ANALYZING IMPACT OF CLIMATE AND LAND USE LAND COVER CHANGES ON THE HYDROLOGIC REGIME: THE CASE OF TEKEZE RIVER BASIN, ETHIOPIA

M.SC. GRADUATE THESIS

GALMA GODANA

FEBRUARY, 2020

ADDIS ABABA UNIVERSITY, ADDIS ABABA

ANALYZING IMPACT OF CLIMATE AND LAND USE LAND COVER CHANGES ON THE HYDROLOGIC REGIME: THE CASE OF TEKEZE RIVER BASIN, ETHIOPIA

A Graduate Project to be submitted to the Post Graduate Program Institute Ethiopian Institute of Water Resource

ADDIS ABABA UNIVERSITY

In Partial Fulfilment of the requirement for the degree of Master of Science in Water Resource Engineering and Management (Surface Water Management)

By

Galma Godana

February, 2020

Addis Ababa University, Addis Ababa

APPROVAL SHEET

ADDIS ABABA UNIVERSITY

ETHIOPIAN INSTITUTE OF WATER RESOURCE

POSTGRADUATE PROGRAM DIRECTORATE

As a graduate project research advisor, here I certify that I have read and evaluated this thesis prepared under my direction entitled: "**Analyzing Impact of Climate and Land Use Land Cover Changes on the Hydrologic Regime: The Case of Tekeze River Basin, Ethiopia"** and recommend that it can be accepted as fulfilling the thesis requirement.

Dr. Elias Tedla	_____	_____
Major Advisor	Signature	Date
Dr. Taye Alemayew	_____	_____
Co-Advisor	Signature	Date

As member of the Examining Board of the final M.Sc. Open Defense, we certify that we have read and evaluated the thesis prepared by, **Galma Godana** and recommend that it can be accepted as fulfilling the thesis requirement for the degree of Master of Science in Water Resource Engineering and Management.

Amanuel Abate	----------	----------
Chairman	Signature	Date
Dr.Ing. Adane Abebe	----------	----------
Internal Examiner	Signature	Date
Dr. Tekalign Ayele	----------	----------
External Examiner	Signature	Date

DEDICATION

This work is dedicated to my lovely Mother **Dima Godana,** for nursing me with affection, love and for her dedication in all success of my life.

STATEMENT OF THE AUTHOR

First, I declare that this project is my authentic work and all sources of materials used for the project work have been used duly acknowledged. The project has been submitted for partial fulfillment of the requirement for an M.Sc. degree at Addis Ababa University. I solemnly declare that this research project is not submitted to any other institution anywhere for the award of any academic degree by the author.

Brief quotations from this thesis are allowable without special permission provided that accurate acknowledgment is made. Requests for extended quotations or reproduction of this manuscript in whole or in part may be granted by the Ethiopian Institute of Water Resource judgment. In all other instances, however, permission must be obtained from the author.

Name	Signature	Date of submission
Galma Godana	_____	_____
School/Department:	Ethiopian Institute of Water Resource (Water Resource Engineering and Management)	
E-mail	godanagalma47@gmail.com	

ACKNOWLEDGMENT

Firstly, I would like to give a glory to almighty God, who made me a person of I am today.

Next, I would like to express my deepest gratitude to my advisors Dr. Elias Tedla and Dr. Taye Alemayew for their expert guidance, constructive comments, suggestions, and encouragement throughout my study period.

The author would like to appreciate also Dr. Yihun Dile for his expertise help.

The author would also like to thank the Ethiopian National Meteorological Agency and Ministry of Water, Irrigation, and Electricity.

I am also grateful to all my friends who supported me by giving comments and suggestions during the preparation of this paper.

The author would like to extend a warm appreciation to the host university (Bule Hora University) without whom this work cannot be accomplished.

My appreciation also goes to all Ethiopian Institute of Water Resource communities (especially the staff and the education coordinator Dr. Azage G/Yohannes).

Lastly, but not least, I remain sincerely, grateful and indebted to all my family for their words of encouragement and support, which served me as a source of strength throughout the study period.

TABLE OF CONTENTS

LIST OF TABLES

LIST OF FIGURES

LIST OF TABLES IN THE APPENDIX

LIST OF FIGURES IN APPENDIX

LIST OF ABBREVIATIONS AND ACRONYMS

AOI	Area of Interest
AR5	Fifth Assessment Report
GIS	Geographic Information System
CC	Climate Change
CCLM	COSMO-Climate Limited Area Model
CDO	Climate Data Operator
CMIP5	Coupled Model Inter-comparison Project Phase 5
CN	Curve Number
CORDEX	Coordinated Regional Climate Downscaling Experiment
COSMO	Consortium for Small Scale Modeling
DEM	Digital Elevation Model
ERDAS	Earth System Data Analysis System
ET	Evapotranspiration
FAO	Food and Agricultural Organization
FCC	False Color Composite
GCM	Global Climate Model
HadGEM2-ES	Hadley Global Environment Model 2 - Earth System
HBV	Hydrologiska Byråns Vattenbalansavdelning model
HEC-HMS	Hydrologic Engineering Center-Hydrologic Modeling system
HRUs	Hydrologic Response Units
IGBP-IHDP	International Human Dimension program on Global Change
IPCC	International Panel on Climate Change
LH-OAT	Latin Hypercube One-factor-At-a-Time
LU/LC	Land Use or Land Cover
LULCC	Land Use land Lover Change
MoWIE	Ministry of Water, Irrigation, and Electricity
NIR	Near-Infrared
NMSA	National Meteorological Services Agency
NSE	Nash Sutcliff Efficiency
PBIAS	Percent Bias
OLI	Operational Land Imager
PET	Potential Evapotranspiration
RCM	Regional Climate Model
RCP	Representative Concentration Pathways
SCS	Soil Conservation System
SPOT	Satellite Pour l'Observation de la Terre

SUFI-2	Sequential Uncertainty Fitting Version 2
SWAT	Soil and Water Assessment Tool
SWAT-CUP	Soil and Water Assessment Tool- Calibration Uncertainty Procedure
TCC	True Color Composite
TM	Thematic Mapper
UNESCO	United Nations Educational, Scientific and Cultural Organization
UNFCCC	United Nations Framework Convention on Climate Change
USDA-ARS	US Department of Agriculture Research Service
USGS	United State Geological Survey
UTM	Universal Transverse Mercator
WCRP	World Climate Research Programme
WGEN	Weather Generator
WGS	World Geodetic System
WMO	World Meteorological Organization

ABSTRACT

Investigating the impacts of land-use and climate change on hydrologic regimes are essential in understanding the patterns and movement of hydrologic processes. The changes in land use land cover and climate change were experienced in the Upper Tekeze River basin in the last three decades (the 1990s, 2000s, and 2010s) and climate changes is likely to occur under near future projections (2020-2040). The paper provides potential implications of land use/ land cover and climate change on streamflow, surface runoff, baseflow, evapotranspiration and water yield of Upper Tekeze River basin using soil and water assessment tool (SWAT) model. The analysis of this study includes an investigation of changes in historical land-use patterns, individual and combined impacts of land use and climate change on hydrology and the factor playing a dominant role in modifying the hydrology of the area. The analysis of three land use/land cover reveals that the decline in forest and grassland and the increment in agricultural land where the predominant land use/land cover change over the past three decades. The hydrologic simulations indicate the influence of climate changes on the hydrologic regime was dominant than land-use change. The variation in evapotranspiration was more pronounced in land use/land cover change. However, the monthly variation in streamflow was mainly related to the seasonal changes in precipitation. The reduction in baseflow was mainly attributed to land-use change. The increment in surface runoff caused by climate change was enhanced by land-use change, while, the decline in evapotranspiration was enhanced by deforestation. Furthermore, the combined action of climate and land use follow the trends similar to the impact of climate change. Under future projection the result reveals that except evapotranspiration all other hydrological components (stream flow, surface runoff, base flow and water yield) show the decline under RCP8.5 while the increment under RCP4.5 except water yield which shows the decline. The finding from this thesis could provide information for local administration, and policymakers to better understand the changes in the hydrology of this region.

Keywords: Land use/land cover, Hydrologic regime, Upper Tekeze River Basin, SWAT model,

CHAPTER ONE

1. INTRODUCTION

1.1. Background

Climate change and land-use/land cover (LULC) change are two factors that produce major impacts on hydrological regimes. Understanding and quantifying their respective influence is of great importance for water resources management and socio-economic activities as well as policy and planning for sustainable development (Yang *et al.*, 2017).

Investigating the impacts of land use land cover, and climate changes on water resources potentials are crucial for an understanding of hydrologic regimes. Hydrologic response to changes in Land-use land cover Changes (LULC), land management practices and climate changes is an integrated indicator of a watershed condition. Watersheds are generally considered as useful units of analysis and action because of several physicals (Natural system, multiple scales, ideal for process studies, integrated framework, assist in addressing complexity) and social (decision-making tool, social organization, upstream and downstream links) characteristics (Mengistu, 2009).

The basin hydrology is sensitive to changes in land cover attributes, with a general pattern of increasing unregulated runoff with the conversion from trees to crops due to decreasing evapotranspiration (Thanapakpawin *et al.*, 2007).

Being one of the very sensitive elements, climate change can cause significant impacts on water resources by resulting in changes in the hydrological cycle. The change in temperature and precipitation components of the cycle can have a direct consequence on the quantity of evapotranspiration component, and on both quality and quantity of the runoff component. Consequently, the Spatio-temporal water resource availability, or in general the water balance, can be significantly affected, which clearly amplifies its impact on sectors like agriculture, industry and urban development (Hailemariam, 1999).

As a result, different studies regarding climate and LULC change impact on the hydrologic response have been undertaken in different parts of the world in general and Ethiopia in particular. Scientists agreed that climate and LULC changes have an adverse impact on the socio-economic development of all nations. However, the degree of impact will vary across nations. It is expected that changes in the earth's climate will hit developing countries like Ethiopia first and hardest because their economies are strongly dependent on crude forms of natural resources and their economies structure is less flexible to adjust to such drastic changes (NMSA, 2001). The other problems of the country are the frequent LULC change because a majority of the people are dependent on agriculture and/or the resettlement in the urban area or expansion of urban land that leaves the forested area barren and contributes to flooding and drought. These natural and anthropogenic environmental problems have been experienced in the Tekeze river basin, one of the major Ethiopian river basins.

Thus, quantifying the relationship between climate and LULC changes and their impact on the hydrology would provide valuable information for land use and urban planning, water resource management, policy formulators, and decision-makers.

Recently, a variety of studies have been carried out on the changes in climate /LULC and their impacts on hydrology by using statistical methods or hydrologic models in various watershed under different scales in the northern part of Ethiopia (most of the studies were in Upper Blue Nile Basin). Some of the studies on the separate impact of climate change e.g. (Bekele, 2009, Nigatu *et al.*, 2016, Yihun, 2009). Some of the current studies on individual impacts of LULC change (Mengistu, 2009, Teklay *et al.*, 2019, Woldesenbet *et al.*, 2017b). One of the limitations in most of the studies is they focus on separate impacts of climate and/or LULC changes on hydrology; which undermines the combined impacts of both climate and LULC changes except studies by (Disse *et al.*, 2018, Legesse *et al.*, 2010, Woldesenbet *et al.*, 2018) which address both separate and combined impacts of climate and land use/land cover changes on hydrology.

The interactive, yet, the overlapping relationship between climate and LUC change is at a juxtaposition of separating their impacts challenging (Lin *et al.*, 2015).

Recent research in understanding these have been based on distributed hydrological models. The hydrological models can extract a significant amount of information from limited existing data. The hydrological model is more effective as it relates model parameters directly to physically observable land surface characteristics (Legesse *et al.*, 2003). From those hydrologic models in general, the Soil and Water Assessment Tool (SWAT) has been widely applied to understand the relationship between climate and LULC change on hydrology (Chang *et al.*, 2015, Natkhin *et al.*, 2015, Zhao *et al.*, 2015).

The Soil and Water Assessment Tool (SWAT), is comprehensive and based on physical mechanisms that offer a framework to conceptualize and investigate the relationships between climate, underlying surface, and hydrological processes in various categories in time and space; (Jothityangkoon *et al.*, 2001, Leavesley, 1994). Integrating remote sensing-based high-resolution temporal LULC classification with hydrological modeling would significantly improve the accuracy in simulating the impacts of the LULC change on the hydrologic regime.

1.2. Statement of the Problem

Understanding watershed hydrology is crucial for effective and sustainable water resource planning, development and management activities. There are a number of factors that control watershed hydrology. Among these changes in climate and LULC have a significant impact on the hydrologic regime by affecting runoff, streamflow, rate of flow and volume of rivers and evapotranspiration (Yang *et al.*, 2017).

Although Ethiopia's water resource is large, very little of it has been developed for agriculture, hydropower, industry, water supply, and other purposes. Most of the Ethiopian river basins are untapped for modern irrigation and energy development. Yet, currently, there are flash spot development in some river basins for energy generation, and large-scale irrigation projects to fulfill energy surplus of the country and attain food self-sufficiency respectively (Abate, 2015).

Besides the financial constraints, the transboundary traits of the rivers, climate and land use land cover changes are the main problem for the development in the sectors. Tekeze is one among these basins which cross the border of the country and drains to the Nile river.

Tekeze is one of the major tributaries of the Nile River (it's the third-largest tributaries of the Nile). It served as a source of irrigation, electric power generation and potable water both for Ethiopia and Sudan. However, the extensive expansion of agricultural activities in the area increases the conversion of forest and grassland to agricultural land. Moreover, rapid urbanization by the increasing population has become prevalent in the Tekeze basin. The transboundary issue is also another challenging problem which needs further research on the basin.

Thus, the growing demands of water use and tension in shared water resources like the Tekeze river require scientific research on climatic and LULC changes to the hydrological regime in order to support sustainable land and water development in the area.

A literature review shows few studies were carried out in the Tekeze basin at the sub-basin level, with most studies focusing on precipitation, temperature, sedimentation, and flow. e.g. streamflow and sedimentation (Welde and Gebremariam, 2017) and temperature and precipitation (Haile and Kassa, 2015). However, there were no comprehensive studies which speculate the impact of climate and LULC changes on the hydrologic regime of the basin.

Considering the data scarcity and the complexity of the hydrometeorological process in mountainous areas like the Tekeze basin; investigating the individual and combined impact of climate and LULC changes on hydrologic regimes in this region could provide an example for water resource assessment in the upstream basins.

Therefore, this research was conducted with the primary objective of understanding and investigating the potential impact of climate and LULC change on the hydrologic regime and the dominant factors that influence the hydrologic regime shift on the Tekeze river basin that has received a little research attention in the past.

1.3.Rationale and Significance of the study

Expansion of agricultural land, urbanization, LULC changes, and climate changes are the observed phenomena in the study area. As a result, developing an approach for assessing the separate and combined impact of climate and LULC changes on the hydrological regime is vital in order to have proper water resource planning, development, and management. Thus, this study has a contribution for local governments, policymakers, and other responsible bodies to formulate and implement; effective and appropriate response strategies to minimize the undesirable effect of climate and LULC changes or modifications.

1.4. Research Questions

This study answers the following questions:

1. What are the historical trends of land use land cover of the Upper Tekeze river basin?
2. What are the combined and separate effects of land use land cover and climate change on the hydrologic regime?
3. Which factor (land use land cover or climate change) plays a dominant role in hydrologic regime changes in the area?

1.5. Research Objectives

The general objective of this study was understanding and investigating the potential impact of climate and land use/land cover change impacts on the hydrologic regime and major driving mechanism on the change exhibited on hydrological regime shift within Upper Tekeze river basin. The following specific objectives were intended to be achieved:

1. Investigating trends in historical land use/ land cover pattern of the Upper Tekeze river basin.
2. Exploring the separate and combined impact of land use/land cover and climate change on the hydrologic regime of the basin.
3. Analyzing the dominant factor affecting the hydrologic regimes of the Upper Tekeze river basin.

1.6. Scope of the study

This study focuses on investigating the impact of land use landcover and climate change on hydrologic regime shifts (mainly steam flow, surface runoff, evapotranspiration, baseflow, and water yield alteration) of the Upper Tekeze river basin of Ethiopian part which takes seasonal change into account. The changes in climate reported in this paper are focused on change taken place over decades. The climate data used in this study was obtained from one GCM model (HadGEM2-ES). The interannual variability was not included in this study

1.7. Structure of the Thesis

This thesis comprises six chapters. In chapter one, a general introduction about Climate and LULC changes impact on hydrology is presented. In addition, the statement of the problem, research questions, general and specific objectives, significance and scope of the study and organization of the thesis are well discussed and presented. A literature review focusing on concepts of the hydrologic regime, climate change overview, climate change in Ethiopia, review of climate change impact on hydrology, LULC concepts, hydrological impacts of LULC change, hydrologic models, model selection and description of SWAT model are presented in chapter two. The third chapter describes the study area by presenting location, topography, climate, soil and land use land cover. Chapter four deals with the methodology of the study. To address objective one, methodology on image analysis, LULC classification, extent and rate of LULC changes are presented. To address objective number two and three, the developed scenarios are discussed. In addition, hydrological modeling, model inputs, and model setup are also presented to achieve the above-mentioned objectives. Chapter five presents results and discussion on LULC classification, extent, and rate of LULC, hydrological modeling, the impact of LULC on hydrologic regimes of the basin. Chapter six dictates the conclusion and recommendation. Finally, references and appendices are presented.

CHAPTER TWO

2. LITERATURE REVIEW

2.1. Concept of Hydrological Regime

The hydrological regime refers to variations in the state and characteristics of a water body that are regularly repeated in time and space and which pass through phases, e.g. Seasonal. Additionally, it's also a change with time in the rates of flow of rivers and in the levels and volumes of water in rivers, lakes, reservoirs, and marshes. The hydrologic regime is closely related to seasonal changes in climate. In regions with a warm climate, the hydrologic regime is affected mainly by atmospheric precipitation and evaporation; in regions with a cold or temperate climate, the air temperature is a leading factor (Thanapakpawin *et al.*, 2007).

2.2. Climate change Overview

Climate is defined as the prevailing condition observed as a long-term average in a location (Grossman-Clarke *et al.*, 2011). Climate change is an accurate threat to global development and efforts to end poverty. Without urgent action, climate change impacts could push an additional 100 million into poverty by 2030. Countries and communities around the world are already experiencing climate change impacts-including droughts, floods, more intense and frequent natural disasters, and the poorest and most vulnerable are being hit the hardest.

In essence, climate variability looks at changes occur within smaller timeframes, such as a month, a season or a year. A climate change considers changes that occur over a longer period of time, typically over decades or longer (Protocol, 1997).

According to the latest IPCC report, the climate consequences of a 2^0 world are far greater than that of 1.5^0 and we are no track for either. A 1.5 ^{0}C world could reduce the number of people both exposed to climate-related risks and susceptible to poverty by up to several hundred million by 2050 compared with 2 ^{0}C.

Climate change is a severe problem that the whole world facing today. It is now widely accepted that climate change is already happening and further change is inevitable; over the last century (between 1906 and 2005), the average global temperature rose by about 0.74 ^{o}c. This has occurred in two phases, from the 1910s to the 1940s and more strongly from the 1970s to the present (Solomon *et al.*, 2007).

Many studies into the detection and attribution of climate change have found that most of the increase in average global surface temperature over the last 50 years is attributable to human activities (Smithson, 2002).

Climate change is perceived to have been driven by global warming, in turn, is resulting in the changes in the temporal and spatial distribution of precipitation patterns (Pachauri *et al.*, 2014). The frequency and intensity of floods (Zhang *et al.*, 2008) and the replenishment and discharge of annual water runoff have also been affected (Immerzeel *et al.*, 2010).

The IPCC finding reveals that developing countries, like Ethiopia, will be more vulnerable to climate change (IPCC-TGICA, 2007).

2.2.1. Climate Change in Ethiopia

According to the Ethiopian National Meteorological Services Agency (NMSA, 2001) study for 42 meteorological stations, the country has experienced both dry and wet years over the last 50 years. Trend analysis of the annual rainfall shows that there was a declining trend in the northern half of the country and southern Ethiopia while there is an increasing trend in the central part of the country. However, the overall trend in the entire country is more or less constant.

The study of NMSA in the same year for 40 stations showed that there have been very warm and very cold years. However, the general trend showed there was an increase in temperature over the last 50 years. The average annual minimum temperature over the country has been increasing by about 0.25 ^{0}c every ten years while the average annual maximum temperature has been increasing by about 0.1 ^{0}c. The study also noted that the minimum temperature is increasing at a higher rate than the maximum temperature.

Associated with rainfall and temperature change and variability, there were recurrent drought and flood events in the country.

There was also the observation of water level rise and dry up of lakes in some parts of the region depending on the general trend of the temperature and rainfall pattern of the regions. Studies on hydro-climatic change of the Northern Ethiopia also reveal that the Tekeze river basin experiences climate change over time (Tesfaye *et al.*, 2019). The report that the stream will show the decline before the year of 2039 under RCP8.5 while it shows the increment until the year of 2039 under RCP 4.5.

2.2.1.1. Climate Change Impact on Hydrology

The climate change is less likely to pose the threat on average water availability. However, temporal variation in river flows is expected to increase in the future (Devkota and Gyawali, 2015).

The study by Habtom (2009) around Gilgel Abay also indicated that the projected maximum and minimum temperature shows an increasing trend for the next century, but the precipitation doesn't show a significant difference from the current condition. This study also reveals the evaporation from open water was showed an increasing trend.

Similarly, according to Yihun (2009) a study in Gilgel Abay sub-basin in Ethiopia, due to climate change there is an increase in temperature which will increase the evapotranspiration of the river. It was observed that climate change has a negligible effect on the low flow condition of the river. Yet, there might be a net annual increase in flow volume in Gilgel Abay due to climate change. This might also aggravate the recurrent flooding problems in the Lake Tana basin. The impact of land-use change on hydrology was neglected in this study. Due to this, there is a need for assessing the combined impact of both climate and land-use impacts on hydrology.

However, another result reveals there is an increment both in precipitation and temperature of Werii watersheds in the future. Climate change projections due to precipitation are higher and significant than that of temperature change (Haile and Kassa, 2015). In this study, only the

impact caused due to climate change was studied which undermine the land-use change impacts. Additionally, it focused only on the precipitation and temperature changes due to climate change.

This result is not in line with the study by Habtom (2009) which dictates no significant changes in precipitation in the future due to climate changes.

2.3. Overview of Climate Change Scenarios

The fifth assessment (AR5) scenario of IPCC adopted new scenarios, called representative concentration pathways (RCPs) in 2009. RCPs are time and space-dependent trajectories of concentrations of greenhouse gases and pollutants resulting from human activities, including changes in land use. RCPs provide a quantitative description of concentrations of the climate change pollutants in the atmosphere over time, as well as their radiative forcing in 2100 (for example, RCP 6 achieves an overall impact of 6 watts per square meter by 2100). There are four categories of RCP pathways:

1. RCP 8.5 (high emissions) is consistent with a future with no policy changes to reduce emissions. It was developed by the International Institute for Applied System Analysis in Australia and is characterized by increasing greenhouse gas emissions that lead to high greenhouse gas concentrations over time. Comparable SRES scenario A1F1. This future is consistent with three times today's CO_2 emissions by 2100, rapid increase in methane emissions, increased use of agricultural lands and grassland which is driven by an increase in population, a world population of 12 billion by 2100, lower rate of technology development, heavy reliance on fossil fuel, high energy intensity and no implementation of climate policies.
2. RCP 6 (Intermediate emissions) is developed by the National Institute for Environmental Studies in Japan. In this case, radiative forcing is stabilized shortly after 2100, which is consistent with the application of a range of technologies and strategies for reducing greenhouse gas emissions. Comparable SRES scenario: B2. This future is consistent with: heavy reliance on fossil fuels, intermediate energy intensity, increase the use of cropland

and declining use of grasslands, stable methane emission and CO_2 emissions peak in 2060 at 75% above today's levels, the decline to 25% above today.

3. RCP 4.5 (Intermediate emissions) is developed by the Pacific Northwest National Laboratory in the US. Here radiative forcing is stabilized shortly after the year 2100, consistent with a future with relatively ambitious emissions reductions. Comparable SRES scenarios: B1.

   This future is consistent with: lower energy intensity, strong reforestation programs, decreasing use of croplands and grasslands due to yield increases and dietary changes, stringent climate policies, stable methane emissions, and CO_2 emissions increase only slightly before decline commences around 2040.

4. RCP 2.6 (Low emissions) is developed by PBL Netherland Environmental Assessment Policy. Here a radiative forcing reaches 3.1 watts per meter squared (W/M2) before it returns to 2.6 W/M2 by 2100. In order to reach such a forcing level, ambitious greenhouse gas emissions reductions would be required over time. Comparable SRES scenario: None. This future would require: declining use of oil, low energy intensity, a world population of 9 billion by 2100, use of cropland increase due to bio-energy production, more intensive animal husbandry, methane emissions reduced by 40%, CO_2 emissions stay at today's until 2020, then decline and becomes negative in 2100 and CO_2 concentrations peak around 2050, followed by a modest decline by 400ppm by 2100.

2.3.1. CORDEX-Africa Domain

Africa is one of the most vulnerable continents to weather and climate variability ((IPCC, 2007). Global Climate Models (GCMs) are the primary tools for understanding the global climate and its projected change under different forcing scenarios. However, the coarse resolution of GCMs precludes them from capturing the effects of local forcing like terrain effect and land-sea contrasts that modulate the signal at a finer scale (Rummukainen, 2010).

For use of GCM outputs in hydrological impact assessment and adaptation studies, downscaling of outputs to a smaller scale is advocated. Recently, a new initiative endorsed by the World Climate Research Programme (WCRP) has emerged in order to produce an improved generation of regional climate change projections world-wide:

The Coordinated Regional Climate Downscaling Experiment (CORDEX) (Giorgi *et al.*, 2009) during the Fifth Assessment Report (AR5). Due to its vulnerability to climate variability, the significant impacts of projected climate change, and the general lack of climate projections based on Regional Climate Downscaling tools, Africa was selected as the first target region for the CORDEX activity: see Jones et al., (2011) for more details on CORDEX Climate Projection Frame-work. The CORDEX downscaled Regional Climate Model (RCM) has relatively fine-scale or resolutions (50km x 50km).

The data include daily, monthly and seasonal variation of CORDEX experiments scaled down onto a 50km grid over Africa (AFR-44) based on the CCLM4-8-17 (Consortium For Small Scale Modeling (COSMO) Climate Limited Area Model) regional climate model. Data from any CORDEX and with any CMIP5 (Coupled Model Inter-comparison Project Phase 5) global model forcing available and transferred from the ESGF (Earth System Grid Federation) are included. These are experiments evaluation, historical, rcp85 and rcp45 using forcing data derived from the CMIP5 models MPI-ESM-LR, EC-EARTH, CNRM-CM5, and HadGEM2-ES. The reference was made to Jones *et al.* (2011) for the description of those models.

Downscaling is through an RCM by using initial conditions and boundary conditions as obtained from selected two GCMs or from re-analysis data which is merged climate model and observed data. The numerical boundary conditions for RCM simulations can, for instance, include a vertical profile of climate variables and surface conditions over oceans. In principle, RCMs cannot remove GCM biases related to large scale variables. However, downscaling GCM output by RCMs may lead to improved simulation at the GCM sub-grid scale as a result of using relatively high-resolution data such as topography and land cover. Whereas simulations by RCMs are spatially more accurate by the much smaller grid element scale it is often assumed and expected that the reliability of the estimates also increases. As such it's assumed that downscaling leads to a reduction of bias and errors though this is not always true as some errors may remain uncorrected or are even amplified by RCM simulations (Laprise *et al.*, 2013). There is uncertainty related to the bias corrections of the climate data. Therefore, one may use the climate without bias correcting to avoid such uncertainties (Liu *et al.*, 2014).

2.4.Land use / Land Cover Concept

The International Geosphere-Biosphere Program, The International Human Dimension Program, and the Land Use and Land Cover Change project have referred to 'land use and land cover change' as follows (Lambin, 1999, Nunes and Auge, 1999). Land cover refers to the physical and biophysical characteristics or state of earth's surface and immediate, captured in the distribution of vegetation, water, desert, ice and other physical features of the land, including those created solely by human activities e.g., settlements. Land use refers to the intended use or management of the land cover type by human beings.

Thus, land use involves both the manner in which the biophysical attributes of land are manipulated and intent underlining that manipulation (the purpose for which the land is used e.g., agriculture, grazing, etc), which are more subtle changes that affect the character of the land cover without changing its overall classification. The definition of land use in this way establishes a direct link between land cover and the actions of people in their environment (Gregrio and Jansen, 2000).

2.4.1. LULC Change Impact on Hydrology in Ethiopia

According to (Bewket and Sterk, 2005) a study in Chemoga sub-basin in north Ethiopia, the hydrology of a sub-basin has been influencing negatively due to the clearance of natural vegetation cover, land degradation, and expanded agricultural land that reduce infiltration, decrease groundwater recharge, and increase runoff.

Similarly, based on the study carried out by (Getahun and Van Lanen, 2015) there was higher streamflow during the main rainy season due to complete deforestation and evapotranspiration was low due to this. The study also shows during the main rainy season, there was slightly increased streamflow due to the expansion of agricultural land but during the dry season it showed a decrement in magnitude. This implies there were a temporal variation and variation in the volume of river flows due to land use/ cover change. This result is in line with the finding of Wolde (2016) which implies the increment in bare land and agricultural land resulted in increased annual and seasonal streamflow and sediment yielded in volumes.

However, during the rainy season, the effect of LULC was more pronounced according to this report which shows the disagreement with the above finding to some extent.

2.5.Remote Sensing Application in Land use Land Cover and Climate Change studies

Remote Sensing (RS) technology has been used for the change detection of land use land cover in many parts of Ethiopia. Remote Sensing (RS), integrated with Geographic Information System (GIS) provides an effective tool for analysis of land use and land cover changes (Afera *et al.*, 2018).

They applied for woreta watershed and comes up with the result that land use land cover change detection using multi-temporal images by means of remote sensing and GIS modeling is a good means of analyzing dynamic changes in time sequence.

Change detection is useful in many applications related to land use and land covers (LULC) changes, such as shifting cultivations and landscape changes, forest degradation and desertification. Andualem *et al.* (2018) applied remote sensing to detect the land use of Upper Rib watershed. Their result implies the huge reduction in grassland and increment in cropland (13.78%) for over an 11year period. This was due to the increased population with great interests in agricultural land.

Asirat (2018) also applied Remote Sensing and GIS for evaluating land use land cover dynamics in Upper Blue Nile and reported the increment in cropland and grassland, while a reduction in forest and shrubland. The changes were due to an increment in the human and livestock population in the area.

However, in the Tekeze River Basin, there are no sufficient studies with regard to the application of remote sensing for land use/land cover change detection. Having this gap, Therefore, there is a necessity of studying the land use land cover change trends in the Tekeze river basin using remote sensing with the integration of GIS.

In recent years, there is no doubt that climate change has observable development impacts, which seriously threatens the ability of individuals and communities at all levels. To halt such disastrous conditions assessing the impact and vulnerability of climate change requires accurate, up to date and improved information. Coupled with this RS technology appears poised to make a great impact on planning agencies and providing a better understanding dynamic of the climate system, predict and mitigate the expected global changes and the effects of human civilization involved in mapping Land use Land Cover (LULC) at a variety of spatial scales. The study in Sudan by Deafalla *et al.* (2014) shows the importance of spatial variables in tackling climate change which promoted the use of maps made in RS. Their result also indicates the use of remote sensing in assessing the combined impacts climate and land use /land cover changes.

2.6.Hydrological Models

Techniques available for analyzing hydrological impacts can be classified into three categories: catchment paired experiment, statistical analysis, and hydrological model (Li *et al.*, 2012). The catchment paired experiment is normally applied in small watersheds and is used to separate the climate factor so that the effects of LULC change can be accurately quantified.

However, Serpa *et al.* (2015) state that this approach is generally not feasible for large watersheds due to differences in locating two similar catchments in close proximity with the same size, land cover pattern, and soil properties. Statistical analysis, on the other hand, is usually easy to access with annual streamflow time series. This method currently in use is frequently misleading in its incapacity to incorporate agronomic and microclimatic effects, and in many cases, particularly egregious in ignoring soil, vadose, and surface storage. Moreover, Wei *et al.* (2013) imply that the experimental and statistical methods treat the study basin as a black box and seldom do they consider the complexity and heterogeneity in underlying surface conditions and the relationships between climate change and hydrological processes (Hu *et al.*, 2015).

Hydrological models are mathematical descriptions of components of the hydrologic cycle. They have been developed for many different reasons and therefore have many different forms. However, hydrological models are in general designed to meet one of the two primary objectives. The one objective of the watershed hydrologic modeling is to get a better understanding of the hydrologic processes in a watershed and of how changes in the watershed may cause these phenomena. The other objective is for hydrologic prediction. They are also providing valuable information for studying the potential impacts of changes in land use and land cover or climate. On the basis of the process description, the hydrological models can be classified into three main categories (Perazzoli *et al.*, 2013).

Lumped models: Parameters of lumped hydrologic models do not vary spatially within the basin and thus, basin response is evaluated only at the outlet, without explicitly accounting for the response of individual sub-basins. The parameters often do not represent the physical features of hydrologic processes and usually involve a certain degree of empiricism.

These models are not usually applicable to event-scale processes. If the interest is primarily in the discharge prediction only, then these models can provide just as good simulations as complex physically-based models.

Distributed models: Parameters of distributed models are fully allowed to vary in space at a resolution usually chosen by the user. The distributed modeling approach attempts to incorporate data concerning the spatial distribution of parameter variations together with computational algorithms to evaluate the influence of this distribution on simulated precipitation-runoff behavior. Distributed models generally require a large amount of (often-unavailable) data. However, the governing physical processes are modeled in detail, and if properly applied, they can provide the highest degree of accuracy.

Semi-distributed models: Parameters of semi-distributed (simplified distributed) models are partially allowed to vary in space by dividing the basin into a number of smaller sub-basins. The main advantage of these models is that their structure is more physically-based than the structure of lumped models, and they are less demanding on input data than fully distributed models.

SWAT (Arnold *et al.*, 1998), HEC-HMS (US-ACE, 2010), HBV (Lindström *et al.*, 1997), are considered as semi-distributed models.

Hydrologic models can be further divided into event-driven models, continuous process models, or models capable of simulating both short-term and continuous events. Event-driven models are designed to simulate individual precipitation-runoff events. Their emphasis is placed on infiltration and surface runoff. Typically, event models have no provision for moisture recovery between storm events and, therefore, are not suited for the simulation of dry-weather flows. On the other hand, continuous-process models simulate instead of a longer period, predicting watershed response both during and between precipitation events. They are suited for simulation of daily, monthly or seasonal streamflow, usually for long-term runoff volume forecasting and for estimates of water yield. Generally, for this study, the semi-distributed model (SWAT) were selected because of their structure is more physically-based than the structure of lumped models. Table *2.* 1 dictates the comparison/difference of three semi-distributed models for hydrological application.

Table 2. 1 : Summary of comparison of specific hydrological models

Descriptions	**SWAT**	**HEC-HMS**	**HBV**
Model Type	Semi-distributed Physically-based Long-term	Semi-distributed Physically-based	Semi-distributed Conceptual Model
Model Objectives	Predict the impact of land management practices on water and sediment	Simulate the rainfall-runoff process of watershed	Simulate the rainfall-runoff process and floods
Temporal Scale	Day	Day	Day
Spatial Scale	Medium	Flexible	Flexible
Process Modeled	Continuous	Continuous and events	Continuous and events
Cost	Public domain	Public domain	Public domain

Source: The author review from different literature.

2.6.1. Model Selection

There are various criteria that can be used for selecting a hydrological model for a specific problem. These criteria are project dependent because every project has its own requirements, need, and objectives. Yet, some criteria are also user-dependent or and therefore subjective. Based on the suggestions from Cunderlik (2003) and Rodda *et al.* (2011) the following factors and criteria were used as being relevant when selecting models:

a. The type of system to be modeled; e.g. small catchment, river reach, reservoir, or large river basin.
b. Hydrologic models that need to be modeled to estimate the desired outputs adequately (is the model capable of simulating a single event or continuous process).
c. The general modeling objective; e.g. hydrological forecasting, assessing human influences on the hydrological regime or climate change impact assessment.
d. The hydrological element to be modeled and required model outputs important to the project and therefore to be estimated by the model; e.g. floods, daily average discharge, monthly average discharge, water quality, and others.
e. Data availability with regard to type, length, and quality of data versus data requirements for model calibration and operation. Can all the inputs required by the model be provided within the time and cost constraint of the project?
f. Model simplicity, as far as hydrological complexity and ease of application are concerned.
g. The possible transition of model parameter value from smaller sub-catchment of the overall catchment or from neighboring catchments.
h. The ability of the model to be updated conveniently on the basis of current hydro-meteorological conditions.
i. Price (openness) or (does the investment appear to be worthwhile for the objective of the project?)

2.6.2. SWAT Model Description

The SWAT (Soil and Water Assessment Tool) watershed model is one of the most recent models developed at the USDA-ARS (Arnold *et al.*, 1998) during the early 1970s.

The SWAT model is a semi-distributed physically-based simulation model and can predict the impacts of land-use change and management practices on hydrological regimes in watersheds with varying soils, land use and management conditions over long periods and primarily as a strategic planning tool (Neitsch *et al.*, 2000).

The interface of the SWAT model is compatible with ArcGIS that can integrate numerous available geospatial data to accurately represent the characteristics of the watershed. In the SWAT model, the impacts of spatial heterogeneity in topography, land use, soil and other watershed characteristics on hydrology are described in subdivisions.

There are two scale levels of subdivisions; the first is that the watershed is divided into a number of sub-watersheds based upon drainage areas of the attributes, and the other one is that each sub-watershed is further divided in to a number of Hydrologic Response Units (HRUs) based on land use and land cover, soil and slope characteristics. The SWAT model simulates eight major components: hydrology, weather, sedimentation, soil temperature, crop growth, nutrients, pesticides, and agricultural management (Neitsch *et al.*, 2000).

Major hydrologic processes that can be simulated by this model include evapotranspiration, surface runoff, infiltration, percolation, shallow aquifer, and deep aquifer flow, and channel routing (Arnold *et al.*, 1998). Streamflow is determined by its components (surface runoff and the groundwater flow from shallow aquifer).

2.6.3. SWAT Model Application

The SWAT model has a good reputation for best use in agricultural watersheds and its uses have been successfully calibrated and validated in many areas of the world (Chien *et al.*, 2013, Tripathi *et al.*, 2003). The studies indicated that the SWAT model is capable of simulating the hydrological process and erosion/sediment yield from complex and data
reasonable model performance statistical values. Tripathi *et al.* (2003) applied the SWAT model

watersheds to develop an effective management plan and the model was verified for both surface runoff and sediment yield.

Michael, (2012) applied SWAT for Upper Blue Nile to investigate the impact of climate and land-use change on water resource and the model was validated successfully for runoff and streamflow. Accordingly, the study concluded that the SWAT model can be used in ungauged watersheds to simulate the hydrological and sediment processes. SWAT has gained international acceptance as a robust interdisciplinary watershed modeling tool as evidenced by international SWAT conferences, hundreds of SWAT-related papers presented at numerous other scientific meetings, and a large number of articles published in peer-reviewed journals (Gassman *et al.*, 2007). However, Cibin *et al.* (2010) indicated that SWAT model parameters show varying sensitivity in different years of simulation suggesting the requirement for dynamic updating of parameters during the simulation.

CHAPTER THREE

3. METHODOLOGY

3.1.Description of the Study Area

3.1.1. Location of Study Area

Tekeze is one of the Ethiopian major river basins. The basin is located in the North-Western part of Ethiopia. The basin consists of three main catchments: Upper Tekeze, Angereb and Goang rivers. This study focuses on the catchment of the Upper Tekeze river basin. The Tekeze river originates in the southern part of the basin near the Ras-Dashen Mountains and flows in the northern direction and then turns towards west flowing into north-eastern Sudan, where the river joins Atbara river (Belete, 2007). It is located at 12^0 0'12.20" N to 14^0 45' 42.29" N and 36^0 32' 07.70" E to 39^0 46' 23.89" E in the North-Western part of Ethiopia. The Tekeze River is one of the major tributaries of the Nile River which drains from the area of 56, 860.190 square kilometers (KM^2) from the outlet. The basin has a minimum elevation of 514 m.a.s.l at the outlet and a maximum elevation of 4528 m.a.s.l at the Ras-Dashen mountain.

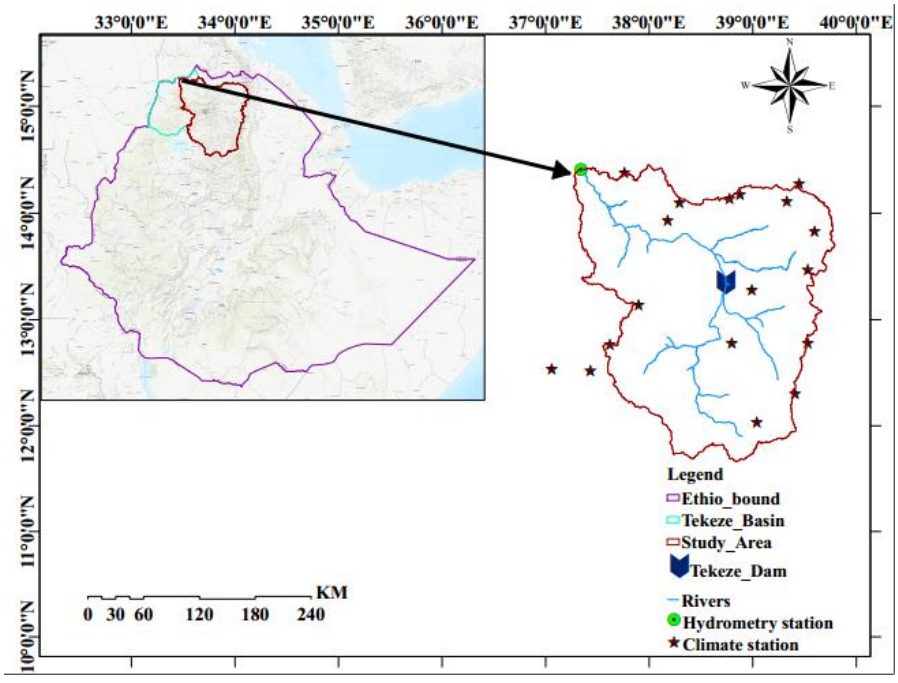

Figure 3. 1 : Location of the study area

3.1.2. Topography

Topographically the basin is characterized by rugged topography consisting of mountains, highlands and terrains of gentle slopes (<5%) to very steep slopes (>60%) (Figure 3. 2). About 33.4% of the basin is included within the slope of less than 15%. The slope ranging from 15%-30% covers about 27% of the basin. About 31.6% and 8% of the area has the slope 30%- 60% and above 60% respectively.

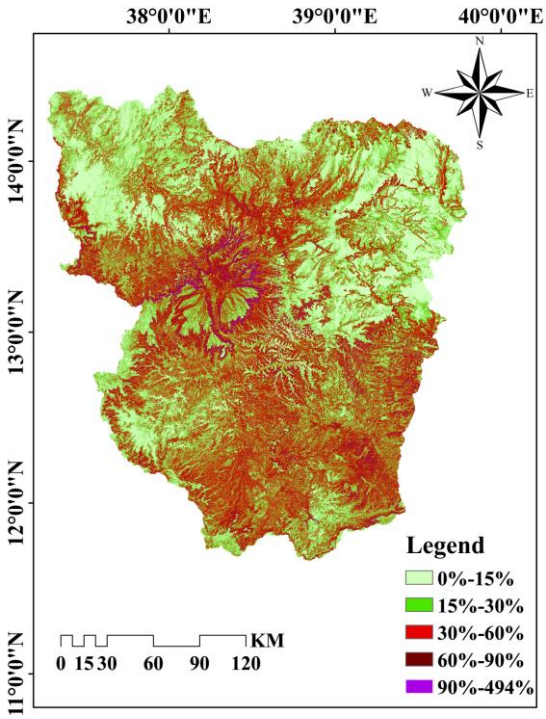

Figure 3. 2 : Topography of the study area

3.1.3. Climate

The climate of the basin is semi-arid in the east and north and partly humid climate in the south (Belete, 2007). Based on the meteorological station used in this study the mean annual rainfall in basin ranges from 400mm in the northern part to over 1400mm in the southern part. Belete (2007) reports the mean annual rainfall in the basin ranges from about 400 mm in the northeast to over 1200 mm in the high lands of the southwest. Amare (1996) also reported the rainfall in the basin is highly affected by local factors like topography and micro-climate in the basin.

The year-to-year variability of annual rainfall in the basin is very high showing coefficient of variability ranging from 0.2 in the high lands of the basin to 0.4 over its low land part (Belete, 2007).

More than 70% of the rainfalls is in two months (July and August). The river flow patterns follow that of the rain. The maximum streamflow occurs in August, and it decreases during the dry period.

The maximum temperature of the basin ranges from 16 ^{0}C (in the wet season) to above 32 ^{0}C (in the dry season), while the minimum temperature ranges between (6-16 ^{0}C) (Figure 3. 4). According to (Gebreselassie and Moges, 2016) the mean temperature in the basin varies from about 10°C in the highlands of the basin to over 26°C on its lowlands.

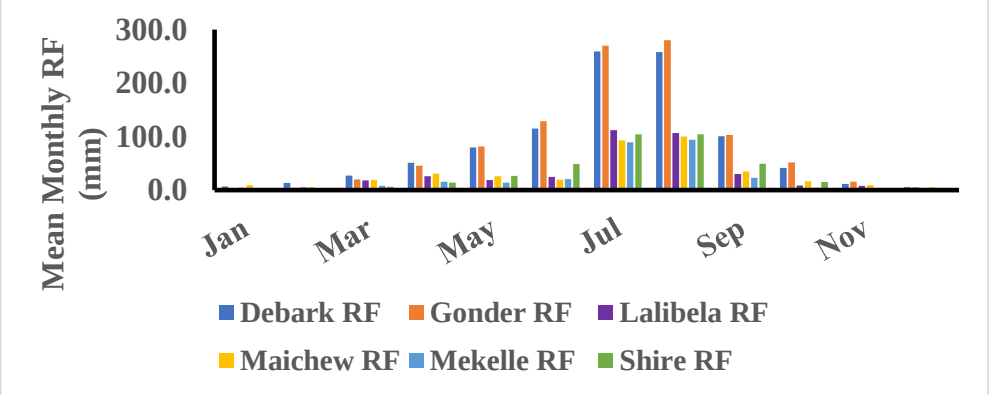

Figure 3. 3 : Average monthly rainfall

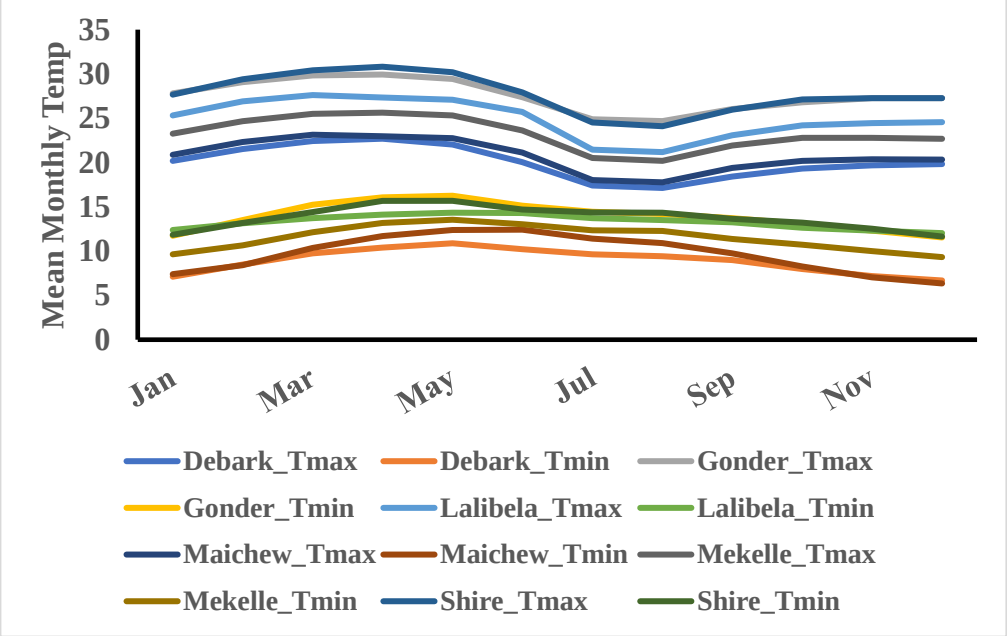

Figure 3. 4 : Mean monthly maximum and minimum temperature

3.1.4. Soil

The basin encompasses 13 types of soil. Lithic Leptosols cover about 43% of the basin which covers most highland parts of the area. The Eutric Leptosols (~22%) which is the second major soil in the area covers the majority of the gentle slope part of the basin. See Figure 3. *6* and/ or Table 3. 1.

Table 3. 1 : Major soil types in the study area.

SN	Soil type name	SWAT Code	Area (km^2)	% of watershed area
1	Petric Calcisols	CLp	105.72	0.19
2	Eutric Cambisols	CMe	2600.97	4.59
3	Vertic Cambisols	CMv	1921.36	3.39
4	Chromic Cambisols	CMx	1743.49	3.08
5	Dystric Leptosols	LPd	2010.30	3.55
6	Eutric Leptosols	LPe	12274.90	21.67
7	Rendzic Leptosols	LPk	44.47	0.08
8	Lithic Leptosols	LPq	24381.15	43.05
9	Haplic Luvisols	LVh	7808.78	13.79
10	Chromic Luvisols	LVx	33.56	0.06
11	Haplic Lixisols	LXh	574.73	1.01
12	Humic Nitisols	NTu	2394.57	4.23
13	Eutric Vertisols	VRe	744.21	1.31

3.1.5. Land Use and Land Cover

The main/dominant land use/ land cover of the basin are Agricultural lands, Grassland, Forest land, Shrub/bushland, Barren land, Built-up land and Waterbody (Figure 3. 6). Agricultural land covers the majority of the area (>67%). The left six constitutes about 33% of the total area. According to Tefera (2003), the dominant land use in basin includes cultivated land (>70.5%), open grassland, sparsely grown woodland, bushes and shrubs, and exposed rock. This basin is characterized by severe land degradation through deforestation, overgrazing, and cultivation on the rugged topography. Yet, it's also known for its more recent experience with soil and water conservation (SWC) Alemayehu *et al.* (2009) in semi-arid parts of the basin.

Another land-use type that may alter the flow regime of downstream is a hydro dam which was established in the year of 2009 in the upper part of this basin.

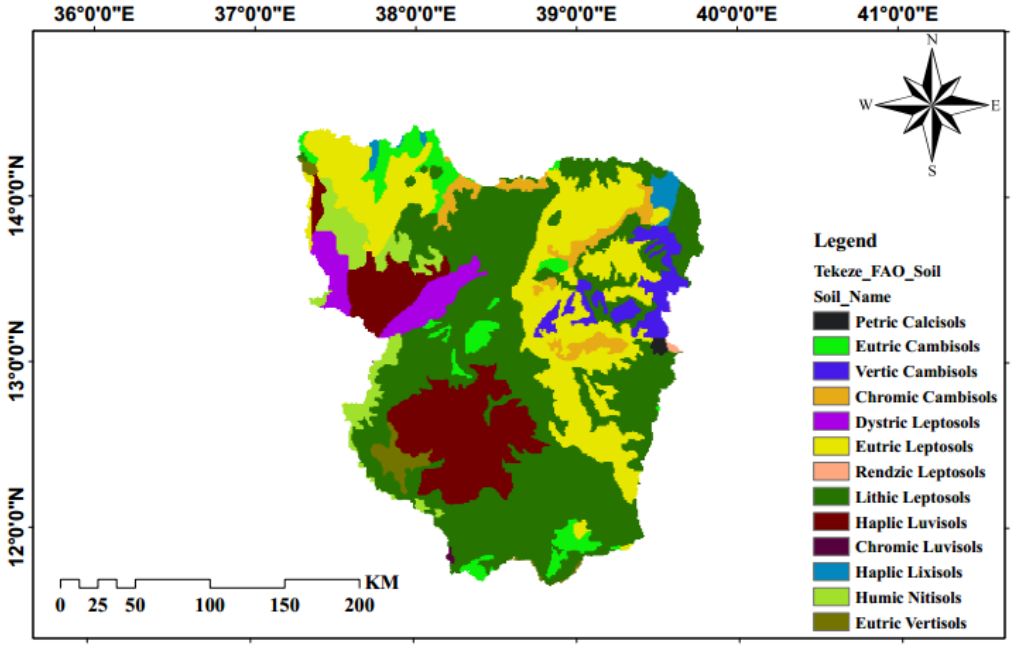

Figure 3. 5 : Soil type of study area

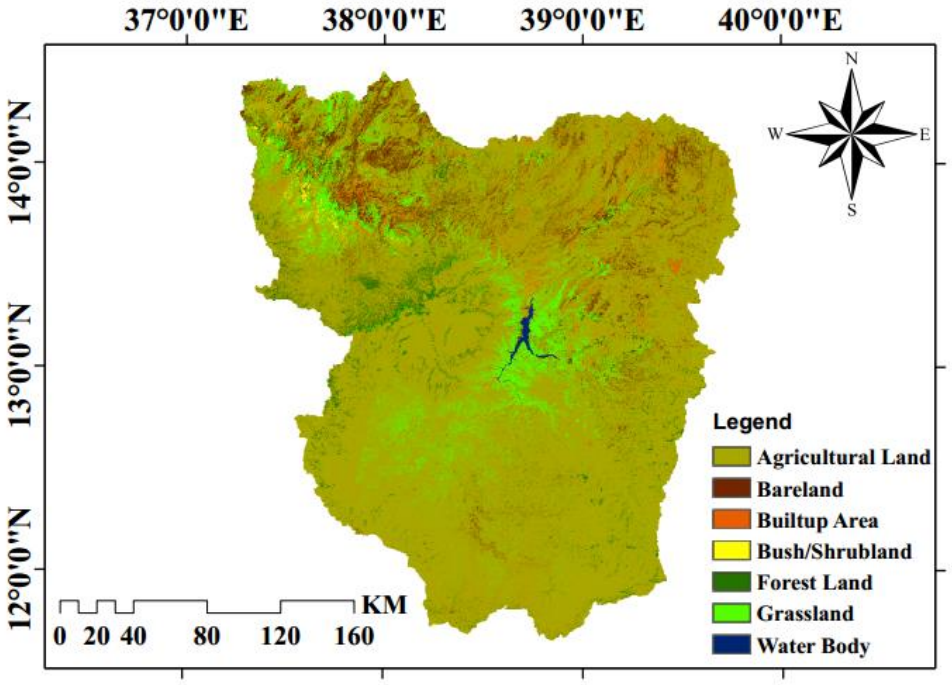

Figure 3. 6 : LULC map of the study area

3.2.Methods

3.2.1. Data types and sources

For this study, Topographic data or Digital Elevation Model (DEM) of 30m*30m were downloaded from http://earthexplorer.usgs.gov/; for delineating the watershed. Soil data were downloaded from the Food and Agricultural Organization- Harmonized World Soil Data Bases (FAO-HWSD). The satellite images of 1992, 2002 and 2015 years or the three years images were obtained from digital satellite imageries of Landsat 5 TM and Landsat 8 OLI.

Daily data of climatic variables (daily data of precipitation, maximum and minimum temperature, relative humidity, wind speed, and solar radiation) of the Tekeze basin were collected from the Ethiopian National Meteorological Agency and the grided climate data of CORDEX-Africa domain (precipitation and temperature) was obtained. The observed streamflow data (1994-2015) of the Tekeze river were collected from MOWIE that were used for calibration and validation of the result.

The ArcSWAT with the help of ArcGIS software version 10.5 was used for catchment delineation and catchment characteristics based on automatic delineation procedure using DEM and digitized stream network. The SWAT tool coupled with Arc GIS 10.5 was used for catchment analysis and SWAT-Cup 2019 was employed for calibration of the result. The ground truth information that was required for the classification and accuracy assessment of imageries were collected through field observation to rectify ground control points (GCPs) for georeferencing, visual interpretation of the images and select reference areas (training areas).

Earth Resource Data Analysis System (ERDAS) imagine version 15.00 and Arc GIS 10.5 software packages were utilized for the classification of LULC changes. The satellite data were imported to ERDAS Imagine 2015 in an image format for geometric correction. Global Positioning System (GPS) was used to collect ground truth points for further analysis of satellite images.

3.2.2. Image Analysis

3.2.2.1. Image Rectification

The Landsat images were preprocessed using standard procedures. The World Geodetic System 1984 (D_WGS_1984) was used as the coordinate system. A subset of Landsat images was rectified from an arbitrary coordinate system in a map projection coordinate system with UTM projection (WGS_1984_UTM_Zone_37) using nearest neighbor resampling algorithm. Image pre-processing was done using ERDAS imagine 2015.

Table 3. 2 : Description of satellite image used

	1992	**2002**	**2015**
Satellite	Landsat TM	Landsat TM	Landsat 8/OLI
Path/Row	168/50, 168/51, 168/52, 169/50, 169/51, 169/52, 170/50, 170/51,	168/50, 168/51, 168/52, 169/50, 169/51, 169/52, 170/50, 170/51	168/50, 168/51, 168/52, 169/50, 169/51, 169/52, 170/50, 170/51
Acquisition date	January 01-31, 1992	January 01-31, 2002	January 01-31, 2015
Spatial resolution (meter)	30	30	30

3.2.2.2. Satellite Images Spectral Band Selection

Satellite imageries may have multiple spectral bands of information. Each band is a set of data file values with a specific portion of the electromagnetic spectrum of reflected light or emitted heat (Red, Green, Blue, Infrared, Near-Infrared, etc.) or other user-defined information created by combining or enhancing the original bands or creating new bands from other sources. The different bands of Landsat, SPOT and other imaging sensors are selected to detect certain features; therefore, knowing the parameters of the bands before performing any image enhancement is crucial (Kacyra *et al.*, 2005). In this study, spectral bands were selected based on the application and specification of each Landsat band with respect to image classification and LULC mapping.

All spectral band of Landsat TM was selected except band 6 namely TIR (Thermal Infrared); and from Landsat 8/OLI, band 1, 9, 10 and 11 for (ocean, cloud, and Temperature respectively) and not mandatory for LULC mapping were exempted (Vermote *et al.*, 2016). The information used for selecting essential bands is described in the ERDAS Imagine field guide.

3.2.2.3. Stacking/Composite, Mosaicking and sub-setting

Once the required bands are selected, a single raster dataset was created from multiple spectral bands of Landsat imageries using a layer stacking tool. Afterward the image mosaicking since the study area lays over the span of eight (8) scenes and finally, sub-setting of mosaicked images was applied so as to include only the area of interest (AOI).

3.2.2.4. Band Combination for Displaying and Image Enhancement

The satellite image color display provides inadequate information for image interpretation. Those image enhancement techniques are required to improve the quality of an image as it increases the transparency of spectral bands. False Color Composition (FCC), True Color Combination (TCC) and other common band combinations were applied; these sets the image to RGB color and those differentiating variety of features were possible. Particularly, for this study, Band 4,3,2 and Band 5, 4, 3 which create a false-color composite were prepared for TM and Landsat 8 respectively for image display, enhancement, and classification.

3.2.3. Land Use Land Cover Classification

The three Landsat imageries namely Landsat TM (1992, 2002) and Landsat 8 (2015) were used to investigate LULC changes (Table 3.2). All images were acquired both for dry and the same season in order to minimize the impact of the seasonal difference in vegetation. Image analysis and LULC classification were made by using ArcGIS 10.5 software.

3.2.3.1. Accuracy Assessment

A total 662 ground truth data (GCP or Ground Control Point); 100 (Global Positioning System or GPS point) and Google Earth (562 X, Y coordinates) regarding land cover types and their spatial locations were collected in October 2018, assuming that there had not been significant land cover change between 2018 and 2015).

As many as 562 points were used for accuracy assessment and 150 were used for developing training sites to generate a signature for each land cover type. The accuracy of the classification was assessed by computing error or confusion matrix that compares the classification result with ground truth information as suggested by (DeFries and Chan, 2000). A confusion matrix lists the value for known cover types of the reference data in the columns and for the classified data in the row (Banko, 1998). From the confusion matrix, four measures of accuracy are estimated overall accuracy, user's accuracy, producer's accuracy, and the Kappa statistics.

3.2.3.2. Image Classification and Post Classification

Image classification mainly comprises supervised and unsupervised types of classification. In this study supervised classification was performed. Supervised classification is the process of the sample of known identity to classify pixels of unknown identity. Samples of known identity are those pixels within training sites. Training sites were developed from the reference data collected to create a signature for each land cover type. The training samples were assigned to individual classes before image classification. The agricultural land with different soil colors was first classified as independent classes. The satellite images were then classified into seven (Built-up area, Forest land, Grassland, Bushland, Barren land, Agricultural land, and Water bod) independent classes.

From the supervised classification methods, maximum likelihood classification algorithm was used to produce the LULC maps.

Classified images were post-processed before assessing classification accuracy and creating LULC maps i.e. by combining classes. To aid image classification using the supervised method, field observation (in October 2018) referencing image information on google earth and previous studies (Alemayehu *et al.*, 2009) were used as a guide for image classification and identification of major LULC.

Table 3. 3 : Description of land use and land cover classes

No.	LULC class	Description	User Code (SWAT Code)
1	Settlement/Urban	Residentials, industrial, transportation/roads, paved areas/way, mixed urban.	STL (URBN)
2	Forest	An area with low to dense trees/woody land	FL (FRST)
3	Shrub/Bushland	Low woody plants with shorter height above ground, with multiple stems	SHL (RNGB)
4	Grassland	Area covered with grass	GL (RNGE)
5	Barren land	The land area of exposed soil/ rocky surface with little or no vegetation	BL (BARR)
6	Agricultural land	Crop field, fallow lands (after harvesting) and bare soil period	AL (AGRL)
7	Waterbody	Rivers, Open water, Lakes, ponds and reservoirs	WB (WATR)

3.2.4. Extent, net change, rate of change and swap

Post classification method was performed for change detection, which requires the comparison of independently produced classified images (Singh, 1989). The post-classification method doesn't need data normalization between two dates. The change detection was performed using a combine tool which is a built-in function in ArcGIS 10.5 and Microsoft Excel. "From to" table extracted from two different LULC maps of different dates were exported to Excel to compute transition of one category to another, Gain, loss, swap and net change in each land cover type using pivot table function.

The computed transition matrix consists of rows that show category at initial state and column that display category at the final state. Gain, loss, and persistence were computed using the method outlined in (Braimoh, 2006). A gain in land covers i between timeline 1 and 2 refers to an increase in the extent of a land cover type i within a period. It was computed using the equation (4.1):

$$g = p_{+J} - P_{JJ} \qquad 4.1$$

where;

P_{+j} = column total of cover type j

p_{jj} = persistence of cover type j of the transition matrix

Loss (l) in a land cover "i" between timeline 1 and 2 is a decrease in the extent of a land cover type "i" within the period. It's computed using equation (4.2.):

$$\mathbf{L = P_{i+} - P_{ii}} \qquad \mathbf{4.2}$$

where;

p_{i+} = the row total of cover type i

p_{ii} = the persistence of cover type i of the transition matrix

The persistence indices from Braimoh (2006) were used to assess the vulnerability of LULC classes to transition in terms of gain and loss. Loss-to-Persistence ratio (Loss/Persistence) denoted by lp indicates the higher tendency of land cover transition to other categories than persistence when the value of lp is greater than one. Likewise, the value of the gain-to-persistence ratio (gain/persistence) denoted by gp greater than one indicates more gain than persistence.

Swap is the change in location between two autonomously classified maps from images of two different dates (Braimoh, 2006, Pontius Jr *et al.*, 2004).

Net change is the difference in the area between two independently classified maps from images of two different dates. Net change can only give change in quantity between time 1 and 2 yet, swap gives the detail of where the change has been occurred and simultaneous gain and loss of a category on the landscape. The amount of net change (Dj), swap (Sj) and total change (Cj) were computed using the following equation:

$$Dj = |gj - lj| \quad 4.3$$

$$Sj = 2 * MIN(pi + - pii, p + j - pjj) or\ 2 * MIN(l, g) \quad 4.4$$

$$Cj = Dj + Sj \quad 4.6$$

Where;

gj is gain of cover type j; lj is loss of cover type j; Pjj is persistence of cover type j; pi+ is row total of cover type i; p+j is column total of cover type j; Dj is net change of cover type j; Sj is swap of cover type j; Cj is total change of cover type j.

3.2.5. Hydrological Modeling

The Soil and Water Assessment Tool (SWAT) model was used for hydrological modeling component of this study. SWAT is an open-source code, physically based, a semi-distributed model with a large and growing number of model applications in a variety of studies (Arnold *et al.*, 2012, Neitsch *et al.*, 2011). It evaluates the impact of LULC and climate change on water resources in a basin with varying soil, land use and management practices over a period of time (Arnold *et al.*, 2012). This physically-based hydrological model allows a number of different physical processes to be simulated in a basin (watershed) and simulation is done in two separate divisions; those are the land phase and routing phase of the hydrologic cycle (Neitsch *et al.*, 2011).

In SWAT, the watershed (catchment) is divided into a variety of sub-basins, which are further separated into hydrological response units (HRUs) consisting of homogenous land use management, soil, and slope (Arnold *et al.*, 2012). HRUs are the smallest unit of the watershed in which essential hydrological components such as evapotranspiration, surface and peak runoff, groundwater flow and sediment yield can be estimated. The driving force behind all the process calculated in the SWAT model is the water balance equation: which is;

$$SWt = SWo + \sum_{i=1}^{t} (Rday - Qsurf - Ea - Wseep - Qgw) \qquad 4.7$$

Where SWt is the final soil water content (mm H20), SWo is the initial soil water content on day i (mm H20), t is the time (days), Rday is the amount of precipitation on day i (mm H20), Qsurf is the amount of surface runoff on day i (mm H20), Ea is the amount of evapotranspiration on day i (mm H2O), Wseep is the amount of water entering the vadose zone from the profile on day i (mm H20), and Qgw is the amount of return flow on day i(mm H20).

SWAT calculates run-off separately for each HRU and route to obtain the total run-off for the basin using the soil conservation (SCS) curve number (CN) method (USDA, 1972) and green and Ampt infiltration methods. The CN method was used in this study because of its ability to use daily input data (Arnold *et al.*, 2012, Neitsch *et al.*, 2011, Setegn *et al.*, 2006) or in other cases the Green and Ampt infiltration method uses the sub-daily scale data which is not available for this study area. The evapotranspiration was calculated using the Penn-man Monteith method (Allen *et al.*, 1989, Monteith, 1965). This study focuses on the effect of LULC and climate change on the hydrologic regime of the basin which includes outflow and change in storage. Precipitation is the main inflow, whereas evapotranspiration (Et), surface run-off (Qs), later flow (Ql) and base flow (Qb) are the outflows. For more description of the SWAT model, one may refer to SWAT theoretical documentation and chapter two of this thesis, the reference also made to Neitsch *et al.* (2011).

3.2.6. Model Input

3.2.6.1. Digital Elevation Model

The Digital Elevation Model (DEM) used in the study was obtained from the Shuttle Radar Topography Mission (SRTM) website (National Aeronautics and Space Administration (NASA)/USGS). Shuttle Radar Topography Mission (SRTM) Global Digital Elevation Model (GDEM) with a resolution of 30m*30m was accessed free of charge from the United State Geological Survey (USGS) center via http://earthexplorer.usgs.gov/ , to identify the watershed, each sub-basin and to analyze terrain parameters (slope length and slope gradient) and stream network characteristics (Length, width and slope). Arc SWAT allows the users to delineate the boundary of the watershed and sub-basins by watershed delineator tool using the Digital Elevation Model (DEM) as input data.

3.2.6.2. Soil Data

Soil is another major input of the SWAT model. The Food and Agricultural Organization – Harmonized World Soil Database (FAO-HWSD) with a spatial scale of 900m was used for this study. The soil parameters required for SWAT was obtained from FAO-HWSD except for some parameters (Hydrologic soil group (HYDGRP), Soil Available Water Content (SWC), Soil Albedo (SOL_ALB), USLE_K) which were absent in database was estimated using Soil-Plant-Air-Water (SPAW) tool and SWAT-user soil-template. There are 13 major soil types in the study area (Table 3. 1).

3.2.6.3. Land Use Data

Land use data in raster format for the three-time period (1992,2002 and 2015) were obtained Landsat as discussed earlier. Land use data is another input of the SWAT model that helps to divide the area into HRUs. Land cover data of the area were prepared using an image of TM and Landsat 8 accessed free of charge from the USGS center via http://earthexplorer.usgs.gov/. A lookup table that identifies the four-letter SWAT code for the different categories of LULC was prepared to associate grid value with the SWAT user land use database.

3.2.6.4. Hydrometeorological Data

Hydrometeorological data required for site descriptions, model setup, calibration and validation originated upon the request from the Ethiopian Ministry of Water, Electricity and Irrigation, and Ethiopian National Meteorological Agency. SWAT requires daily precipitation (PCP), Maximum and Minimum Temperature (TMP), Relative Humidity (RHM), Wind Speed (WND) and Solar Radiation (SLR). Value for meteorological data may be read from records of observed data or generated using weather generator. The daily data of 30 years (1988-2017) for 16 stations were collected from the National Meteorological Agency (NMA) for the detail of meteorological data see Appendix Table 1.

The collected meteorological data have missing values. The precipitation and temperature data with missing values were filled using the method mentioned in the next section. Since SWAT uses a weather generator called WGEN which treats the missing values with -99, all other elements other than PCP and TMP were treated with this tool.

SWAT-WEATHERDATABASE- version01803 was used to calculate the weather station statistics needed to create user weather station files for SWAT.

Arc SWAT needs daily solar radiation; unfortunately, the data acquired from NMA is a sunshine hour. Therefore, converting sunshine hour to solar radiation is necessary because SWAT requires solar radiation as input.

The daily mean of solar radiation was calculated from sunshine hour using eqn. (4.8) described by (Ahmed *et al.*, 2009; Medugu and Yakubu, 2011; Prescott, 1940):

$$H = H_0 \left[a + b\frac{n}{N}\right] \qquad 4.8$$

Where

H is daily mean value of solar radiation (MJ/m^{2}day), N is the daily average value of day length, a and b values are regression constant dependent on location and site's climatic conditions and for Ethiopia the suggested values are α = 0.29 and b = 0.50 (Bayou and Assefa, 1989); the value

is also applied for this study, N is the maximum daily bright hours of sunshine assuming no obstruction in the horizon, and n/N is the percent possible sunshine (relative sunshine duration). H_o is monthly mean values of extraterrestrial radiation (MJ/m^{2}day), n is the monthly average of daily hours of bright sunshine calculated using eqn. (4.8.1.) described by (Ahmed *et al.*, 2009, Medugu and Yakubu, 2011, Prescott, 1940):

$$Ho = \frac{24 * 3600}{\pi} * 4.9212 * E_0 \left[\cos(\varphi)\cos(\delta)\sin(\omega_s) + \frac{\pi\omega_s}{180}\sin(\varphi)\sin(\delta)\right] \quad 4.9$$

Where Eo is the eccentricity correction and estimated using Eqn. (4.10)

$$E_0 = 1 + 0.033\cos\left(\frac{360n_d}{365}\right) \quad 4.10$$

Where n_d is the day of the year/Julian day (1st Jan, n_d =1 and 31st December, n_d = 365), φ is the latitude of the site, $\boldsymbol{\delta}$ is the solar declination and, ω_s is the mean sunset hour angle for the given month. The solar declination ($\boldsymbol{\delta}$)and the mean sunset hour angle (ω_s) can be computed as suggested by DuffieBeckman (2013):

$$\delta = 23.45sin\left[360\frac{284+n_d}{365}\right] \quad 4.11$$

And

$$\omega_s = \cos^{-1}(-tan\varphi tan\delta) \quad 4.12$$

For a given day, the maximum possible sunshine duration (monthly values of the day length, (N) can be computed using:

$$N = \frac{2}{15}\omega_s \quad 4.13$$

3.2.6.5. Meteorological Data Quality Control

Before using the rainfall record of any station, it's necessary to check the continuity and consistency of the data set. The continuity of the record may be broken with missing data due to many reasons such as damage or fault in a rain-gauge during a period.

Checking for the inconsistency of record was done by the double mass curve technique (Subramanya, 2013) for this study. The double mass curve is a simple, visual and practical method, and it is widely used in the study of the consistency and long-term trend test of hydrometeorological data (Gao *et al.*, 2011). The theory of the double-mass curve is based on the fact that a plot of two accumulative quantities during the same period exhibits a straight line so long as the proportionality between the two remains unchanged, and the slope of the line represents the proportionality. The accumulated totals of the gauge in question were compared with the corresponding totals for a representative group of nearby gauges. So that, data gap checking, wrong record, negative values and non-dated data recordings which can affect data quality were checked before used for analysis. These data should be consistent and homogeneous when they are to be used for simulation of the hydrological system.

Woldesenbet *et al.* (2017a) made a comparison of four methods of data gap filling (normal ratio method, the modified normal ratio method, the coefficient of correlation weighting method and inverse distance weighting method) and reports the coefficient of correlation weighting method outperforms the left three methods for filling rainfall and minimum and maximum temperature.

For this study the R climatol package (https://CRAN.R-project.org/package=climatol) which contains the function of quality control, homogenization, outliers removals and infilling of the missing data in a set of series of any climatic variables. The detail of these methodologies can be seen in the work by (Aguilar *et al.*, 2003, Peterson *et al.*, 1998). For this study, the quality control of Rainfall and Temperature data were done by using the R package "climatol" which could be installed in R software. The climatol package categorize stations based on the location, elevation, and distance from each other or mostly the station within 100km are categorized into a similar category and the missed value is filled using the coefficient of correlation method.

For the homogeneity test, the climatol package uses the Standard Normal Homogeneity Test or SNHT (Alexandersson, 1986). For more detail please review the climatol documentation by Guijarro (2018).

3.2.6.6. Discharge data

The daily streamflow (discharge) data of 1994-2015 at the outlet (Tekeze near Shiraro and Near Embamadre) were collected from the Tekeze-Athbara project and Ministry of Water, Irrigation and Electricity (MOWIE).

3.2.6.7. Climatic Data and its Processing

In this study, the dynamically downscaled output of one GCMs from CMIP5 (Coupled Model Inter-comparison Project Phase 5) was employed. The CMIP5 GCM has different ensemble members (r1, r2, r3, etc.) and differs only in initial conditions around 1850, but the physics and greenhouse gas forcing is the same. For the simulation in this study, since different versions of the same model often exhibit similarities, only the first member from the GCMs was used, one ensemble member per model to avoid model bias. The utilized ensemble was r1i1p1, where, r, i and p represents the realization, initialization method indicator and perturbed physics ensemble, respectively. The GCM model used in this study is HadGEM2-ES (Hadley Global Environment Model 2 - Earth System). HadGEM2-ES is a coupled Earth System Model that was used by the Met Office Hadley Centre for the CMIP5 centennial simulations in the UK. HadGEM2 is a configuration of the Met Office Unified Model (UM) developed from UM version 6.6. HadGEM2-ES was the first Met Office Hadley Centre model to include Earth system components as standard.

The downscaling was accomplished by COSMO-CLM or CCLM4 (Consortium for Small Scale Modeling (COSMO) Climate Limited Area Model). For the detail description of the CCLM4 model, reference is made to Panitz *et al.* (2014).

Spatially, the CCLM4 simulations cover the CORDEX-Africa domain at a resolution of 0.44^0 x 0.44^0 (~50km x50km) for the period of 1951-2100 time period which is divided into: historical (1951-2005) and scenario (2006-2100) periods.

CORDEX-Africa Prioritizes the RCP4.5 and RCP8.5 scenarios following the priority by CMIP5.

In this study the Climate model selection was based on the study by Tesfaye *et al.,* (2019) over Tekeze basin and Hussein S. et al., 2013 over East Africa. Hussein S. et al., 2013 evaluated performance of 10 CORDEX-Africa RCMs over East Africa and reported; apart from REMO and CCLM most of the model showed bias under wet and dry season. Tesfaye et al., 2019 made a comparison of 30 GCM models outputs. Their report implies, CanESM2 and HadGEM2-ES performed best in terms of the correlation coefficient between gauged and simulated rainfall amounts. Accordingly, the researcher selects the data from HadGEM2-ES which was downscaled by the regional climate model of CCLM4 purposely assuming that both of the model will produce a result which is near to each other.

Therefore, for the climate scenarios, the daily inputs of precipitation and temperature (maximum and minimum) were obtained from downscaled projections for two representative concentration pathways (RCP 4.5 and RCP 8.5) of the CORDEX_Africa domain. The researcher selects these two RCPs to compare their results because the RCP4.5 works under the policy of ambitious emission reduction while RCP8.5 works under the policy without any control on emission. The future scenario was made only up to 2040 years (near future) in this study and the impact was analyzed per decades. This is due to the uncertainty in the future LULC changes. For this specific study, no future LULC projection was made. The current/existing LULC was assumed to be the same for the coming two decades (up to 2040). The data from NMA was used as a reference data and bias correction of the RCM data sets. The climate data (both precipitation and temperature) for the year of 1988-2040 was selected for the analysis. This was based on the data obtained from NMA with the starting year of 1988 which was highlighted earlier. The RCMs climate data obtained from CORDEX-Africa is in a NetCDF (Network Common Data Form) format with a rotated pole (rotated longitude and latitude). And the unit of the elements (precipitation and temperature) is $kg/m^2/s$ and Kelvin respectively. Therefore, there is a need for correcting the rotated pole and units before using the data in any hydrological impact analysis.

To do this, the Climate Data Operator (CDO) software was utilized. CDO is a collection of many operators for the standard processing of climate and forecast model data. The operators include simple statistical and arithmetic functions, data selection and subsampling tools, and spatial interpolations. The rotated pole was corrected using CDO. In the case of unit conversions, the kg per square meter is assumed as equivalent to mm.

Therefore, to obtain mm/day the given data was multiplied by 86400 (24 * 60* 60) conversion factor. For the conversion of Kelvin to Celsius, the conversion factor (273.15) was subtracted from the given data. More information about the measurement and unit conversion of rainfall can be found in "basic documents No.2", Technical regulations by the World Meteorological Organization (WMO) or see the link: http://www.wmo.int. For the detail of how CDO works the reference was made to (Kaspar *et al.*, 2010, Schulzweida *et al.*, 2009).

3.2.7. Model Setup

3.2.7.1. Watershed Delineation

The SWAT model setup can be done using the ArcSWAT tool in ArcGIS environment. Digital Elevation Model (DEM) with 30m*30m resolution was used for watershed delineation. DEM was projected from its arbitrary coordinate system into a map projection (Geographic coordinate system with UTM projection (WGS_1984_UTM_ZONE_37). The manual mask was performed so as to include only the area of interest and to reduce the time of processing for delineating watershed. DEM-based stream definition was used to define flow direction and accumulation with a minimum threshold of 100000 ha and manually edited. As a result, the 30 watersheds were produced for the study area.

3.2.7.2. Hydrological Response Unit

After watershed delineation, the determination of HRUs for the whole sub-basin was executed. HRU is a unique combination of land use, soil, and slope classes. HRU uses these inputs to subdivide sub-basin into HRUs. All datasets were projected to map projection coordinate system (WGS_1984_UTM_ZONE_37). The lookup table was prepared both for land use/land cover and soil to link with the SWAT database.

Multiple HRU definition option was used to define the threshold level for land use, soil and slope. The threshold definitions can be based on the function of the project and the aim of the modeler to achieve the desired objectives. As a result, the threshold level of 2% land use, 10% soil and 20% slope were adopted and about 550 HRU were identified.

3.2.7.3. Weather data definition

The last step in the model setup is writing all climatic variables (Precipitation, Temperature, Humidity, Solar radiation, and Wind) required by SWAT. All climatic variables were prepared in text (.txt) format using SWAT-WEATHERDATABASE- version01803. The variables were uploaded with their respective station locations.

3.2.7.4. SWAT Simulation

To undertake the simulations of the result, the climate data was split into the decades, with the first decades starting in the 1990s. Accordingly, the researcher classified the climate data of 1988-2040 into three (3) categories 1990s and 2000s (Past), 2010s (current), 2020s and 2030s (future). Therefore, the results reported in this paper were based on the decadal analysis.

In this study, four different scenarios were adopted for SWAT simulation. The first three scenarios are dealt with the changes occurred on hydrology in the current and past two decades due to climate and LULC changes (the 2010s, 2000s, and 1990s) respectively. The last scenario dealt with the impact of future climate change on hydrology or in this case the projection is made up to 20 years from now. To achieve this the simulation period (1988-2040) was divided into four periods. The first period (1988-1999) was treated as a baseline period and 2000-2009 and 2010-2019 were used as the changing periods and 2020-2030 and 2031-2040 were used as future projection. The LULC map of 1992, 2002, 2015 and 2015 produced from Landsat images were used to represent the LULC patterns of the 1990s (1988-1999), 2000s (2000-2009), 2010s (2010-2019) and 2020s (2020-2040) respectively (Table 3.4). Therefore, the difference between the scenarios represents the change occurred either due to land use or climate change alone or the combined impacts of both (changes of both climate and LULC at the same time).

The first scenario (S1) is simulations to analyze the individual effect of LULC changes to achieve the second objective and to give the direction for the third objective. To achieve this the similar climate data of the 1990s (1988-1999) with LULC maps of 1992, 2002 and 2015 was used separately. Then the model was run separately for the three distinct LULC maps with constant climate data. First, the model was calibrated for the baseline period (the 1990s) using the LULC map of 1992 and climate data of the 1990s (1988-1999), then the same calibrated parameters were applied for the changing period (2000s and 2010s).

The second scenario (S2) works in a similar way as the first scenario however the simulation is set to analyze the separate effect of climate change. To do this the model again runs three times the same as in the first scenario but with constant LULC (the 1990s or 1992) in this case with different climate data (1990s, 2000s, and 2010s).

The third scenario (S3) is simulations to attribute changes in the hydrologic regime to combined LULC and climate change. The simulation represents the hydrology affected by the combination of both LULC and climate change simultaneously. In this case, land use and climate were in the same period for each model run as indicated in Table 3.4 or both climate and LULC were changing for the three-model run.

The fourth scenario (S4) is simulations made to attribute the effect of future climate change. This was made only for future climate change assuming the LULC of the current time unchanged. In this case, climate data of 20 years from the current year onwards was used. Then the data was divided into two decades: 2020s (2020-2029) and 2030s (2030-2039). To achieve this the climate data of the 2020s and 2030s was run keeping the LULC constant (2015 or current LULC). This was done by assuming no changes happen in LULC for the coming two decades.

Table 3. 4 : Scenario set to analyze the combined and individual effect of climate and LULC change on the hydrologic regime (Both RCP4.5 and 8.5).

Scenario	Combined effect of climate and LULCC		Separate effect of LULC change		Separate impacts of Climate changes	
	Climate data	LULC map	Climate data	LULC map	Climate data	LULC map
S1	1990s	1992	1990s	1992	1990s	1992
S2	2000s	2002	1990s	2002	2000s	1992
S3	2010s	2015	1990s	2015	2010s	1992
Future climate scenario						
S4					2020s	2015
					2030s	2015

3.2.7.5. Sensitivity Analysis

Sensitivity analysis is the process of determining the rate of change in model output with respect to changes in model parameters (Arnold *et al.*, 2012). It helps to select the parameter having a high effect on the simulation output and/or to reduce the number of parameters so that it's easy to achieve the desired result.

The sensitivity analysis was performed using SWAT-CUP, the interface developed for the SWAT. As a result, the Sequential Uncertainty Fitting version 2 (SUFI-2) which is a built-in program of SWAT-CUP was used to undertake sensitivity analysis.

SWAT-CUP uses Global sensitivity and the One-At-a-Time sensitivity analysis method. Global sensitivity uses the regression system to determine sensitive parameters, which regress the Latin hypercube generated parameters against the objective function values. The t-stat and p-value are used to get a sensitive parameter. The t-stat is the coefficient of parameter divided by its standard error. If a coefficient large compared to its standard error, it's probably different from 0 and the parameter is sensitive. The p-value for each term tests the null hypothesis that the coefficient is equal to zero. The parameter with a low p-value (<0.05) indicates high sensitivity. The requirement for a large number of simulations is the drawback of Global sensitivity (Arnold *et al.*, 2012). One-At-a-Time shows the sensitivity of a variable to the changes in the parameter if all other parameters are kept constant at some value. The difficulty of knowing the value of those other constant parameters is the limitation of this method. In this study, the global

sensitivity analysis method was used to select sensitive parameters. The sensitivity analysis was performed on twenty-seven (27) hydrological parameters (Table4.5).

3.2.7.6. Model Calibration

Calibration is a major aspect of hydrological modeling which intended to fit the simulated outputs of the model to the recorded streamflow data of the watershed by adjusting the model parameters, thereby reducing the prediction uncertainty. The calibration method is categorized into three (manual trial and error, automatic and combination of both) based on Refsgaard (1997). The manual trial and error method is adjusting model input parameter values manually that within a certain range to fit simulated output with observed streamflow data. The combination of both manual and automatic or numerical parameter optimization method were used in this study for the calibration of 1994-1999 as indicated in Table 3.5. The detail of the warming up period, calibration and validation period is presented in Table 3.5. To perform manual trial-and-error method the usual approach was used: SWAT runs to perform simulation; compare measured and simulated values; analyze whether reasonable results achieved; if not, adjust input parameters based expert judgment and other guidance within reasonable parameter value ranges; and loops the process until the sound result obtained.

In this study, statistical values for acceptable calibration were considered based on Moriasi *et al.* (2015), acceptable calibration value of $r^2 > 0.6$ and NSE > 0.5 on the monthly time step.

3.2.7.7. Model Validation

Model validation is the process of testing a given site-specific model performance of the calibrated model parameter set against an independent set of measured data (Refsgaard, 1997). For this study validation was performed using parameters that were determined during the calibration process, and comparing the predictions to observed data not used for calibration was executed. For the validation, streamflow data for the period of 2004-2009 were used as indicated in Table 3.5.

Table 3. 5 : The summary of data used for model calibration and validation.

Periods	Baseline period
Warming up period	1988-1993
Calibration period	1994-1999
Validation	2004-2009

3.2.7.8. Model Performance Evaluation

Model performance was performed by SWAT-CUP using statistical measures to assess the extent of its accuracy and consistency. For this study, Coefficient determination (r^2), Nash-Sutcliffe simulation efficiency (NSE) and Percent of bias (PBIAS). The coefficient of determination is an indicator of the strength of the relationship between the observed and simulated values. The closer the value of r^2 to one implies a higher agreement between the simulated and observed flow (Singh *et al.*, 2005). The equation 4.9 depicts how it works:

$$R^2 = \frac{[\sum(Qm,i-\overline{Q_m})\,(Qs,i-\overline{Q_m})\,]^2}{\sum(Qm,i-\overline{Q_m})\text{^}2\;\;(Qs,i-\overline{Q_m})^2} \qquad 4.9$$

Where Q is a discharge, and m and s stands for measured and simulated respectively, i is the i^{th} measured or simulated data and the bar stands for average.

The Nush-Sutcliffe simulation efficiency (NSE) indicates how well the plots of observed and simulated value fits. When the value of NSE is 1, the simulated value is the same as observed. When the value is between 0 and 1, it indicates the deviations between observed and simulated data. If the value of NSE is negative, predictions are very poor, and the average value of output is a better estimate than predictions (Nash and Sutcliffe, 1970). It's calculated using eqn. 4.10:

$$NSE = 1 - \frac{\sum(Qm-Qs)i^2}{\sum(Qm,i-\bar{Q}_m)^2} \qquad 4.10$$

Where Q is a discharge, and m and s stand for measured and simulated flow respectively, and the bar stands for average.

The Percent Bias (PBIAS) measures the average tendency of the simulated data to be larger or smaller than their observed counterparts Gupta *et al.* (1999). The optimal value of PBIAS is 0.0, with low-magnitude values indicating accurate model estimation. Positive values indicate model underestimation bias, and negative values indicate model overestimation bias Gupta *et al.* (1999). PBIAS is calculated with eqn. 4.11:

$$PBIAS = \frac{\sum_{i=1}^{n}(Qm,i - Qs,i) * 100}{\sum_{i=1}^{n}(Qm,i)} \qquad 4.11$$

Table 3. 6 : performance evaluations for the monthly time step. (Moriasi et al., 2015).

Performance Rating	NSE	R^2	PBIAS
Very good	0.75<NSE≤1	0.7< R^2≤1	PBIAS< ± 10
Good	0.65<NSE≤0.75	0.6<R^2≤0.7	±10≤PBIAS< ± 15
Satisfactory	0.5<NSE≤0.65	0.5<R^2≤0.6	±15≤PBIAS< ± 25
Unsatisfactory	NSE≤0.5	R^2≤0.5	PBIAS≥ ±25

3.3.A Framework of the Study

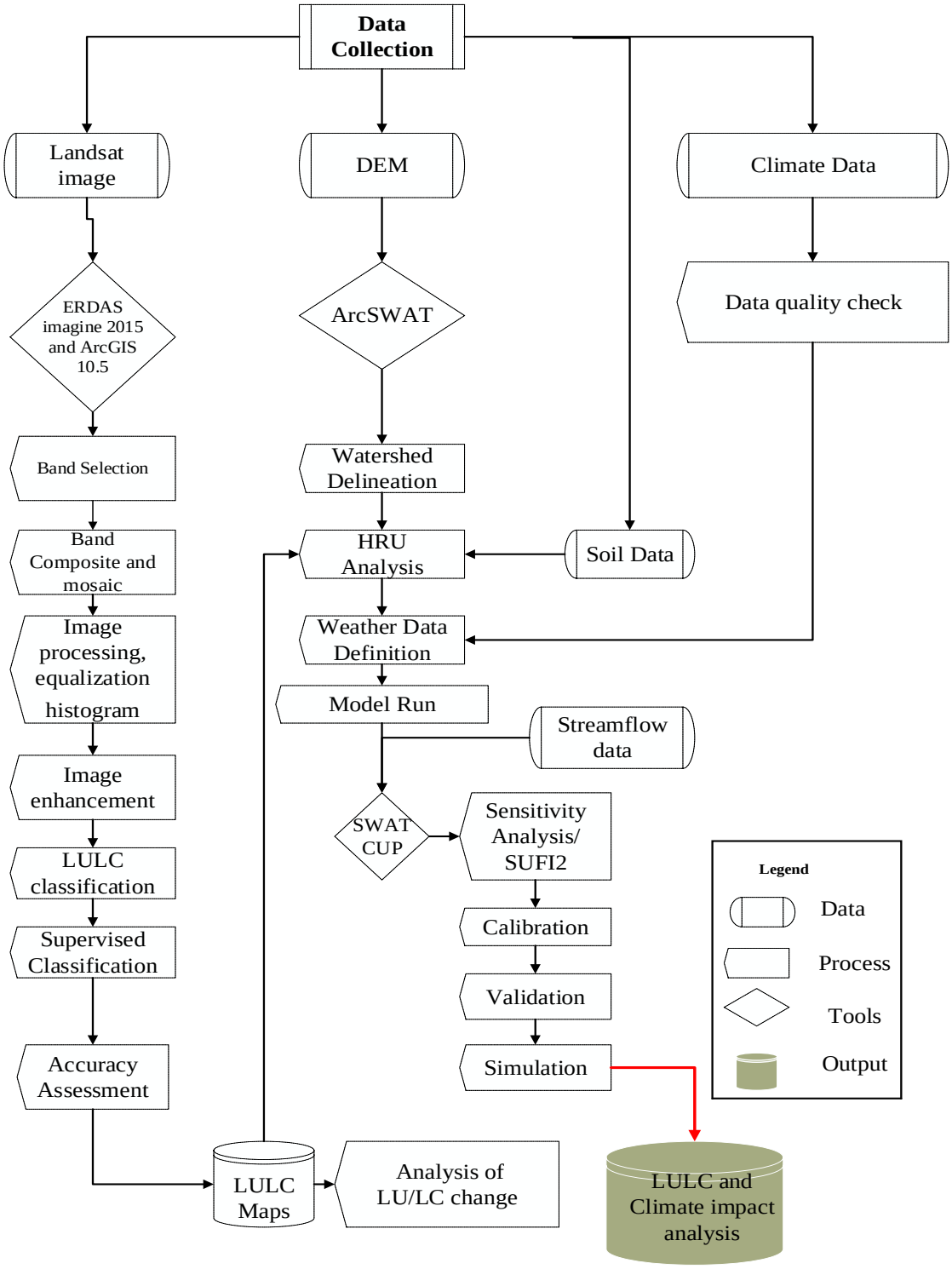

Figure 3. 7 : Framework of the research

CHAPTER FOUR

4. RESULT AND DISCUSSION

4.1.Land Use Land Cover Classification Accuracy Assessment

The accuracy of the classified images of 2015 was assessed using 562 ground truth points collected from field surveys as discussed in the methodology part. Using these reference data and classified maps, confusion (error) matrix was constructed. The confusion matrix report (Table 4.1) describes that about 95.2% overall accuracy and 94.35 Kappa coefficient values were attained for the classified map of 2015. According to CongaltonGreen (2009), the above results represent a strong agreement between the ground truth and classified images and accepted for the subsequent analysis and change detection.

Table 4. 1 : Confusion Matrix for the 2015 Classification Map

Class	**STL**	**FL**	**SHL**	**GL**	**BL**	**AL**	**WB**	**Ground truth Total**	**User's Accuracy (%)**
STL	70	0	1	0	2	0	0	73	95.89
FL	0	75	2	1	0	2	0	80	93.75
SHL	0	1	68	1	0	0	0	70	97.14
GL	0	1	1	84	0	2	0	88	95.45
BL	0	0	0	0	58	2	0	60	96.67
AL	0	3	4	2	1	110	1	121	90.91
WB	0	0	0	0	0	0	70	70	100.00
Column Total	70	80	76	88	61	116	71	562	
Producer's Accuracy (%)	100.00	93.75	89.47	95.45	95.08	94.83	98.59		

NB: Overall Accuracy = 95.2% and Kappa Coefficient = 94.35

4.2.Land Use/Land Cover Maps

The spatial analysis was conducted using approaches adopted in the methodology, and the land use land cover (LULC) maps of the Upper Tekeze River Basin were generated for three years (1992, 2002 and 20015). The change detections and analyses were done for two separate periods (1992-2002 or period 1 and 2002-2015 or period 2).

The seven major LULC classes were developed (namely: Built-up (BU), Forest Land (FL), Shrub/bushland (SHL), Grassland (GL), Bare Land (BL), Agricultural Land (AL) and Water Body (WB)). Figures 4.1, 4.2 and 4.3 show the classified maps of 1992, 2002 and 2015 respectively.

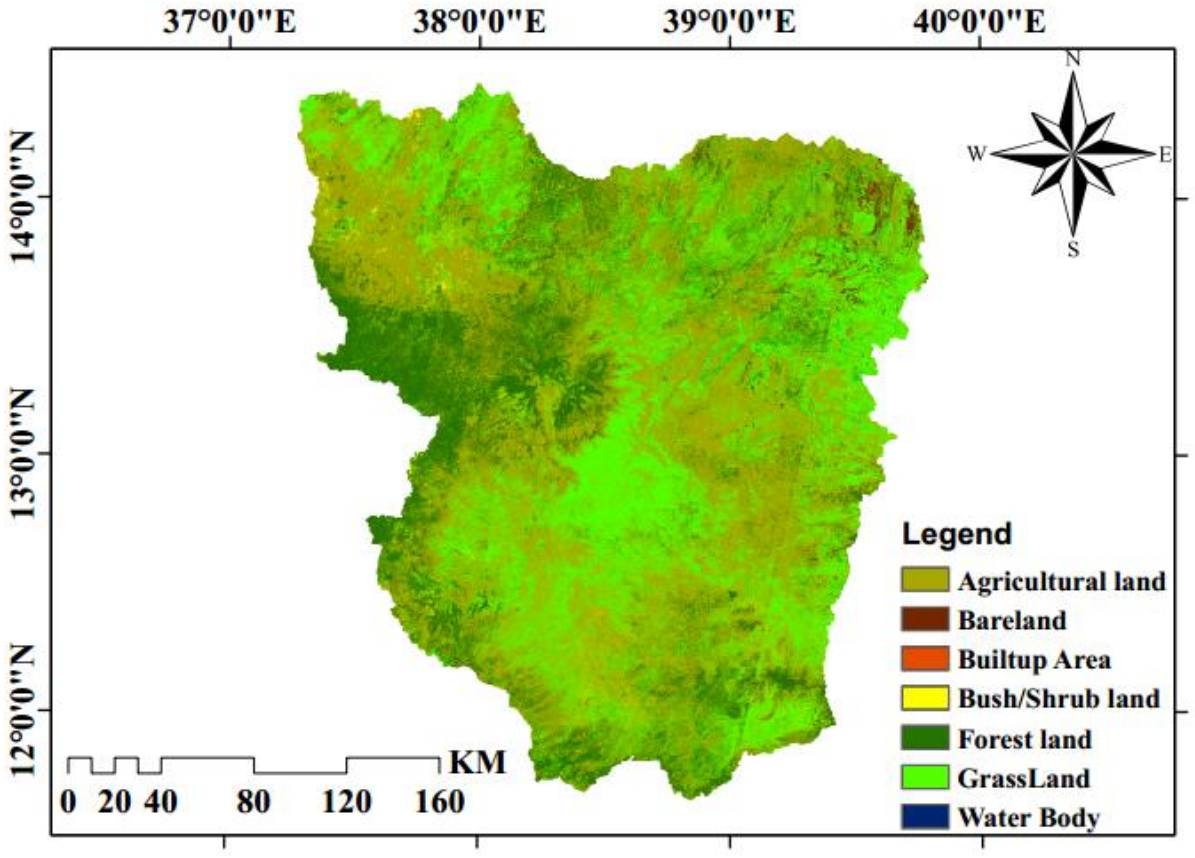

Figure 4. 1 : LULC maps of 1992

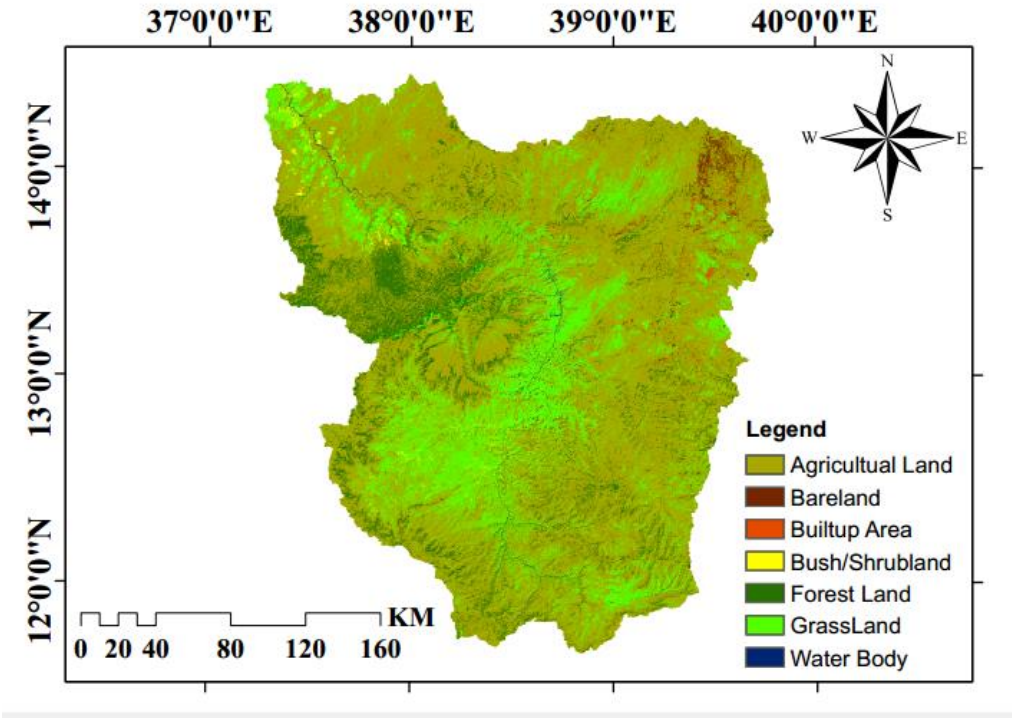

Figure 4. 2 : LULC maps of 2002

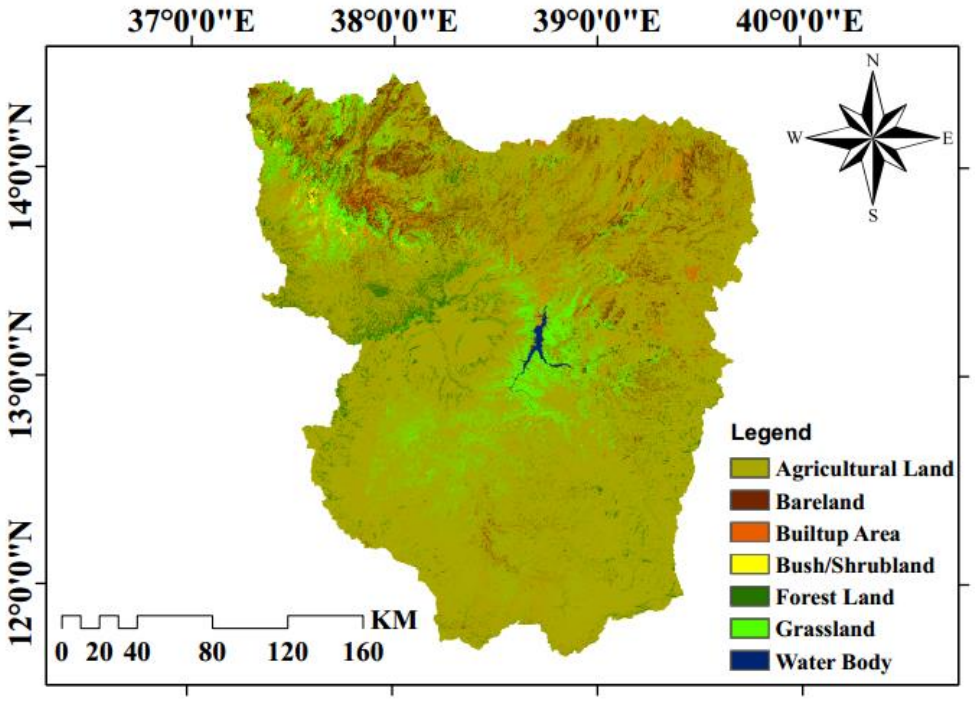

Figure 4. 3 : LULC maps of 2015

4.3.Extent and Rate of Land Use Land Cover Change

4.3.1. Gross Gains, Gross Losses and Persistence

Figure 4.4 indicates area coverage (Percentages) of each land use during the study period (1988-20017). Initially (1992) Agricultural land and Grassland were the dominant LULC classes in comparison to another LULC class constituting 43.78% and 31.88% respectively. The two LULC classes (Agricultural land and Grassland) stays dominant throughout the whole study period.

Table 4.2 illustrates the transition of individual land use land cover types from one category to another through both phases (first period or 1992-2002 and second period or 2002-2015). During the first phase the highest gain in agricultural land (~35.94%) and highest lost in Grassland (~25.97%), followed by agricultural land (~22.38%) and forest land (~16.42%) were experienced in the area. In the period 1992-2002 the Agricultural land, Built-up area and Waterbody increase with 13.56%, 1.17%, and 0.28% respectively. The increment in water bodies may be due to soil and water conservation practices in the area and the development of small dams. On the other hand, Barren land, Bushland, Grassland, and Forest land shows the decrement by 0.19%, 0.13%, 9.09%, and 5.60% respectively. The reduction of barren land was insignificant, but it might be related to the reforestation at the watershed level. The significant changes were observed in Agricultural land (increment), Grassland (reduction) and forest land (reduction). During the second period (2002-2015), the highest gain in agricultural land (23.72%), grassland (8.97%) and bare land (7.03), followed by the highest lost in agricultural land (24.01%), grassland (15.82%) and forest land (9.13%) were observed. During the second period, agricultural land shows the relative increment (8.72%) but at a slower rate than the first period. This may be due to the land protection policy of the government. In the same period, bare land and settlement (Built-up) areas were increased at the rate higher than the first period (6.56% and 2.54% respectively). While grassland and forest land show the decline at the rate which exceeds the first period (12.85% and 7.24% respectively).

The diagonal values in Table 4.2 illustrate the percentage of unchanged land use land cover class of both periods. About 32. 35% and 48.50% of the landscape was persisted while, 67.65% and 51.50% were undergone the change in the first and second periods of the study respectively, indicating the change dominates in both periods. This indicates the basin undergone significant LULC changes as compared to the persistency throughout the study period.

Agricultural land, grassland, and forest land contribute to 64.77% of changes during the first period. Similarly, in the year 2002-2015 agricultural land, grassland and forest land contributes to 48.95% of changes occurred in the basin. Based on the persistence indices of Braimoh (2006) the value of gain-to-persistence (gp) ratio exceeding 1 indicates that a LULC experience more gain than persistence, and the value of loss-to-persistence (lp) ratio exceeding 1 implies a higher tendency of transition to other LULC classes than persist. During the period of 1992-2002, the area experiences more gain than persistence because the majority of the classes gp ratio exceeds 1. In this period the lp ratio of shrubland, grassland and forest were exceeding 1which means the classes are more likely to loss than persist.

During the second period, bare land, settlement, and shrubland show a high tendency to gain than persist. Grassland, forest land, shrubland and water body indicate a high tendency to loss than to persist in the period of 2002-2015. As discussed earlier the gp and lp of shrubland and water body during the first and second periods is greater than 1 which implies a tendency to loss or gain rather than persist. During this period (2002-2015), gp and lp of agricultural land were below 1 indicating the tendency to persist instead of gain or loss.

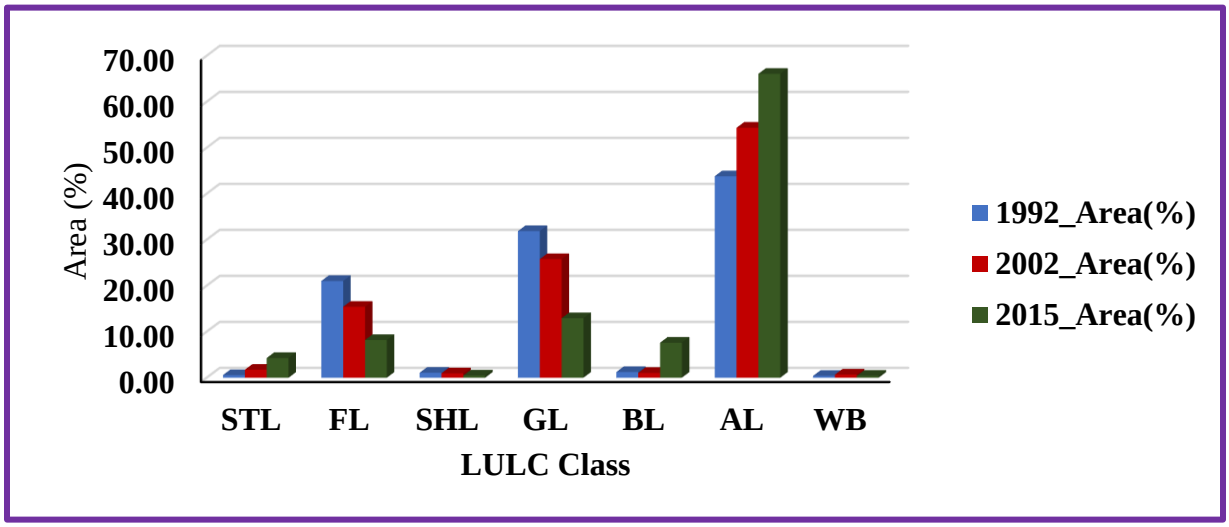

Figure 4. 4 : Percentage area cover comparison of LULC classes of 1992, 2002 and 2015

Table 4. 2 : LULC transition matrix in percentages. (1992-2002 and 2002-2015).

LULC Classes	**STL**	**FL**	**SHL**	**GL**	**BL**	**AL**	**WB**	**1992 Total**	**Loss**
STL	0.02	0.04	0.01	0.11	0.00	0.38	0.01	0.57	0.55
FL	0.09	4.60	0.09	2.29	0.15	13.70	0.09	21.03	16.42
SHL	0.00	0.25	0.04	0.18	0.00	0.59	0.02	1.09	1.05
GL	0.36	1.25	0.43	8.91	0.31	20.26	0.36	31.88	25.97
BL	0.01	0.01	0.00	0.06	0.35	0.81	0.00	1.24	0.89
AL	1.22	9.24	0.39	14.14	0.20	18.41	0.19	43.79	22.38
WB	0.03	0.03	0.00	0.10	0.03	0.21	0.01	0.41	0.40
2002 Total	1.74	15.42	0.96	25.79	1.05	54.35	0.68	100.00	67.65
Gain	**1.72**	**10.82**	**0.92**	**16.88**	**0.70**	**35.94**	**0.67**	**67.65**	
LULC Classes	**STL**	**FL**	**SHL**	**GL**	**BL**	**AL**	**WB**	**2002 Total**	**Loss**
STL	0.17	0.03	0.00	0.02	0.01	0.51	0.01	0.74	**0.57**
FL	0.56	1.29	0.01	0.06	0.07	8.41	0.01	10.42	**9.13**
SHL	0.05	0.01	0.05	0.11	0.04	0.70	0.01	0.96	**0.91**
GL	0.75	0.42	0.11	3.97	1.06	13.24	0.25	19.79	**15.82**
BL	0.04	0.01	0.00	0.02	0.58	0.40	0.00	1.05	**0.47**
AL	2.61	6.43	0.30	8.75	5.86	42.35	0.07	66.36	**24.01**
WB	0.11	0.00	0.02	0.01	0.00	0.45	0.09	0.68	**0.59**
2015 Total	4.28	8.19	0.49	12.94	7.61	66.07	0.43	100.00	51.50
Gain	**4.11**	**6.89**	**0.44**	**8.97**	**7.03**	**23.72**	**0.34**	**51.50**	

4.3.2. Net Change and Swap

Table 4.3 and Table 4.4 reflects the summary of LULC changes in the study area. The basin experienced land cover changes about 82.24% and 80.37% of total landscape changes for the period of 1992-2002 and 2002-2015 respectively. During the period of 1992-2002 agricultural land, grassland and forest land experienced both swap and net changes, while the change in the water body, barren land, shrubland and settlement area was insignificant. In this period agricultural land (50%) experienced a major change in location (swap). This is because of the higher gain of agricultural land from other categories which increases the area coverage. During the period of 2002-2015, even-though the watershed experienced both swap and net changes, the swap change was predominant for agricultural land (47%), grassland (17%) and forestland (13%). The higher swap of agricultural land in this period might related to the land degradation in the area due to agricultural practices in mountains. The swap (1.2%) and net change (3.5%) for settlement were higher in this period than the first period with the net change exceeding the swap change.

Table 4. 3 : Summary of LULC changes in percentages (1992-2002).

LULC class	1992 Total	2002 Total	Loss	Gain	Persistence	Net change	Swap	Total change
STL	0.57	1.74	0.55	1.72	0.02	1.17	1.09	2.26
FL	21.03	15.42	16.42	10.82	4.60	5.60	21.64	27.24
SHL	1.09	0.96	1.05	0.92	0.04	0.13	1.84	1.97
GL	31.88	25.79	22.97	16.88	8.91	6.09	33.77	39.85
BL	1.24	1.05	0.89	0.70	0.35	0.19	1.39	1.59
AL	43.79	54.35	25.38	35.94	18.41	10.56	50.76	61.32
WB	0.41	0.68	0.40	0.67	0.01	0.28	0.79	1.07
Total	100.00	100.00	67.65	67.65	32.35	24.02	111.28	135.30

Table 4. 4 : Summary of LULC changes in percentages (2002-2015)

LULC class	2002 Total	2015 Total	Loss	Gain	Persistence	Net change	Swap	Total change
STL	0.74	4.28	0.57	4.11	0.17	3.54	1.15	4.69
FL	10.42	8.19	9.13	6.89	1.29	2.24	13.79	16.02
SHL	0.96	0.49	0.91	0.44	0.05	0.47	0.88	1.35
GL	19.79	12.94	15.82	8.97	3.97	6.85	17.93	24.78
BL	1.05	7.61	0.47	7.03	0.58	6.56	0.94	7.50
AL	66.36	66.07	24.01	23.72	42.35	0.29	47.44	47.73
WB	0.68	0.43	0.59	0.34	0.09	0.26	0.67	0.93
Total	100	100	51.50	51.50	48.50	20.21	82.79	103.01

4.3.3. Rate of Land Use and Land Cover Change

The annual increment in built-up was 60.43 km^2 during the period of 1992-2002 then it gets higher by 103.19 km^2 during the period of 2002-2015. Initially (1992-2002) the bare land area shows the decrement by 9.88 km^2 annually, on the contrary during the second period (2002-2015), its annual coverage was increased by 266.63 km^2 which implies the high degradation or loss of vegetation and other LULC types annually. Grassland and forest had experienced higher degradation throughout the study period, the decrement in the area of coverage was observed in both categories. The annual rate of decline from 314.66 km^2 in the period of 1992-2002 to 521.99 km^2 in the period of 2002-2015 (Grassland) and 289.68 km^2 in the period of 1992-2015 to 293.88km^2 (forest) in the period of 2002-2015 were experienced.

The annual rate of increase in agricultural land during the first period of study was 636.92 km2 yet during the second period the increment gets slow down and shows about 332.87km2 increment in area per annum.

4.4.Hydrological Modeling

4.4.1. Data Quality Check

Data quality check (consistency, homogeneity, and outliers) of all stations used in this study was tested using the approach discussed under the methodology section. Based on a double mass curve plot analysis, all stations didn't show significant slope change. This indicates the consistency between all stations. Figure 4.5 shows the double mass curve of the Mekelle gauge station based on which the study period was divided and the other stations are listed in the Appendix. Homogeneity of annual rainfall and hydrological data were tested using the method mentioned in the methodology section.

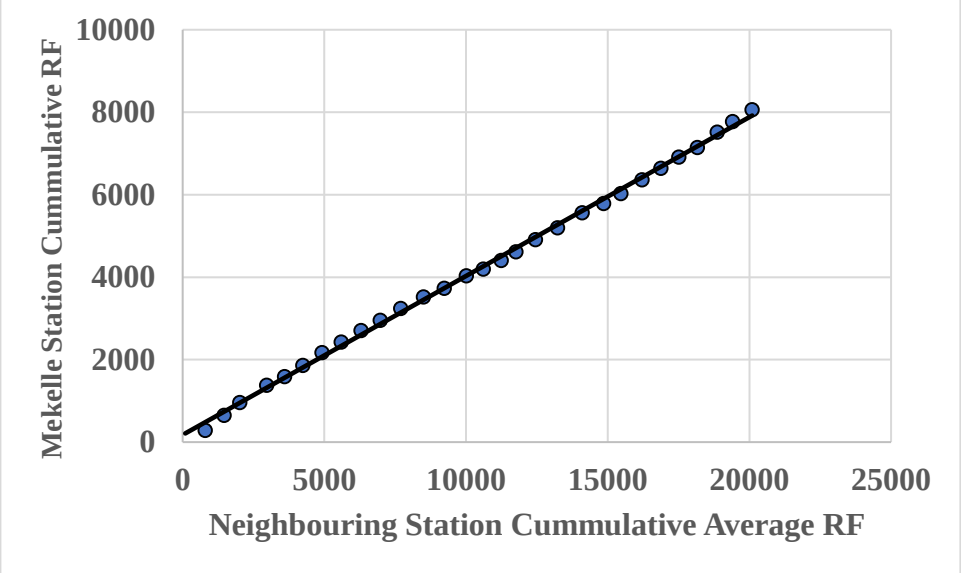

Figure 4. 5 : Mekelle station double mass curve

4.4.2. Sensitivity Analysis

A sensitivity analysis was performed using the method outlined in the methodology section. The sensitivity analysis was performed on 27 (twenty-seven) hydrological parameters (Table 4.5). The simulation number was set to 500 (five hundred) and iterated four times with which the first iteration is used to select the most sensitive parameter.

Accordingly, 9 parameters were selected as the most sensitive parameters out of 27 parameters. Those sensitive parameters (9), in their priority sequence, are presented in Table 4.6.

Table 4. 5 : Parameters used for sensitivity analysis and their descriptions

S. N	Parameters Name (SWAT Code)	Absolute Range (Default Value)		Description
		Max	Min	
1	r__CN2.mgt	-0.25	0.25	SCS runoff curve number
2	v__ALPHA_BF.gw	0	1	Baseflow alpha factor (days)
3	v__GW_DELAY.gw	30	450	Groundwater delay
4	v__GWQMN.gw	0	5000	Threshold depth of water in the shallow aquifer required for return flow to occur (mm)
5	r__SOL_Z().sol	-0.25	0.25	Depth from soil surface to bottom of layer
6	r__SOL_K().sol	-0.25	0.25	Saturated hydraulic conductivity
7	r__SOL_ALB().sol	-0.25	0.25	Organic carbon content
8	r__SOL_AWC().sol	-0.25	0.25	Available water capacity of the soil layer
9	r__SOL_CBN().sol	-0.25	0.25	Organic carbon content
10	r__SOL_BD().sol	-0.25	0.25	Moist bulk density
11	r__USLE_K().sol	-0.25	0.25	USLE equation soil erodibility (K) factor
12	v__ALPHA_BNK.rte	0	1	Baseflow alpha factor for bank storage
13	v__CH_K2.rte	-0.01	500	Effective hydraulic conductivity in main channel alluvium
14	v__CH_S2.rte	-0.01	10	Manning's "n" value for the main channel
15	v__GWHT.gw	0	25	Initial groundwater height (m)
16	v__REVAPMN.gw	0	100	Threshold depth of water in the shallow aquifer for "revap" to occur (mm)
17	v__SHALLST_N.gw	0	5	Initial depth of water in the shallow aquifer (mm)
18	r__BIOMIX.mgt	0	1	Biological mixing efficie
19	v__SURLAG.bsn	0	24	Surface runoff lag time
20	r__OV_N.hru	-0.25	0.25	Manning's "n" value for overland flow
21	v__EPCO.hru	0	1	Plant uptake compensation factor
22	r__ESCO.hru	0	1	Soil evaporation compensation factor
23	v__SLSOIL.hru	0	150	Slope length for lateral subsurface flow
24	v__CANMX.hru	0	100	Maximum canopy storage
25	v__SLSUBBSN.hru	10	150	Average slope length
26	v__CH_N2.rte	0	0.3	Manning's "n" value for the main channel
27	v__GW_REVAP.gw	0.02	0.2	Groundwater "revap" coefficient

R – is the method by which value from SWAT database is multiplied by a given value; V – is the method of replacing the initial parameter by the given value

4.4.3. Model Calibration and Validation

The model calibration and validation were performed as discussed under the methodology section of 3.6.7.4.

With the objective of identifying whether the calibration and validation of the model are required or not, the default simulated output of the model was compared with the recorded streamflow data; the performance of the model was evaluated as well. As a result, Nash Sutcliffe Model Efficiency (NSE) of 0.60, Coefficient of Determination (R^2) of 0.65 and Percent of Bias (PBIAS) of -28 were obtained from default simulation. This implies the statistical measures are under acceptable range. Thus, the need for adjusting the most sensitive parameter is mandatory. After the most sensitive parameters identified in sensitivity analysis, manual calibration was performed before automatic calibration. Figure 4.6 showed the calibration and validation result of monthly streamflow hydrographs. This was again verified by the statistical performance measures of NSE, R^2 and PBIAS as presented in Table 4.7. For the calibration period, the value of NSE, R^2 and PBIAS were 0.84, 0.86 and -6.6 and for the validation period were 0.89, 0.90, and 2.4 respectively. According to the rating of Moriasi *et al.* (2015), the performance of the SWAT model over Upper Tekeze Basin could be categorized as a very good, although underestimation was observed in the base flow simulation.

The final adjusted values of sensitive parameters for three model have described in their sequence order in Table 4.6. A change was observed in some of the parameters, such changes indicates the change of the catchment response behavior. For instance, an increase in the CN2 values in the 2000s and 2010s from -0.227 to 0.1795 and 0.491 as compared to 1990s respectively, indicates the reduction of forest coverage and expansion of agricultural land in the area which is in line with the result of LULC maps.

Table 4. 6 : SWAT model sensitive parameter and their final calibrated values for the three-model run

Rank	**1990s**		**2000s**		**2010s**	
	Parameters	Adjusted value	Parameters	Adjusted value	Parameters	Adjusted value
1	CN2.mgt	-0.22745	CN2.mgt	0.1795	CN2.mgt	0.491
2	ALPHA_BF.gw	0.778	ALPHA_BF.gw	0.766	ALPHA_BF.gw	0.766
3	ALPHA_BNK.rte	0.915	ALPHA_BNK.rte	0.797	ALPHA_BNK.rte	0.798
4	GWQMN.gw	2995	GWQMN.gw	3075	GW_DELAY.gw	68.2
5	ESCO.hru	0.45	CANMX.hru	20.5	GWQMN.gw	3075
6	SOL_AWC.sol	0.06	SOL_AWC.sol	-0.0495	ESCO.hru	0.53
7	CANMX.hru	68.5	ESCO.hru	0.46	SOL_AWC.sol	0.08
8	GW_DELAY.gw	63.18	GW_REVAP.gw	0.1523	CANMX.hru	20.5
9	SURLAG.bsn	20.184	SURLAG.bsn	20.184	SURLAG.bsn	18.02

Table 4. 7 : Statistical performance values of the SWAT model

Period		R2	NSE	PBIAS
	Default calibration	0.65	0.6	-28
1990s	Calibration (1994-1999)	0.86	0.84	-6.6
2000s	Validation (2004-2008)	0.90	0.89	2.4

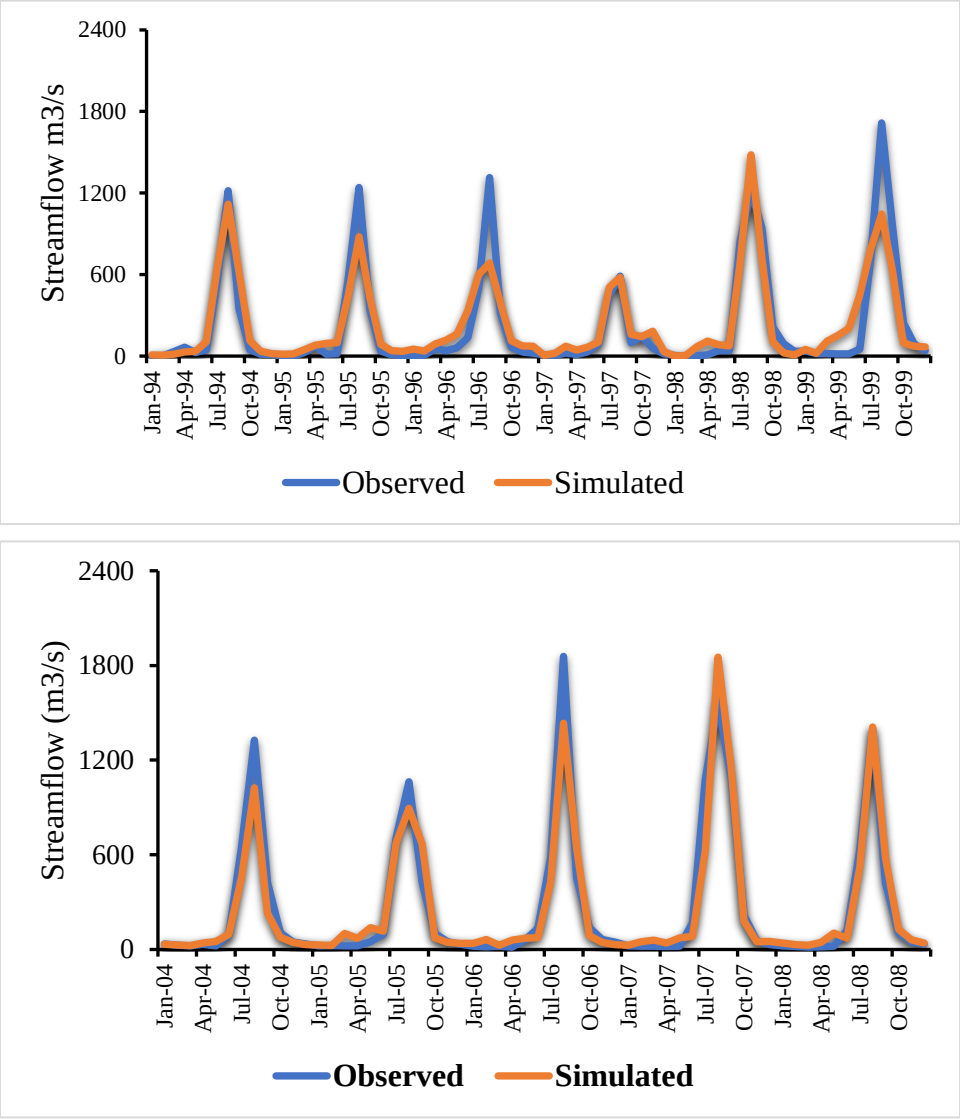

Figure 4. 6 : Calibration and Validation of the SWAT hydrological model (up and down) respectively

4.5.Hydrologic Impact of Climate and Land Cover Change

4.5.1. Impact on Annual Averages of Hydrologic Component

The changes in simulated average annual streamflow, surface runoff, baseflow, Evapotranspiration, and water yield were compared for different scenarios to explore changes of a hydrologic regime (Table4.8, Table4.9, and Table4.10).

4.5.1.1. Separate Impact of LULC Change

Once the SWAT model had been calibrated and validated for the baseline period, the model again runs two times for the altered period. Then the output from three different LULC was compared. This was achieved by keeping the climate data of the 1990s (1988-1999) and calibrated parameter value for 9 sensitive parameters similar while the LULC was changed for all models to identify the individual impact of LULC as expressed by Hassaballah *et al.* (2017). Table 4.8 indicates the annual average hydrologic response to land-use change, with a change ranging from -9 to 14% and -13% to 10% because of the great offset of internal conversions among land use classes under RCP4.5 and RCP8.5 respectively. The streamflow (Qt), surface runoff (Qs) and water yield (WY) were increased, while baseflow (Qb) and evapotranspiration (ET) shows the decrement throughout the study period (RCP4.5). Yet, under RCP8.5 all except ET shows an increment. The streamflow shows the increment of 10.49mm/year (2.06%) and 27.69mm/year (5.26%) in scenario 2 (S2) or 2002 LULC map with 1988-1999 climate and scenario 3 (S3) or 2015 LULC map with 1988-1999 climate respectively from baseline scenario (S1). The Qs also increased by 17.65mm/year (7.11%) and 38.85mm/year (14.42%) during S2 and S3 from the baseline period (S1) respectively. Similarly, WY shows the increment as expressed in table 5.8. On the contrary, ET and Qb show the decrement by 46.49mm (8.66%) and 102.29mm (17.09%) or ET, 7.16mm (2.75%) and 11.16 (4.35%) or Qb in S2 and S3 from S1 respectively. This is due to the reduction in forest and grassland which leads to the reduction in canopy interception and plant transpiration which ultimately reduces evapotranspiration. On the other hand, expansion in agricultural land and reduction in forest land affect the properties of topsoil that cause a lower permeability and less infiltration; as a result, a fraction of precipitation converted to surface runoff is increased while the fraction of baseflow is getting reduced. This result is in line with Woldesenbet *et al.* (2017b) which found that expanded cultivation land results in an increment of surface runoff, water yield and decreased groundwater flow and evapotranspiration.

Similarly, (Bewket and Sterk, 2005) found that the hydrology has been influencing negatively due to the clearance of natural vegetation cover, land degradation, and expanded agricultural land that reduce infiltration, decrease groundwater recharge, and increase runoff.

The finding by (Getahun and Van Lanen, 2015) dictates there was higher streamflow during the main rainy season due to complete deforestation and evapotranspiration was low due to this. The study also shows during the main rainy season, there was slightly increased streamflow due to the expansion of agricultural land but during the dry season, it showed a decrement in magnitude. This implies a temporal variation and variation in the volume of river flows due to LULC change.

Table 4. 8 : Mean and changes in annual hydrologic regime caused by land-use change alone under RCP4.5 and RCP8.5

Change in Hydrologic variables	**Qt RCP4.5(8.5)**	**Qs RCP4.5(8.5)**	**Qb RCP4.5(8.5)**	**ET RCP4.5(8.5)**	**WY RCP4.5(8.5)**
S1 (mm)	249.17(251.23)	115.27(150.74)	133.90(100.49)	613.71(662.50)	288.07(295.85)
S2 (mm)	259.66(265.11)	132.92(159.07)	126.74(106.04)	567.22(665.23)	298.30(298.45)
S3 (mm)	276.86(298.75)	154.11(185.23)	122.74(113.53)	511.43(508.32)	322.57(328.45)
S2-S1 (mm)	10.49(13.88)	17.65(8.33)	-7.16(5.55)	-46.49(2.73)	10.24(2.60)
S3-S1 (mm)	27.69(47.52)	38.85(34.49)	-11.16(13.03)	-102.29(-154.18)	34.50(32.60)
S3-S2 (mm)	17.20(33.64)	21.19(26.16)	-4.00(7.48)	-55.79(-156.91)	24.27(30.00)
S2-S1 (%)	2.06(2.69)	7.11(2.69)	-2.75(2.69)	-8.66(0.21)	1.74(0.44)
S3-S1 (%)	5.26(8.64)	14.42(10.27)	-4.35(6.09)	-17.09(-13.17)	5.65(5.22)
S3-S2 (%)	3.21(5.97)	7.38(7.60)	-1.60(3.41)	-5.17(-13.37)	3.91(4.79)

Note: S1, S2, and S3 represent 1992, 2002 and 2015 LULC maps respectively with the same climate data set (1988-1999) under three scenarios. The number in bracket indicates the values from RCP8.5.

4.5.1.2. Separate Impact of Climate Change

The impact of climate change was analyzed by running the three scenarios (two past and one current) using the unique LULC of 1992 with its model parameter with changing the three different data set of climates (1988-1999 or S1, 2000-2009 or S2, and 2010-2019 or S3). The simulated water balance component shown in Table4.9 indicate that Qt, Qs, and WY show the decrement by 14.25mm/annum (3.3%), 9.88mm/annum (5.86%), and 25.62mm/annum (4.65%) in S2 from S1 (baseline) respectively (RCP4.5).

This is related to a slight decrement in precipitation between S1 and S2. While Qt, Qs, and WY show the increment (19.91mm (3.84%), 43.49mm (15.87%) and 11.12mm (1.89%) respectively) between S3 and baseline period (S1). This implies the small change in precipitation affects the surface runoff more. The ET experienced the increment between S1 and S2 or 3.95mm (0.32%); S1 and S3 or 39.35mm (2.49%). This may be induced by the combined impact of increased net solar radiation, temperature and wind speed (Yang *et al.*, 2017). (Yihun, 2009) also suggests that the increment in temperature plays a significant role in the increment of ET. Yet, the change was insignificant when compared with impact due to land-use change. On the other hand, Qb experienced the decrement throughout both scenarios i.e. 4.37mm (1.66%) and 23.58mm (2.65%) between S1 and S2 and S3 respectively. The change in Qb due to climate change is also smaller than the change caused by land-use change.

Table 4. 9 : Mean and changes in annual hydrologic regime caused by climate change alone under RCP4.5 and RCP8.5

Change in Hydrologic variables	**Qt RCP4.5(8.5)**	**Qs RCP4.5(8.5)**	**Qb RCP4.5(8.5)**	**ET RCP4.5(8.5)**	**WY RCP4.5(8.5)**
S1 (mm)	249.17(251.23)	115.27(150.74)	133.90(100.49)	613.71(662.50)	288.07(295.85)
S2 (mm)	235.92(239.22)	106.39(122.00)	129.53(117.22)	617.66(622.92)	262.45(266.23)
S3 (mm)	269.08(269.98)	158.76(167.39)	110.32(102.59)	713.06(745.31)	299.19(312.32)
S2-S1 (mm)	-14.25(-12.01)	-8.88(-28.74)	-4.37(16.73)	3.95(-39.58)	-25.62(-29.62)
S3-S1 (mm)	19.91(18.75)	43.49(16.65)	-23.58(2.10)	39.35(82.81)	11.12(16.47)
S3-S2 (mm)	33.16(30.76)	52.37(45.39)	-19.21(-14.63)	95.40(122.39)	36.74(46.09)
S2-S1 (%)	-3.3(-2.45)	-4.01(-10.54)	-1.66(7.68)	0.32(-3.08)	-4.65(-5.27)
S3-S1 (%)	3.84(3.60)	15.87(5.23)	-2.65(1.03)	2.49(5.88)	1.89(2.71)
S3-S2 (%)	6.57(6.04)	19.75(15.68)	-8.01(-6.65)	7.17(8.95)	6.54(7.97)

Note: S1, S2, and S3 represent the climate of 1988-1999, 2000-2009 and 2010-2019 respectively with the same LULC map (1992) under three scenarios. The number in bracket indicates the values from RCP8.5.

4.5.1.3. Combined Impacts of Climate and Land Use Land Cover Change

In terms of combined impact, a legible clue could be observed in Table4.10. Because ET was more sensitive to land-use change than climate change, the change in ET under both climate

and land-use change scenarios was consistent with that under the LULC change scenario. However, the change in surface runoff was mainly affected by climate change.

Changes in baseflow were influenced both by climate and land-use change. Generally, a decrease in average annual surface runoff (1.9mm or 1.1% i.e. the change between S2 and S1) and baseflow (8.8mm or 3.4% i.e. the change between S3 and S1) caused by climate change was promoted by land-use change, whereas a decrease of average annual ET (23.3mm or 1.9% and 44.5mm or 3.8% i.e. the change between S2 and S1; and S3 and S1 respectively) was enhanced by deforestation in the area. With regard to the reduction of base flow, the increment in agricultural land or deforestation also plays a significant role. This might be because of less infiltration due to compactions in topsoil pores in the area devoid of forests. The streamflow and water yield show the increasing trend under combined actions. The result also indicates average annual increment in water yield is more affected by both climate and LULC change under both altered periods (S2 and S3).

Table 4. 10 : Mean and changes in annual hydrologic regime caused by the combined action under RCP4.5 and RCP8.5

Change in Hydrologic variables	**Qt RCP4.5(8.5)**	**Qs RCP4.5(8.5)**	**Qb RCP4.5(8.5)**	**ET RCP4.5(8.5)**	**WY RCP4.5(8.5)**
S1 (mm)	223.2(232.1)	89.3(92.8)	133.9(139.3)	613.7(618.4)	288.1(293.9)
S2 (mm)	236.2(236.2)	87.4(87.4)	144.1(148.8)	590.4(592.3)	328.4(328.4)
S3 (mm)	320.8(341.3)	195.7(208.2)	125.1(133.1)	569.2(576.5)	452.0(457.3)
S2-S1 (mm)	13.0(4.1)	-1.9(-5.5)	10.2(9.5)	-23.3(-26.0)	40.3(34.5)
S3-S1 (mm)	97.7(109.2)	106.4(115.4)	-8.8(-6.2)	-44.5(-41.8)	163.9(163.5)
S3-S2 (mm)	84.7(105.2)	108.3(120.8)	-18.9(-15.7)	-21.2(-15.8)	123.7(128.9)
S2-S1 (%)	2.8(0.9)	-1.1(-3.0)	3.7(3.3)	-1.9(-2.2)	6.5(5.5)
S3-S1 (%)	18.0(19.0)	37.3(38.3)	-3.4(-2.3)	-3.8(-3.5)	22.2(21.8)
S3-S2 (%)	15.2(18.2)	38.3(40.9)	-7.0(-5.6)	-1.8(-1.4)	15.8(16.4)

Note: S1, S2, and S3 represent the climate of 1988-1999, 2000-2009 and 2010-2019 with 1992, 2002 and 2015 LULC maps respectively under three scenarios. The number in bracket indicates the values from RCP8.5.

4.5.2. Impact on Mean Monthly of hydrologic Components.

The changes in simulated average monthly streamflow, surface runoff, baseflow, Evapotranspiration, and water yield were compared for different scenarios to explore changes in the hydrologic regime. The result discussed under monthly mean fluxes was based on RCP4.5.

The change from the baseline period (S1) for the basin is shown in Figure 4.7, 4.8 and 4.9, which describes the impact of individual LULC change, climate change alone and the combined impacts respectively.

4.5.2.1. Separate Impact of LULC Change

For the entire basin (Figure 4.7), changes in ET followed decreasing trend in all months except for April, May, and November which shows a slight increment, whereas changes in base flow experienced a consistent decline in all months between S2 and S1. The ET was increased by 0.6%, 1.5% and 1.2% in April, May, and November respectively. The inconsistency of increasing ET might be due to the reforestation in some parts of the watershed. Surface runoff also exhibited an increasing trend in all months excepts for April, May, and November. The abnormity of decreasing surface runoff might be caused by the uncertainties in the model. The changes in streamflow followed a similar trend as surface runoff. Overall, all the hydrologic variable change under land-use change was below 10%. For example, ET shows a change of -4.3% in July, while baseflow shows the decline by 2.1% between S2 and S1. Under the land-use change scenario, the ET was more likely affected than other hydrologic variables. In terms of surface runoff, almost no significant change for the wet season (July, August, and September). The changes happened in the dry season (December-February) was higher. For example, surface runoff has experienced a change of 2.2%, 3.99% and 3.78% in the month of December, January and February respectively.

This can be explained by the soil moisture condition and evaporation which is most likely increased during the dry period.

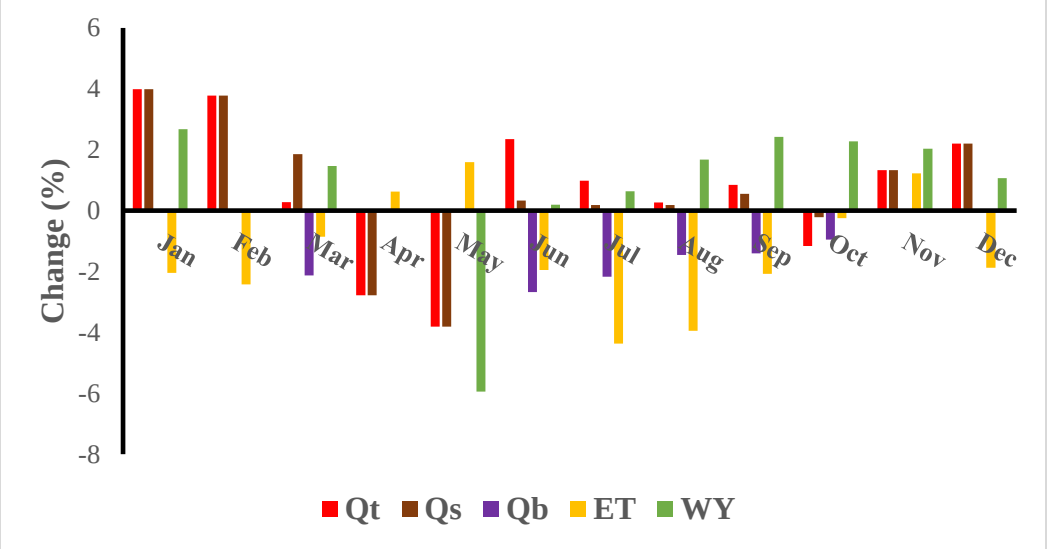

Figure 4. 7 : Changes in monthly mean values for the basin: under LULC change (RCP4.5)

The increment may be different from year to year depending on environmental and atmospheric conditions. However, in the wet season, the infiltration rate is relatively stable and the soil is often saturated, which leads to little changes in surface runoff under the same precipitation condition.

4.5.2.2. Separate Impact of Climate Change

Compared with a monthly hydrologic response under land use, Variations of mean monthly values under climate change scenarios were relatively significant (Figure 4.8). The ET increased in January, February, April, July, August, and September because of an increase in precipitation between S2 and S1. But, in June, regardless of an increment in precipitation by 7.5%, the ET experienced the decrement by 6.3%, which is consistent with the finding discussed in the previous section.

Comparing with ET, monthly surface runoff was more sensitive to climate variability except for February and March. Influenced by the variation in precipitation, surface runoff decreased by 25.5%, 26.7%, 27.4%, 37.1% and 19.5% in May, July, October, November and December, respectively, whereas significant rise where in April (15.9%), June (25.4%), August (5.5%), and September (9.5%). Moreover, in January, surface water was decreased by 7.2% in spite of

an increment of 6.6% in precipitation. This can be attributed to the model uncertainty or the reforestation in some parts of the area as discussed in the previous section. These changes were between S2 and S1. The change in baseflow followed the trend similar to the change in ET in most of the months. Though, the precipitation experienced an increment of 7.5%, baseflow in June shows the decline by 5.5%. This might be caused by the delaying effect from baseflow because groundwater has a longer time of concentration.

The variation in streamflow represented the combined effect of changes in baseflow and surface runoff. The higher increment of streamflow was observed in April (21.2%) and June (19.9%) between S2 and S1. In other months the changes do not have consistent trends. The water yield in the basin shows the decrement in the majority of months. These all changes discussed under climate change impact were based on the changes between S2 and S1.

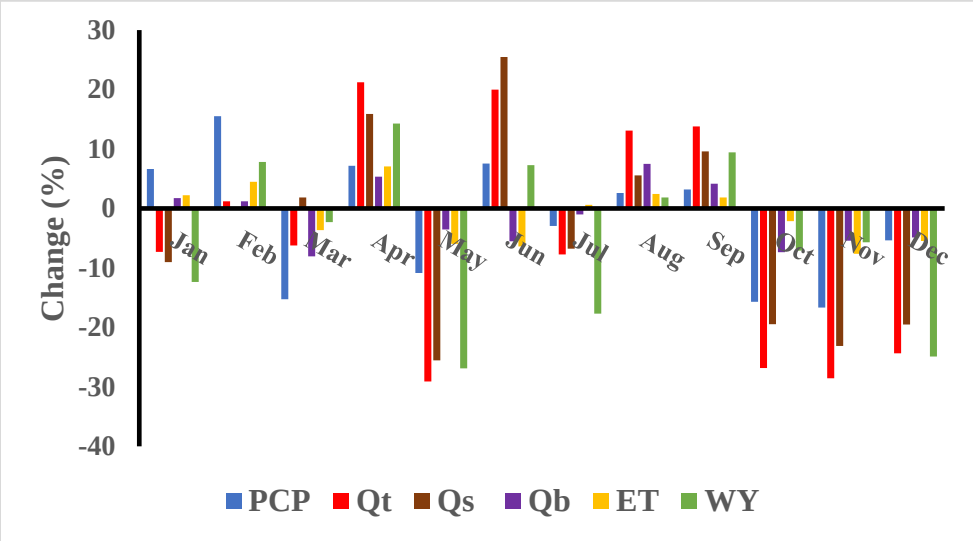

Figure 4. 8 : Changes in monthly mean values of the basin: under climate change (RCP4.5)

4.5.2.3. Combined Impacts of Climate and Land Use Land Cover Change

Figure 4.9 illustrates the impact of combined action on monthly fluctuation was mainly determined by climate change. However, the changes in baseflow were different in months of October, November, and December which shows the slight increment. This may also be attributed to model uncertainty.

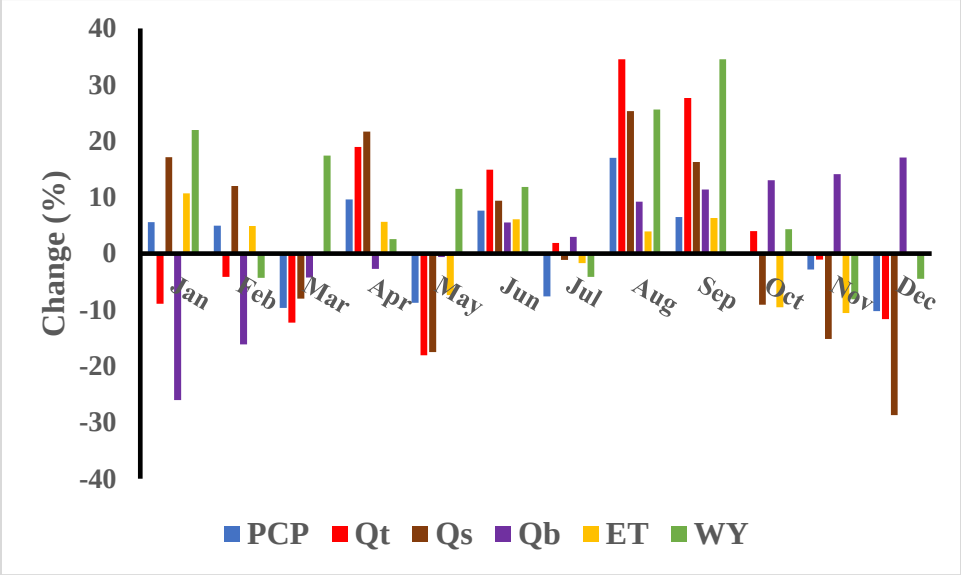

Figure 4. 9 : Changes in monthly mean values of the basin: under the combined action (RCP4.5)

4.5.3. Projected Hydroclimatic Change

This was done based on the fourth scenario discussed under section 3.6.7.4. The projected hydrologic change under a future climate of 2020-2040 years was assessed and the change occurred in Qt, Qs, Qb, ET, and WY were presented under section 4.5.3.1 and 4.5.3.2.

4.5.3.1. Annual Changes Under Projected Climate Change

The potential impact of future climate change on the hydrology of the Tekeze river till the year of 2040 was studied using downscaled P(precipitation) and T(temperature) as a predictor input to the SWAT model. Table 4.11 indicates the streamflow (Qt) for the projected period shows the decline under RCP8.5 and increment under RCP4.5 when compared with the baseline period (S1). The average simulated Qt decreases by 0.3% under RCP8.5 and increases by 8.6% under RCP4.5 for the period of 2020-2040 years. A similar result was found by Tesfaye *et al.* (2019) which reports, due to the projected higher temperature and lower precipitation, streamflow over Northern Ethiopia shows the decline by the end of the twenty-first century. They expect a 3% decrease in mean annual streamflow in comparison with the period 1981-1990. Tesfaye *et al.* (2019) report also indicates the streamflow increment until the year 2039 under RCP4.5 and starts declining.

The disagreement not only in magnitude but also in direction of simulated changes in streamflow, with this result might be that the other investigations had other approaches and reference periods.

Such differences, unfortunately, complicate it to reaches a consensus on how climate change affects hydrological response and what the implications are for the development and management of water resources in Northern Ethiopia.

Under RCP8.5 all elements except evapotranspiration show the decline during the projected change. This response is plausible in view of increasing temperature, which would increase evapotranspiration and reduce water storage and discharge. However, under RCP4.5 all elements except water yield show an increment for the period of 2020-2040 (Table 4.10).

Table 4. 11 : Annual mean and changes in hydrologic components under projected scenario (2020-2040)

Changes in variables	QtRCP4.5(8.5)	QsRCP4.5(8.5)	QbRCP4.5(8.5)	ETRCP4.5(8.5)	WYRCP4.5(8.5)
S4 (mm)	296.1(249.6)	143.4(149.8)	152.7(99.9)	654.9(696.2)	265.4(261.5)
S4-s1 (mm)	46.9(-1.6)	28.2(-1.0)	18.8(-0.6)	41.2(33.7)	-22.7(-34.3)
S4-s1(%)	8.6(-0.3)	10.9(-0.3)	6.6(-0.3)	3.2(2.5)	-4.1(-6.2)

Note: S1 and S4 represent the baseline period (first scenario) and future or projected (fourth scenario) respectively.

4.5.3.2. Monthly Mean Fluxes Under Projected Climate Change

Table 4.12 dictates the values of simulated hydrological components under RCP4.5 and RCP8.5 for the S4 scenario. The result shows the variation of hydrological components under both RCPs. There are also seasonal variations of the hydrological components. For instance, the ET shows the increment under RCP8.5 with respect to RCP4.5. However, the increment is not sharp i.e. it shows the decline at some moths (April). Other than ET, almost all of the element shows the increment under RCP4.5 in relative to RCP8.5 regardless of their seasonal variations, which may show increment or decrement.

Table 4. 12 : Monthly simulated values of hydrological components under RCP4.5 and RCP8.5 for future projection.

Monthly simulated values of hydrological components under RCP4.5					Monthly simulated values of hydrological components under RCP8.5				
Month	Qt(mm)	Qs(mm)	Qb(mm)	ET(mm)	Month	Qt(mm)	Qs(mm)	Qb(mm)	ET(mm)
Jan	46.02	28.8916	85.1284	66.97	Jan	34.21	26.7999	81.9654	70.602
Feb	35.62	14.8596	10.7604	96.49	Feb	23.09	16.7679	7.5974	88.122
Mar	118.23	96.9734	4.2566	112.88	Mar	96.68	94.8817	1.0936	119.512
Apr	193.51	41.6358	5.8742	98.05	Apr	126.51	39.5441	2.7112	95.682
May	376	206.48	149.52	74.17	May	359.97	204.3883	146.357	82.0203
Jun	645.96	363.0568	262.9032	30.25	Jun	635.55	360.9651	259.7402	36.882
Jul	2223.09	651.3922	47.6978	15.89	Jul	1113.44	649.3005	44.5348	15.522
Aug	2153.58	611.0764	44.5036	19.86	Aug	1013.08	608.9847	41.3406	20.492
Sep	825.11	461.1638	33.9462	39.26	Sep	785.89	459.0721	30.7832	35.892
Oct	592.62	626.3196	236.3004	46.24	Oct	562.12	624.2279	233.1374	49.872
Nov	298.25	153.845	111.405	33.76	Nov	255.85	151.7533	108.242	45.392
Dec	184.38	72.1404	52.2396	30.61	Dec	122.18	70.0487	49.0766	36.6807

Note: Monthly simulated values of hydrological components under RCP4.5 (with black color on the left) and RCP8.5 (with blue color on the right).

4.5.4. Streamflow change

Figure 4.10 represents a summary of the monthly simulated streamflow under RCP4.5 and RCP8.5 for the past (1988-2009), present (2010-2019) and future (2020-2040).

The streamflow shows the increment and decline for RCP4.5 and RCP8.5 respectively under future projection except for March and April which does not show a significant shift under RCP8.5.

The comparison between past and present periods of the simulated streamflow shows the increment under both RCPs specifically during the wet season (July, August, and September). While during the dry period (December-February) there is no sharp increment of the streamflow. For example, under RCP4.5 the comparison indicates the decline for the month of December and increment for February. Under RCP8.5 there is a decline of streamflow for April and slight increment for December and March.

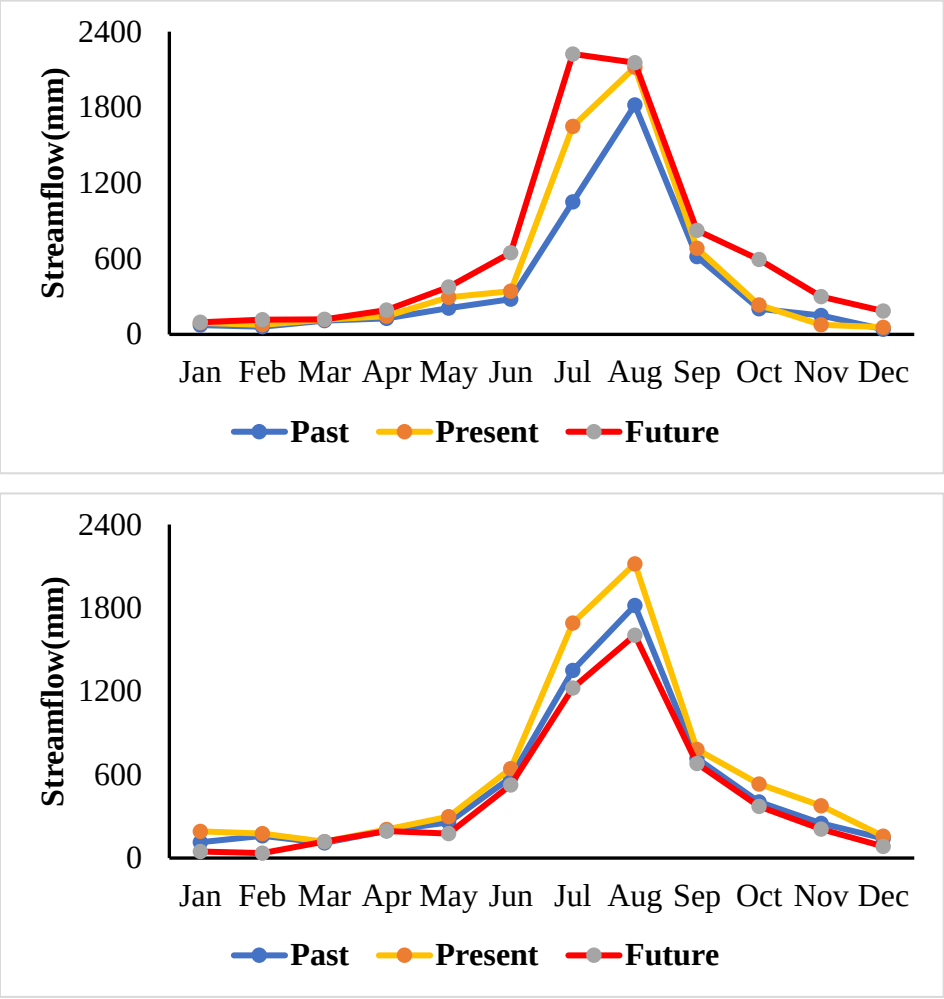

Figure 4. 10 : Simulated monthly streamflow under RCP4.5 (up) and RCP8.5(down).

4.6. Uncertainties Description

The hydrologic modeling in this study has limitations, which inevitably influence the output individually or when combined.

The various uncertainties in current studies including:

(a) input uncertainty. This is caused by insufficient data availability or unreasonable parameter value. For instance, the distributions in rain gages, introduce errors in the data used in a hydrologic model, especially in the region with a poor network.

(b) model uncertainty.

(c) method uncertainty. The method used in this study, like the single factor fixed method for differentiating the impact of land use and climate change often does not take into account atmospheric feedback of land surface process. The homogenous parameter may magnify the possible error in a diverse area.

(d) simulations uncertainty. The impact of external factors like irrigation and hydropower dam on simulations result was not included in this study which may produce different outputs. Combined with simulation uncertainty induced by ignoring the iteration between land surface and atmosphere, may result in possible bias when differentiating the impact of climate and land-use changes.

The data inconsistency even if data quality checking is done, impacts of other catchment characteristics like the implication of the water conservation practices, geology etc., and human interventions including implication of the population growth and future climate change scenarios on flows, estimation of the unknown user-defined model parameters for the model set-up process of satellite image analysis were essentially the limitations of the study.

Generally, in addition to individual uncertainties, the above-mentioned uncertainties may affect the output significantly when combined.

CHAPTER FIVE

5. CONCLUSION AND RECOMMENDATION

5.1. Conclusion

In this study, The SWAT model was applied to the Upper Tekeze river basin to analyze the impact of climate and LULC changes on the hydrologic regime over the period of 1988-2040. Model calibration and validation were carried out to select the most appropriate parameter for the simulation. The agreement between observed and simulated streamflow demonstrated that the model can provide a good estimate of the hydrologic regime in the basin.

Over the past three decades, the predominant patterns of LULC change were the transitional conversions among Agricultural land, Barren land, Built-up area, Forest, Grassland, Shrub/bushland, and Waterbody. The LULC change detection was assessed by comparing the classified images and the result showed that the dominant process is the expansion of agricultural land and decline in forest and grassland. In general, there was an increase in agricultural land (13.56%), Built-up (1.17%) and Waterbody (0.28%), along with a decrease in Barren land (0.19%), Shrub/bushland (0.13%), Grassland (9.09%) and forest land (5.6%) between 1992 and 2002. The area under forest and grassland was reduced by 7.24% and 12.85%, respectively, whereas the area coverage of barren land and settlement increased by 6.56% and 2.54% respectively between 2002 and 2015. Agricultural land coverage showed an increment of 8.72% during this period.

The effect of LULC change on hydrology for the basin was mainly attributed to the internal conversion among different land-use classes. However, the expansion in agricultural land and decline in forest area resulted in an obvious increment in surface runoff and reduction in ET and baseflow. Moreover, ET was more sensitive to land-use change than climate change in the study area.

The result also indicates the effect of climate change on hydrology was more pronounced than LULC change, regardless of average annual and mean monthly values in the basin.

Generally, climate change in the study area leads to a decline in annual streamflow (3.3%/2.45% under RCP4.5/RCP8.5) and surface runoff (4.01%/10.54% under RCP4.5/RCP8.5) between S2 and S1, while an increased between S3 and S1 (3.84/ 3.60 (Qt) and 15.87/5.23(Qs) under RCP4.5/RCP8.5 respectively); which is directly related to the decline in precipitation between S2 and S1 and increment between S3 and S1. Under future projection, the Qt shows the increment (8.6%) under RCP4.5 and declines under RCP8.5.

Annual and Monthly hydrologic changes were mainly influenced by the variation in precipitation and other climatic factors. Moreover, the changes in surface runoff under climate change was more significant than other hydrologic alterations.

The combined impact of climate and LULC change was more on changing the monthly distributions of the hydrologic modification than on altering average annual values. The increase in surface runoff and decrement in baseflow caused by climate was boosted by changes in LULC.

5.2.Recommendation

Even after considering the aforementioned uncertainties, the results and methodology in this study still have an implication for land use and water resource management in the future for the study area.

The quantitative result of this thesis, such as graphs and tabulated data, can provide information for local administration and policymakers to better understand the changes in hydrologic regimes in this region and hence develop better land use planning and water resource management.

Adequate and good quality meteorological and hydrological data is essential to have a desirable simulation result and advance model performance; therefore, it is useful to put an effort into improving quality and quantity along with establishing a good network of both hydrological and meteorological station.

For further hydrological simulation and assessment, values of calibrated parameters and database created in this study have paramount importance to be considered. Generally, the effort to address the potential uncertainties included in the current study are needed.

The expansion of agricultural land and the built-up area will increase surface runoff which would eventually lead to flash flood and landslides on the downstream and erosions on the upstream areas. On the other hand, the reduction of precipitation and the rise of temperature in the future would lead to the decline of surface runoff which will affect negatively agricultural practices of both downstream and upstream dwellers. Yet, the extent that the downstream users will be affected is more than the upstream users if the condition continues as it is. Therefore, there is a need to invest more in collaborative conservation practices from both upstream and downstream dwellers.

The current best prediction is that the water resource in the Tekeze basin, based on the result of this study, are become under more stress due to climate and LULC changes. This impact could be minimized by the development of future mitigation, conservation, and adaptation measures.

In terms of climatic variables, it appears to be rational to consider multi-GCM ensemble means, rather than single GCM results in this region of Tekeze river, in its sub-river basins and in other similarly complex regions.

6. REFERENCE

ABATE, S. 2015. *Assessment of Surface Water Potential and Demands in Tekeze River Basin, Northern Ethiopia.* Addis Ababa.

AFERA, H., ASIRAT, T., ERMIAS., DEEPAK, K., MIHRET, D., LAKWINDER, S.andDESSALEW, T. 2018. Application of Remote Sensing and GIS Land Use/Land Cover change detection: A Case Study of Woreta Zuria Watershed, Ethiopia. .

AGUILAR, E., AUER, I., BRUNET, M., PETERSON, T. C. and WIERINGA, J. 2003. Guidance on metadata and homogenization. *Wmo Td,* 1186**,** 1-53.

AHMED, M. A., FIROZ, A. and AKHTAR, M. W. 2009. Estimation of global and diffuse solar radiation for Hyderabad, Sindh, Pakistan. *Journal of Basic & Applied Sciences,* 5**,** 73-77.

ALEMAYEHU, F., TAHA, N., NYSSEN, J., GIRMA, A., ZENEBE, A., BEHAILU, M., DECKERS, S. and POESEN, J. 2009. The impacts of watershed management on land use and land cover dynamics in Eastern Tigray (Ethiopia). *Resources, Conservation and Recycling,* 53**,** 192-198.

ALEXANDERSSON, H. 1986. A homogeneity test applied to precipitation data. *Journal of climatology,* 6**,** 661-675.

ALLEN, R. G., JENSEN, M. E., WRIGHT, J. L. and BURMAN, R. D. 1989. Operational estimates of reference evapotranspiration. *Agronomy journal,* 81**,** 650-662.

AMARE, B. Climatic resources, agro-ecological zones and farming systems in Tigray. Extension Intervention Programme workshop, Mekele, 1996.

ANDUALEM, T., BELYA, G. and GUADIE, A. 2018. Land Use Change Detection Using Remote Sensing Technology. . *J Earth Sci Clim Change* 9**,** 488-496.

ARNOLD, J. G., MORIASI, D. N., GASSMAN, P. W., ABBASPOUR, K. C., WHITE, M. J., SRINIVASAN, R., SANTHI, C., HARMEL, R., VAN GRIENSVEN, A. and VAN LIEW, M. W. 2012. SWAT: Model use, calibration, and validation. *Transactions of the ASABE,* 55**,** 1491-1508.

ARNOLD, J. G., SRINIVASAN, R., MUTTIAH, R. S. and WILLIAMS, J. R. 1998. Large area hydrologic modeling and assessment part I: model development 1. *JAWRA Journal of the American Water Resources Association,* 34**,** 73-89.

ASIRAT, T. 2018. Evaluating the Dynamics of Land Use/Land Cover Change Using GIS and Remote Sensing Data in case of Yewoll Watershed, Blue Nile Basin, Ethiopia. . *Applied Research Journal of Geographic Information System. ,* 1**,** 10-24.

BANKO, G. 1998. A review of assessing the accuracy of classifications of remotely sensed data and of methods including remote sensing data in forest inventory.

BAYOU, T. and ASSEFA, A. 1989. Solar radiation maps fot Ethiopia. *Zede Journal,* 8**,** 7-15.

BEKELE, H. M. 2009. Evaluation of climate change impact on upper blue Nile Basin reservoirs. *Arba Minch University***,** 109.

BELETE, K. 2007. *Sedimentation and sediment handling at dams in Tekeze River Basin, Ethiopia.* Norwegian University of Science and Technology Trondheim, Norway.

BEWKET, W. and STERK, G. 2005. Dynamics in land cover and its effect on stream flow in the Chemoga watershed, Blue Nile basin, Ethiopia. *Hydrological Processes: An International Journal,* 19**,** 445-458.

BRAIMOH, A. K. 2006. Random and systematic land-cover transitions in northern Ghana. *Agriculture, ecosystems & environment,* 113**,** 254-263.

CHANG, J., WANG, Y., ISTANBULLUOGLU, E., BAI, T., HUANG, Q., YANG, D. and HUANG, S. 2015. Impact of climate change and human activities on runoff in the Weihe River Basin, China. *Quaternary International,* 380**,** 169-179.

References

CHIEN, H., YEH, P. J.-F. and KNOUFT, J. H. 2013. Modeling the potential impacts of climate change on streamflow in agricultural watersheds of the Midwestern United States. *Journal of Hydrology,* 491**,** 73-88.

CIBIN, R., SUDHEER, K. and CHAUBEY, I. 2010. Sensitivity and identifiability of stream flow generation parameters of the SWAT model. *Hydrological Processes: An International Journal,* 24**,** 1133-1148.

CONGALTON, R. G. and GREEN, K. 2009. *Assessing the accuracy of remotely sensed data: principles and practices*, CRC press, Taylor and Fransis Group, Boka Raton

CUNDERLIK, J. 2003. *Hydrologic model selection for the CFCAS project: assessment of water resources risk and vulnerability to changing climatic conditions*, Department of Civil and Environmental Engineering, The University of Western ….

DEAFALLA, T. H., CSAPLOVICS, E. and EL-ABBAS, M. M. The application of remote sensing for climate change adaptation in Sahel region. Earth Resources and Environmental Remote Sensing/GIS Applications V, 2014. International Society for Optics and Photonics, 92451R.

DEFRIES, R. and CHAN, J. C.-W. 2000. Multiple criteria for evaluating machine learning algorithms for land cover classification from satellite data. *Remote Sensing of Environment,* 74**,** 503-515.

DEVKOTA, L. P. and GYAWALI, D. R. 2015. Impacts of climate change on hydrological regime and water resources management of the Koshi River Basin, Nepal. *Journal of Hydrology: Regional Studies,* 4**,** 502-515.

DISSE, M., FENTA MEKONNEN, D., DUAN, Z. and RIENTJES, T. Analysis of the combined and single effects of LULC and climate change on the streamflow of the Upper Blue Nile River Basin (UBNRB): Using statistical trend tests, remote sensing landcover maps and the SWAT model. EGU General Assembly Conference Abstracts, 2018. 18688.

DUFFIE, J. A. and BECKMAN, W. A. 2013. *Solar engineering of thermal processes*, John Wiley & Sons.

GAO, P., MU, X.-M., WANG, F. and LI, R. 2011. Changes in streamflow and sediment discharge and the response to human activities in the middle reaches of the Yellow River. *Hydrology and Earth System Sciences,* 15**,** 1-10.

GASSMAN, P. W., REYES, M. R., GREEN, C. H. and ARNOLD, J. G. 2007. The soil and water assessment tool: historical development, applications, and future research directions. *Transactions of the ASABE,* 50**,** 1211-1250.

GEBRESELASSIE, M. G. and MOGES, S. A. 2016. Spatial and temporal variability of dry spell lengths and indication of climate change in rainfall extremes at Tekeze River Basin, Ethiopia. *International Journal of Water Resources and Environmental Engineering,* 8**,** 39-51.

GETAHUN, Y. S. and VAN LANEN, H. 2015. Assessing the impacts of land use-cover change on hydrology of Melka Kuntrie subbasin in Ethiopia, using a conceptual hydrological model. *Hydrology: Current Research,* 6**,** 1.

GIORGI, F., JONES, C. and ASRAR, G. R. 2009. Addressing climate information needs at the regional level: the CORDEX framework. *World Meteorological Organization (WMO) Bulletin,* 58**,** 175.

GREGRIO, A. and JANSEN, J. 2000. Land cover classification system (LCCS); Classification concepts and user manual for software version 2.

GROSSMAN-CLARKE, S., STEFANOV, W. L. and ZEHNDER, J. A. 2011. Urban weather, climate and air quality modeling: increasing resolution and accuracy using improved urban morphology. *Urban remote sensing: Monitoring, synthesis and modeling in the urban environment,* 250**,** 305-319.

GUIJARRO, J. A. 2018. Homogenization of climatic series with Climatol. *Reporte técnico, State Meteorological Agency (AEMET), Balearic Islands Office, Spain*.

GUPTA, H. V., SOROOSHIAN, S. and YAPO, P. O. 1999. Status of automatic calibration for hydrologic models: Comparison with multilevel expert calibration. *Journal of Hydrologic Engineering,* 4**,** 135-143.

References

HABTOM, M. 2009. *Evaluation of Climate Change Impact on Upper Blue Nile Basin Reservoir*. Doctoral Dissertation, MSc Thesis, Case Study on Gilgel Abay Reservoir.

HAILE, G. G. and KASSA, A. K. 2015. Investigation of precipitation and temperature change projections in Werii watershed, Tekeze River Basin, Ethiopia; application of climate downscaling model. *Journal of Earth Science & Climatic Change,* 6**,** 1.

HAILEMARIAM, K. 1999. Impact of climate change on the water resources of Awash River Basin, Ethiopia. *Climate Research,* 12**,** 91-96.

HASSABALLAH, K., MOHAMED, Y., UHLENBROOK, S. and BIRO, K. 2017. Analysis of streamflow response to land use and land cover changes using satellite data and hydrological modelling: case study of Dinder and Rahad tributaries of the Blue Nile (Ethiopia–Sudan). *Hydrology and Earth System Sciences,* 21**,** 5217.

HU, Z., WANG, L., WANG, Z., HONG, Y. and ZHENG, H. 2015. Quantitative assessment of climate and human impacts on surface water resources in a typical semi-arid watershed in the middle reaches of the Yellow River from 1985 to 2006. *International Journal of Climatology,* 35**,** 97-113.

IMMERZEEL, W. W., VAN BEEK, L. P. and BIERKENS, M. F. 2010. Climate change will affect the Asian water towers. *Science,* 328**,** 1382-1385.

IPCC-TGICA, A. 2007. General guidelines on the use of scenario data for climate impact and adaptation assessment. version 2. Tech. rep.

IPCC 2007. The physical science basis. *Contribution of Working Group I to the fourth assessment report of the Intergovernmental Panel on Climate Change,* 996.

JONES, C., GIORGI, F. and ASRAR, G. 2011. The Coordinated Regional Downscaling Experiment: CORDEX–an international downscaling link to CMIP5. *CLIVAR exchanges,* 16**,** 34-40.

JOTHITYANGKOON, C., SIVAPALAN, M. and FARMER, D. 2001. Process controls of water balance variability in a large semi-arid catchment: downward approach to hydrological model development. *Journal of hydrology,* 254**,** 174-198.

KACYRA, B. K., DIMSDALE, J. and KUNG, J. A. 2005. Integrated system for quickly and accurately imaging and modeling three-dimensional objects. Google Patents.

KASPAR, F., SCHULZWEIDA, U. and MULLER, R. Climate data operators as a user-friendly processing tool for cmsaf's satellite-derived climate monitoring products. the Proc. of the EUMETSAT Meteorological Satellite Conference, 2010.

LAMBIN, E. F. 1999. Land-use and land-cover Change (LUCC)-implementation strategy. *A core project of the International Geosphere-Biosphere Programme and the International Human Dimensions Programme on Global Environmental Change*.

LAPRISE, R., HERNÁNDEZ-DÍAZ, L., TETE, K., SUSHAMA, L., ŠEPAROVIĆ, L., MARTYNOV, A., WINGER, K. and VALIN, M. 2013. Climate projections over CORDEX Africa domain using the fifth-generation Canadian Regional Climate Model (CRCM5). *Climate Dynamics,* 41**,** 3219-3246.

LEAVESLEY, G. H. 1994. Modeling the effects of climate change on water resources—a review. *Assessing the Impacts of Climate Change on Natural Resource Systems.* Springer.

LEGESSE, D., ABIYE, T., VALLET-COULOMB, C. and ABATE, H. 2010. Streamflow sensitivity to climate and land cover changes: Meki River, Ethiopia. *Hydrology and Earth System Sciences,* 14**,** 2277.

LEGESSE, D., VALLET-COULOMB, C. and GASSE, F. 2003. Hydrological response of a catchment to climate and land use changes in Tropical Africa: case study South Central Ethiopia. *Journal of Hydrology,* 275**,** 67-85.

LI, H., ZHANG, Y., VAZE, J. and WANG, B. 2012. Separating effects of vegetation change and climate variability using hydrological modelling and sensitivity-based approaches. *Journal of Hydrology,* 420**,** 403-418.

References

LIN, B., CHEN, X., YAO, H., CHEN, Y., LIU, M., GAO, L. and JAMES, A. 2015. Analyses of landuse change impacts on catchment runoff using different time indicators based on SWAT model. *Ecological Indicators,* 58**,** 55-63.

LINDSTRÖM, G., JOHANSSON, B., PERSSON, M., GARDELIN, M. and BERGSTRÖM, S. 1997. Development and test of the distributed HBV-96 hydrological model. *Journal of hydrology,* 201**,** 272-288.

LIU, F., YUAN, L., YANG, Q., OU, S., XIE, L. and CUI, X. 2014. Hydrological responses to the combined influence of diverse human activities in the Pearl River delta, China. *Catena,* 113**,** 41-55.

MEDUGU, D. and YAKUBU, D. 2011. Estimation of mean monthly global solar radiation in Yola, Nigeria, Using Angstrom Model. *Advances in Applied Science Research,* 2**,** 414-421.

MENGISTU, K. T. 2009. Watershed hydrological responses to changes in land use and land cover, and management practices at Hare Watershed, Ethiopia.

MONTEITH, J. 1965. Evaporation and the environment. Soc. for Exp. Biol. 19, 205-234. In the state and movement of water in living organisms, XIXth Symposium, Swansea. Cambridge University Press.

MORIASI, D. N., GITAU, M. W., PAI, N. and DAGGUPATI, P. 2015. Hydrologic and water quality models: Performance measures and evaluation criteria. *Transactions of the ASABE,* 58**,** 1763-1785.

NASH, J. E. and SUTCLIFFE, J. V. 1970. River flow forecasting through conceptual models part I—A discussion of principles. *Journal of hydrology,* 10**,** 282-290.

NATKHIN, M., DIETRICH, O., SCHÄFER, M. P. and LISCHEID, G. 2015. The effects of climate and changing land use on the discharge regime of a small catchment in Tanzania. *Regional Environmental Change,* 15**,** 1269-1280.

NEITSCH, S., ARNOLD, J., KINIRY, J. E. A., SRINIVASAN, R. and WILLIAMS, J. 2000. Soil and water assessment tool user's manual. *Blackland Research Center, Temple, TX*.

NEITSCH, S. L., ARNOLD, J. G., KINIRY, J. R. and WILLIAMS, J. R. 2011. Soil and water assessment tool theoretical documentation version 2009. Texas Water Resources Institute.

NIGATU, Z. M., RIENTJES, T. and HAILE, A. T. 2016. Hydrological impact assessment of climate change on Lake Tana's water balance, Ethiopia. *American journal of climate change,* 5**,** 27.

NMSA 2001. Initial National Communication of Ethiopia to the United Nations Framework Convention on Climate Change (UNFCC). Report.

NUNES, C. and AUGE, J. 1999. Land use and land cover changeimplementation strategy.

PACHAURI, R. K., ALLEN, M. R., BARROS, V. R., BROOME, J., CRAMER, W., CHRIST, R., CHURCH, J. A., CLARKE, L., DAHE, Q. and DASGUPTA, P. 2014. *Climate change 2014: synthesis report. Contribution of Working Groups I, II and III to the fifth assessment report of the Intergovernmental Panel on Climate Change*, Ipcc.

PANITZ, H.-J., DOSIO, A., BÜCHNER, M., LÜTHI, D. and KEULER, K. 2014. COSMO-CLM (CCLM) climate simulations over CORDEX-Africa domain: analysis of the ERA-Interim driven simulations at 0.44 and 0.22 resolution. *Climate dynamics,* 42**,** 3015-3038.

PERAZZOLI, M., PINHEIRO, A. and KAUFMANN, V. 2013. Assessing the impact of climate change scenarios on water resources in southern Brazil. *Hydrological Sciences Journal,* 58**,** 77-87.

PETERSON, T. C., EASTERLING, D. R., KARL, T. R., GROISMAN, P., NICHOLLS, N., PLUMMER, N., TOROK, S., AUER, I., BOEHM, R. and GULLETT, D. 1998. Homogeneity adjustments of in situ atmospheric climate data: a review. *International Journal of Climatology: A Journal of the Royal Meteorological Society,* 18**,** 1493-1517.

PONTIUS JR, R. G., SHUSAS, E. and MCEACHERN, M. 2004. Detecting important categorical land changes while accounting for persistence. *Agriculture, Ecosystems & Environment,* 101**,** 251-268.

PRESCOTT, J. 1940. Evaporation from a water surface in relation to solar radiation. *Trans. Roy. Soc. S. Aust.,* 46**,** 114-118.

References

PROTOCOL, K. 1997. United Nations framework convention on climate change. *Kyoto Protocol, Kyoto*, 19.

REFSGAARD, J. C. 1997. Parameterisation, calibration and validation of distributed hydrological models. *Journal of hydrology,* 198**,** 69-97.

RODDA, G. H., JARNEVICH, C. S. and REED, R. N. 2011. Challenges in identifying sites climatically matched to the native ranges of animal invaders. *PloS one,* 6**,** e14670.

RUMMUKAINEN, M. 2010. State-of-the-art with regional climate models. *Wiley Interdisciplinary Reviews: Climate Change,* 1**,** 82-96.

SCHULZWEIDA, U., KORNBLUEH, L. and QUAST, R. 2009. Climate Data Operators. User's Guide. MPI for Meteorology Brockmann Consult.

SERPA, D., NUNES, J., SANTOS, J., SAMPAIO, E., JACINTO, R., VEIGA, S., LIMA, J., MOREIRA, M., CORTE-REAL, J. and KEIZER, J. 2015. Impacts of climate and land use changes on the hydrological and erosion processes of two contrasting Mediterranean catchments. *Science of the Total Environment,* 538**,** 64-77.

SETEGN, S. G., SRINIVASAN, R. and DARGAHI, B. Streamflow Calibration and Validation of SWAT2005/ArcSWAT in Anjeni Gauged Watershed, Northern Highlands of Ethiopia. International SWAT Conference, July 02-06, UNESCO-IHE, Delft, The Netherlands., 2006.

SINGH, A. 1989. Review article digital change detection techniques using remotely-sensed data. *International journal of remote sensing,* 10**,** 989-1003.

SINGH, J., KNAPP, H. V., ARNOLD, J. and DEMISSIE, M. 2005. Hydrological modeling of the Iroquois river watershed using HSPF and SWAT 1. *JAWRA Journal of the American Water Resources Association,* 41**,** 343-360.

SMITHSON, P. A. 2002. IPCC, 2001: climate change 2001: the scientific basis. Contribution of Working Group 1 to the Third Assessment Report of the Intergovernmental Panel on Climate Change, edited by JT Houghton, Y. Ding, DJ Griggs, M. Noguer, PJ van der Linden, X. Dai, K. Maskell and CA Johnson (eds). Cambridge University Press, Cambridge, UK, and New York, USA, 2001. No. of pages: 881. Price£ 34.95, US 49.95,ISBN0-521-01495-6(paperback).£90.00,US 130.00, ISBN 0-521-80767-0 (hardback). *International Journal of Climatology: A Journal of the Royal Meteorological Society,* 22**,** 1144-1144.

SOLOMON, S., QIN, D., MANNING, M., AVERYT, K. and MARQUIS, M. 2007. *Climate change 2007-the physical science basis: Working group I contribution to the fourth assessment report of the IPCC*, Cambridge university press.

SUBRAMANYA, K. 2013. *Engineering Hydrology, 4e,* Tata McGraw-Hill Education.

TEFERA, W. D. Integrating Geo-information for the Management of River Basins in the Ethiopian part of the Nile Basin. 2003. ITC.

TEKLAY, A., DILE, Y. T., SETEGN, S. G., DEMISSIE, S. S. and ASFAW, D. H. 2019. Evaluation of static and dynamic land use data for watershed hydrologic process simulation: A case study in Gummara watershed, Ethiopia. *Catena,* 172**,** 65-75.

TESFAYE, S., TAYE, G., BIRHANE, E. and VAN DER ZEE, S. E. 2019. Observed and model simulated twenty-first century hydro-climatic change of Northern Ethiopia. *Journal of Hydrology: Regional Studies,* 22**,** 100595.

THANAPAKPAWIN, P., RICHEY, J., THOMAS, D., RODDA, S., CAMPBELL, B. and LOGSDON, M. 2007. Effects of landuse change on the hydrologic regime of the Mae Chaem river basin, NW Thailand. *Journal of Hydrology,* 334**,** 215-230.

TRIPATHI, M., PANDA, R. and RAGHUWANSHI, N. 2003. Identification and prioritisation of critical sub-watersheds for soil conservation management using the SWAT model. *Biosystems Engineering,* 85**,** 365-379.

US-ACE 2010. Hydrologic Modeling System HEC–HMS, Technical Reference Manual. *Davis, CA: Hydrologic Engineering Center*.

References

VERMOTE, E., JUSTICE, C., CLAVERIE, M. and FRANCH, B. 2016. Preliminary analysis of the performance of the Landsat 8/OLI land surface reflectance product. *Remote Sensing of Environment,* 185**,** 46-56.

WEI, X., LIU, W. and ZHOU, P. 2013. Quantifying the relative contributions of forest change and climatic variability to hydrology in large watersheds: a critical review of research methods. *Water,* 5**,** 728-746.

WELDE, K. and GEBREMARIAM, B. 2017. Effect of land use land cover dynamics on hydrological response of watershed: Case study of Tekeze Dam watershed, northern Ethiopia. *International Soil and Water Conservation Research,* 5**,** 1-16.

WOLDE, E. 2016. Identification and prioritization of sub watersheds for land and water management in Tekeze Dam watershed, Northern Ethiopia. Int. *Soil Water Conserv. Res,* 4**,** 30-38.

WOLDESENBET, T. A., ELAGIB, N. A., RIBBE, L. and HEINRICH, J. 2017a. Gap filling and homogenization of climatological datasets in the headwater region of the Upper Blue Nile Basin, Ethiopia. *International Journal of Climatology,* 37**,** 2122-2140.

WOLDESENBET, T. A., ELAGIB, N. A., RIBBE, L. and HEINRICH, J. 2017b. Hydrological responses to land use/cover changes in the source region of the Upper Blue Nile Basin, Ethiopia. *Science of the Total Environment,* 575**,** 724-741.

WOLDESENBET, T. A., ELAGIB, N. A., RIBBE, L. and HEINRICH, J. 2018. Catchment response to climate and land use changes in the Upper Blue Nile sub-basins, Ethiopia. *Science of the total environment,* 644**,** 193-206.

YANG, L., FENG, Q., YIN, Z., WEN, X., SI, J., LI, C. and DEO, R. C. 2017. Identifying separate impacts of climate and land use/cover change on hydrological processes in upper stream of Heihe River, Northwest China. *Hydrological Processes,* 31**,** 1100-1112.

YIHUN, D. 2009. Hydrological Modeling to Assess Climate Change Impact at Gilgel Abay River, Lake Tana Basin, Ethiopia. *Unpublished Master's thesis, Lunds Universitet, Sweden*.

ZHANG, X., ZHANG, L., ZHAO, J., RUSTOMJI, P. and HAIRSINE, P. 2008. Responses of streamflow to changes in climate and land use/cover in the Loess Plateau, China. *Water Resources Research,* 44.

ZHAO, Y., ZOU, X., GAO, J., XU, X., WANG, C., TANG, D., WANG, T. and WU, X. 2015. Quantifying the anthropogenic and climatic contributions to changes in water discharge and sediment load into the sea: a case study of the Yangtze River, China. *Science of the Total Environment,* 536**,** 803-812.

Websites Reference

The official website for SWAT software and related documentations [Online]: Available at: http://swatmodel.tamu.edu/software/arcswat [Accessed 15 October 2018].

U.S Geological Survey (USGS): Official Website for downloading Landsat images and DEM [Online]: Available at: http://earthexplorer.usgs.gov/ official Website for downloading Landsat images and DEM, [Accessed 01 January 2018]

CORDEX_ Africa Domain: Official website for downloading climate data [Online]: Available at: https://esg-dn1.nsc.liu.se/search/esgf-liu/ (or https://esgf-index1.ceda.ac.uk/search/esgf-ceda/), [Accessed 01 May 2018]

Climatol Package: The official website for installing package on R software [Online]: Available at: (https://CRAN.R-project.org/package=climatol): [Accessed 01 January 2019]

7. APPENDICES

Appendix A: Meteorological and Hydrological Data Tables

Appendix Table 1: List of neighboring and target Meteorological stations for the Tekeze river basin.

S.No	Station name	Latitude	Longitude	Elevation	Period of Record	
					Rainfall	Temerature
1	Adigrat	14.28	39.45	2497	1988-2017	1988-2017
2	Adwa	14.18	38.88	1911	1988-2017	1988-2017
3	Alamata	12.31	39.41	1589	1988-2017	1988-2017
4	Ambagorgis	12.77	37.62	2900	1988-2017	1988-2017
5	Axum	14.14	38.78	2113	1988-2017	1988-2017
6	Ayikel	12.53968	37.0587	2254	1988-2017	1988-2017
7	Debark	13.14213	37.8979	2836	1988-2017	1988-2017
8	Edagahamus	13.84	38.63	2670	1988-2017	-
9	Enda aba guna	13.94	38.18	1761	1988-2017	1988-2017
10	Gonder	12.52115	37.4319	1973	1988-2017	1988-2017
11	Lalibela	12.039	39.039839	2487	1988-2017	1988-2017
12	Maichew	12.78413	39.5337	2432	1988-2017	1988-2017
13	Mekele	13.47051	39.5312	2257	1988-2017	1988-2017
14	Shiraro	14.4006	37.7597	1033	2002-2017	2002-2017
15	Shire	14.10172	38.29457	1897	1988-2017	1988-2017
16	wukro	13.83	39.6	1972	1988-2017	1988-2017

Appendix Table 2: Ayikel Monthly Precipitation (mm)

Year	Jan	Feb	Mar	Apr	May	Jun	Jul	Aug	Sep	Oct	Nov	Dec	Total
1988	0	34.4	7.9	39.1	25.2	112.9	348.6	379.7	93.1	188.9	0.2	0.2	1230.2
1989	0.1	7	32.3	39.6	139	66.9	246.1	243.4	78.3	0	0	10	862.7
1990	2.6	0	11.5	28.8	32.2	86.9	301.6	182.2	116.4	0	0	20	782.2
1991	46.7	152.4	143.2	315.8	402.7	91.5	128.5	44.9	1	0.3	0	2.6	1329.6
1992	4	0.8	10.8	45.8	65.3	88.8	260.7	231	69.5	46.4	18.9	19.9	861.9
1993	1.3	3.8	29.7	141.6	73.1	63.3	230.2	176	108	58.2	2.7	0.7	888.6
1994	1	3.6	2.7	25.2	38.9	122.1	309.2	280.5	126.9	39.3	8	5.9	963.3
1995	0	7.2	30.5	49.8	72.9	102.6	266	264.5	47.4	0	0.7	20.9	862.5
1996	19.2	18.2	75.8	39.3	86.1	175.8	237.3	224.8	84.2	29.4	25.1	0.3	1015.5
1997	4.4	2.8	27.1	44.1	82	144.6	220.1	196.3	72.5	73	33.9	5.4	906.2
1998	1.6	2.7	16.4	9	44.1	112.7	292.4	298.5	119.2	70.6	1.9	0	969.1
1999	21.2	0.6	2.4	28.3	59.6	126.9	311.7	302.3	130.2	100.9	14.3	7.2	1105.6
2000	0	0.4	27.4	47	56.4	115.1	260.7	236.8	152.6	99.4	5.2	4.5	1005.5
2001	0	2.6	15.6	31.4	73.6	169.7	351.2	292.8	79.4	60.8	5.6	3.6	1086.3
2002	12.8	6.1	23.3	17.7	52.3	150.4	203.3	250.7	95.6	31.3	2.4	4.6	850.5
2003	9.1	15.2	15	24.7	37.1	137.2	224	293.7	102.8	22.5	1.8	1.8	884.9
2004	1.2	4.1	17.2	33.5	1.1	112.4	195.5	224.6	58	35.3	3.7	0	686.6
2005	14.3	2.1	44	43.3	51.5	170.1	268.5	254.6	111.9	0	0	0.8	961.1
2006	1.3	37.7	47.3	74.7	78.2	75.8	263.2	323.4	145.9	47.9	11.3	8.5	1115.2
2007	4.7	2.7	3.8	29.9	63.5	245.1	370.2	338.4	191	28.9	16.3	0	1294.5
2008	9.4	0.5	2	60.6	74.3	124.2	298.9	306.5	126.9	31.2	17.8	11.2	1063.5
2009	1.5	28.1	20.1	37.8	46.1	34.8	332.4	304.9	19.6	0	20.2	4.8	850.3
2010	11.5	26.2	34.8	50.4	60.8	87.5	290.9	367.2	62	0.6	10.8	5.8	1008.5
2011	27.5	25.8	31.8	21.7	92.7	95.8	221.1	273.2	117.6	5	30.7	0	942.9
2012	0	0	1.8	2	88.7	119.3	242.9	202.4	105.6	25.2	25.5	11.3	824.7
2013	0	0	26.2	20.5	76.2	146.7	303.7	259.5	96.5	88.8	0	0	1018.1
2014	0	0.1	41.6	46.1	99	79.3	215.6	246.6	181.9	44.1	23.8	0	978.1
2015	0	0	25.5	32.2	103.3	84.2	103.5	203.4	145.9	33.8	50.6	5.6	788
2016	0	0	12.6	97.3	130	97.2	218.5	271.1	73.7	33.2	8.2	0.8	942.6
Mean	6.7	13.3	26.9	50.9	79.5	115.2	259.2	257.7	100.5	41.2	11.7	5.4	968.2

Appendix Table 3: Gondar Monthly Precipitation (mm)

Year	Jan	Feb	Mar	Apr	May	Jun	Jul	Aug	Sep	Oct	Nov	Dec	Total
1988	0	35.2	0	13.2	67.4	107.9	345.6	375	99.5	40.6	8.3	0.8	1093.5
1989	0	1.5	41.8	35.1	27.9	173.8	291	253.8	116.9	37.3	7.6	12.9	999.6
1990	4.6	0	7.1	32.1	14.1	64.1	335.8	213.3	139.9	1.5	1.3	0	813.8
1991	0	10.1	120.4	255.2	374.3	109.4	217.9	265.6	80.8	39.5	5.2	0	1478.4
1992	0	0	2.9	55.9	56.4	93.7	268.1	212.2	98.8	50.9	12.9	23.4	875.2
1993	0	3.8	33.3	157.7	85.6	50.5	239.6	171.1	105	73	2	0.5	922.1
1994	0	1	0	7.5	54.9	150.9	280.1	229.9	90.7	36.7	19.5	2.7	873.9
1995	0	0	33.4	23.2	96.1	102.5	273.8	296.9	59.1	11.6	0.9	19.2	916.7
1996	0	4.3	21.5	80.7	110.4	165	249.2	251.6	72.6	34.9	22.5	0.4	1013.1
1997	0	1.7	27.3	41.5	120.1	179	182	202	32.1	78.3	38.9	13.2	916.1
1998	0	0	9.7	3.6	54.6	142.5	336.5	326.6	121.7	122.5	4.6	0	1122.3
1999	34.3	0	0	11.1	82.3	141.7	292.5	364.6	147.7	162.7	10.9	17.2	1265
2000	0	1.4	3.8	37.4	58.9	155.6	312.8	254.6	139.1	173.3	1.9	2.4	1141.2
2001	0	0.9	3.2	28.1	61.8	220.9	409.5	348.2	88.2	88.6	15.5	0	1264.9
2002	8.9	5.1	13.6	16.1	84.3	168.4	186.9	239.6	74.5	20.4	5.7	4	827.5
2003	0	21.4	10.8	0	36.8	179	238.6	304.1	94.1	20.6	0	5.5	910.9
2004	1.5	3.5	5.7	36.5	1.4	117.1	218	211.6	100	27	5.7	0	728
2005	0	0	47.2	21.1	17.8	196.1	276.9	229.1	142.1	23.7	3.6	0	957.6
2006	0	0	18.7	48.4	140.3	89	275.8	335.5	163.7	71.7	5.8	14.3	1163.2
2007	0	0	1.5	62.8	87.1	189.2	325	358.9	176.3	42.5	0.4	0	1243.7
2008	8.1	0	0	85.5	90.4	138.8	289.6	233.6	110.8	15	17.9	15.1	1004.8
2009	1.2	15.2	31	38.9	26	23.4	346.4	318.3	22.7	17.3	26.4	9	875.8
2010	19.7	0	31.2	45.4	90.2	99.3	270.8	384.3	71.7	37.4	14.6	0	1064.6
2011	2.5	7.9	19.9	23.8	74.8	93.6	230.9	338.6	103.5	52.3	46.6	0	994.4
2012	9.8	0	8.9	0	31.2	117.3	304.6	285.3	135.2	43.9	51.1	11.1	998.4
2013	0	0	2.6	10.1	69.8	154.6	244.4	291.6	63.3	62.8	43.6	0	942.8
2014	9.2	8.1	53.5	52.3	81.7	96.9	200.2	333.8	158.5	40.8	17.6	0	1052.6
2015	0	3.3	20.7	16.5	130.4	87.7	104.9	207.9	92.2	35.1	52.4	5.8	756.9
2016	2.8	0	12.2	76.9	144.7	126.9	280.6	278.6	81.6	40.6	6.6	0.6	1052.1
Mean	3.5	4.3	20.1	45.4	81.8	128.8	269.9	279.9	102.8	51.8	15.5	5.5	1009.3

Appendix Table 4: Lalibela Monthly Precipitation (mm)

Year	Jan	Feb	Mar	Apr	May	Jun	Jul	Aug	Sep	Oct	Nov	Dec	Total
1988	7.9	27.9	0	18.9	3.9	14.6	160.5	125.1	48.8	5.6	0.1	0	413.3
1989	0.1	4.6	36.5	30.6	18.4	8.8	84.4	94.1	43.6	9.9	2.2	2.7	335.9
1990	1	0	4.1	11	12	32.7	113.7	68.8	49.6	5	0.1	2.4	300.4
1991	5.4	19	39.5	81.6	129.2	42.3	57.9	66.2	16.5	10.4	0.9	0.8	469.7
1992	2.9	0.7	20.4	23	5.5	10.5	82.9	107.7	22.3	6.4	34.3	30.9	347.5
1993	3.3	3	22.1	95	13.3	2	99.9	56.9	34.1	6.9	3.1	1.3	340.9
1994	0	2	5.4	30.1	2.2	26.8	169.7	130.1	32.4	2.3	1.2	0.6	402.8
1995	0	18.5	6.7	39.8	27.3	2.7	136.6	106.3	30.4	0.5	0	13.4	382.2
1996	4.3	1.2	42.1	16.1	36.4	65.7	90.2	116.7	13.2	0.5	22.5	0.5	409.4
1997	10.2	5.5	31.8	21.8	15.7	37.3	117.8	83.9	5.4	29.6	38.1	1.6	398.7
1998	3.8	4.9	17.1	7	21.5	10.3	129.9	124.9	25.9	14	0	0	359.3
1999	12.5	0	0	14.4	0.5	12.9	175.4	160	35	24.4	2.1	1.2	438.4
2000	0	0	16.8	28.4	8.6	10.6	114.7	123	25.8	19	7.5	6	360.4
2001	0	3.3	34.1	20.3	1.2	45.4	146.4	133.6	4.5	0	0	4.6	393.4
2002	22.2	12.5	29.5	22.4	4.4	23.8	66.3	109.4	20.8	0	1	8.3	320.6
2003	1.3	12.7	28.6	14.9	1.2	35.7	76.9	157.1	35.7	0	1.1	0	365.2
2004	1.8	7.5	9.7	13.2	0	29.4	103.9	104.3	12.4	6.6	0.5	0	289.3
2005	4	0	27.4	17.5	36.8	23.6	134.6	72.3	26	0.3	4	0	346.5
2006	0	0.6	25.9	27	13.1	15.5	117.5	151.5	28.2	14.8	15.3	9.9	419.3
2007	10.6	6.9	3.3	14	15.2	60.8	156.1	107.2	44.1	0.2	2.5	0	420.9
2008	2.5	1.2	0.6	31.1	11.8	35.4	95.8	99.6	33.7	6.7	14.4	0	332.8
2009	0.5	1.8	19.3	13.7	1.5	3.3	120.1	116.8	13.1	15.8	14.9	0	320.8
2010	2.9	0	10.6	27.9	12.4	6	145.4	161.3	22.9	0.3	0.5	10.2	400.4
2011	7.2	0	21	23.3	14	26.2	109.1	110.5	43.7	1	12.8	0	368.8
2012	0	0	20	22.2	12.7	50.3	111.2	91.2	31.4	0.7	3.7	0	343.4
2013	8.6	0	7.2	20.5	13	35.3	105.2	97.4	28.9	23.5	8.4	0	348
2014	0.7	8.2	6	22.4	40.2	27.6	77.5	112.5	56	11.7	12.1	0.5	375.4
2015	3.8	5.7	24.3	0	40.5	0	52.6	10.1	53.3	12.9	19.2	2.2	224.6
2016	8.7	0.3	11.5	44.3	38.2	22.4	91.1	95.4	27.7	13.5	5.2	0.4	358.7
Mean	4.4	5.1	18.0	25.9	19.0	24.8	111.8	106.7	29.8	8.4	7.9	3.4	365.1

Appendix Table 5: Maichew Monthly Precipitation (mm)

Year	Jan	Feb	Mar	Apr	May	Jun	Jul	Aug	Sep	Oct	Nov	Dec	Total
1988	2.6	11.5	0.5	14.4	7.5	19.5	129.2	129.5	37.2	15.8	0	0	367.7
1989	0.1	3.8	21.8	20.6	24.3	30.3	94.6	98.3	45	9.4	2.4	2.7	353.3
1990	0.7	0	5.6	10.5	12.7	33.7	116.5	70.7	49.5	4.1	0.1	2.4	306.5
1991	5.8	19.7	35.8	72.1	123.3	44.4	53.2	72.2	19.2	3	2.1	0.5	451.3
1992	4.8	1.2	24.5	25.8	16.3	0.9	90.5	122.5	31.3	23.3	29	31.4	401.5
1993	33.2	10.4	7.2	72.2	24.5	2.9	61.8	37.8	31.5	29.2	0	1.2	311.9
1994	0	2.8	33.8	20.7	15.3	27	121.6	135.4	39.2	4.7	2.2	4	406.7
1995	0	27.4	11.9	44.6	37.5	6.6	83.9	92.2	32.2	14.7	0	16.7	367.7
1996	8.3	1.1	42.7	23	49.5	47.2	98.3	86.9	40	3.8	20.7	9.7	431.2
1997	1.5	0	48.3	56.1	22.3	41.1	108.1	60.2	25.6	41.3	52.3	0	456.8
1998	26.4	11	20.9	11.2	26.5	17.5	118.9	121.1	46.5	10.3	0	0	410.3
1999	9.5	0	10.1	10.1	3.9	12.1	121.9	138.6	59.5	35.4	0.4	1.8	403.3
2000	0	0	5.5	16.5	19.4	11.2	111.1	114.4	32.7	30.9	10.5	10.2	362.4
2001	0	1.9	40.3	8.6	21.8	25	130.1	97.8	48	10	0	10.3	393.8
2002	36	0	21	22.7	26.5	19.8	35.8	75.7	40.9	4.5	0	12.3	295.2
2003	9.2	12.3	35.2	21.5	1.2	12.9	60.4	154.7	29.3	4.4	2.2	16.8	360.1
2004	11.8	5	7.3	33.3	1.1	19	55.5	95.2	12.4	22.2	3	0	265.8
2005	6	2.5	47.9	57.2	43.2	17	91.5	103.7	21.2	20	4.2	0	414.4
2006	0	0.1	37.3	28	27.6	12	77.7	117.5	28.2	11.7	10.6	17.8	368.5
2007	19.6	13	9	29.7	6.8	27.3	162.4	87	44.8	9.1	3.6	0	412.3
2008	11.4	0	0	12.7	24	26.5	78.4	69.8	58.5	29.1	20.4	0	330.8
2009	0.5	0	8.1	16.5	0	2.6	157	126	5.2	10.8	12.4	14.3	353.4
2010	0.9	0.5	18.1	66.2	29.7	1.3	108.6	169.1	40.3	20.2	0	13.1	468
2011	16	0	10	19.5	31.3	8.1	109	101.3	25.9	10	27.2	0	358.3
2012	0	0	13.8	40.6	24.7	19.5	78.7	75.4	11.6	12.6	0	0	276.9
2013	17.5	13.6	9.6	27.6	10.5	31.3	61.6	101.7	19.3	34.9	24.4	0	352
2014	5.2	10.5	0	34	51.6	21.7	70.5	113	57.6	13.4	14.8	0	392.3
2015	8.2	0	13.1	0	36	9.7	32.2	45	54.7	12.9	19.2	2.2	233.2
2016	29.3	10.5	4.8	67.5	33.2	14.9	82.2	90.7	31.3	19.5	8.7	0.5	393.1
Mean	9.1	5.5	18.8	30.5	25.9	19.4	93.1	100.1	35.1	16.2	9.3	5.8	368.9

Appendix Table 6: Mekelle Monthly Precipitation (mm)

Year	Jan	Feb	Mar	Apr	May	Jun	Jul	Aug	Sep	Oct	Nov	Dec	Total
1988	0	2.1	0	10.1	1.1	6.7	106.7	131.6	27	0	0	0	285.3
1989	0	4.1	15.2	16.1	26.2	39.1	100.5	102.2	47.5	9	2.4	2.4	364.7
1990	0.6	0	6.7	10	13.2	35.3	119.6	72.3	49.8	3.4	0.1	2.3	313.3
1991	5.1	17.9	31.7	62	117.3	46.6	43.9	77.1	12.2	0.8	0	0	414.6
1992	8.7	2.1	8.5	1	2.6	6.2	64.4	90.9	1.3	2.1	12.9	8.3	209
1993	8	7.7	7	60.9	12.9	12.8	95	49	15.2	6.8	0	0	275.3
1994	0	5.3	0.4	14.3	0.8	35.4	106.6	108.8	33.8	0	1.8	2	309.2
1995	0	5.9	9.8	14.4	9.1	6.8	110.8	73.4	18.1	3	0	2.7	254
1996	1.4	0	20.7	4.9	24.8	37.6	79.6	93.1	7.1	0	12.8	1.1	283.1
1997	0	0	13	23.9	2.9	20.4	94.2	57.4	6.3	20.1	9.6	0	247.8
1998	10	1.2	0	3.8	12.2	15.9	104.6	121.4	13.9	7.2	0	0	290.2
1999	8.1	0.3	3.5	0	0	7.4	101	110.3	32.6	11.9	0	0	275.1
2000	0	0	0	10.4	9.6	5.4	75.3	87	15.8	2.2	1.7	3.5	210.9
2001	0	0	16.8	11.8	8.7	30.1	125.9	95.1	9.2	2.9	0	0	300.5
2002	2.8	0	11.3	4.2	5.9	17	40.4	73	7.5	0	0	0.3	162.4
2003	0	16.9	2.7	0.1	1.6	25.4	38.8	110.4	14.2	0.7	0	0.1	210.9
2004	1.6	4.7	2.7	21.9	7.1	16.6	44.3	104.4	1.4	3.1	0.8	0	208.6
2005	0	1.4	21	30	9.6	11.4	86.6	108.6	27.2	0	0	0	295.8
2006	0	0	13.2	15	11.1	28.8	76	118.1	23.9	3	0	0.3	289.4
2007	1.1	2.3	0.3	7.6	7.3	39.2	143.2	97.3	63.1	0	0	0	361.4
2008	7.5	0	0	13.5	5.5	13	77.1	73.9	24.8	7.7	4.1	0	227.1
2009	0	0	1.6	8.4	0.8	3.9	101.7	105	3.7	4.4	5.6	2.8	237.9
2010	0	3.2	14.2	21	17.2	16.4	102.5	133.2	27.5	0	0	0.3	335.5
2011	0	2.5	4.2	10.1	13.5	22.7	89.9	108.9	19.9	0	7.1	0	278.8
2012	0	0	3.4	17.8	12.6	34	100.2	83.6	15.3	4.2	0.4	0	271.5
2013	0.3	0	2.2	14	16.4	12.7	65.4	86.9	19.2	13.5	6.9	0	237.5
2014	0	5	12.8	18.6	20.5	12.1	105.2	117	58.8	13.8	3.2	0.1	367.1
2015	0	0	13.6	0	13.6	12.8	76.3	55.1	55.3	12.9	19.2	2.2	261
2016	0	0	1.5	37.2	21.1	17.1	106.6	83.1	19.2	0	0	0.3	286.1
Mean	1.9	2.8	8.2	16.0	14.0	20.3	89.0	94.1	23.1	4.6	3.1	1.0	278.1

Appendix Table 7: Shire Monthly Precipitation (mm)

Year	Jan	Feb	Mar	Apr	May	Jun	Jul	Aug	Sep	Oct	Nov	Dec	Total
1988	0	0	1	14.9	35.4	43.9	128.6	112.4	44.6	28.7	0	0	409.5
1989	0	7	0	3.9	20.8	65.4	120.4	125.1	62.5	9.8	3.8	1.5	420.2
1990	0	0	10.7	8.7	14.5	39	127.8	78.2	49.3	1	0	0	329.2
1991	0	0	14.4	17.6	90	57.6	60.7	96.9	56.7	5.7	11.7	1	412.3
1992	0	0	5.7	7.8	55.3	61.5	125.1	83.1	48	30.8	1.9	3	422.2
1993	0	0	6.1	28.7	25.9	51.3	86.3	94.8	64	28.1	0	0	385.2
1994	1.3	0	0	11.4	9.6	50.1	133.3	134.7	68.6	23.1	0	1.5	433.6
1995	0	0	1.8	26.2	12.8	50.3	87.4	85.6	54.1	43.8	1.2	0	363.2
1996	0	0	0	1.4	26.1	82.5	93.1	64.5	49	14.9	2.1	0.1	333.7
1997	0.6	0	7	13.2	6.4	44	96	81.2	35.8	9.6	0.7	0.7	295.2
1998	0	1	2.9	6.4	8.6	37.3	95.6	98.9	56.2	2.9	0	0	309.8
1999	5.2	1	3.5	17.3	0.1	51.2	113.3	94.5	38.4	26.8	10.6	0	361.9
2000	0	0	27.8	6.2	26.5	42.4	83.9	73.9	87.5	2.7	1.7	0	352.6
2001	0	0	0	7.5	36	48.6	151.3	104.4	33.4	25.8	0.8	2.7	410.5
2002	0	0	4.8	4.9	8.4	59.8	100.4	100.7	49.6	9.2	0.4	0	338.2
2003	12.7	2.2	0	27.1	23.1	42.9	84.1	110.2	36.2	1.8	2	0	342.3
2004	0	0	12.6	4.1	0	45.3	64.1	90.1	12.3	24.4	1.8	0	254.7
2005	19	0	6.5	36.4	31	96	107.5	140.1	51.2	30.8	0	0	518.5
2006	5	0	9	14.1	62	25	98.6	110.6	55.5	3.5	5.1	0	388.4
2007	0	0	0	5.8	14.6	148.8	190.6	168.6	125.8	0.2	12.6	0	667
2008	0	0	2.7	8	7.6	39.7	155	183.7	59.8	20.8	1.9	0	479.2
2009	0	0	15.5	11	7.4	7.1	122.4	113.6	6.4	10.6	8.8	4.2	307
2010	2.4	3.8	10.2	13.7	68.5	25.7	99.4	138.4	29.4	6	2.3	2.9	402.7
2011	0	0	6.5	13.7	28	40.4	99.1	108.2	64.9	2	1.6	0	364.4
2012	0	0	3.7	11.3	23.3	37	92.9	80.6	28.6	9	7	2.3	295.7
2013	3.4	2.4	6.2	12.5	20	40	87.2	94.7	25.9	25.1	9.3	0	326.7
2014	1.5	3.7	13.1	19.6	35.1	27.4	82.9	103.9	60.7	14.8	7.8	0	370.5
2015	1.5	0.8	9.1	5.6	33	23.3	47.9	62	56.5	12.9	19.2	2.2	274
2016	5.3	1.8	4.1	40.3	39.3	30.2	92.3	97.3	25.4	9.8	2.9	0.3	349
Mean	2.0	0.8	6.4	13.8	26.5	48.7	104.4	104.5	49.5	15.0	4.0	0.8	376.5

Appendix B: Appendix Figures

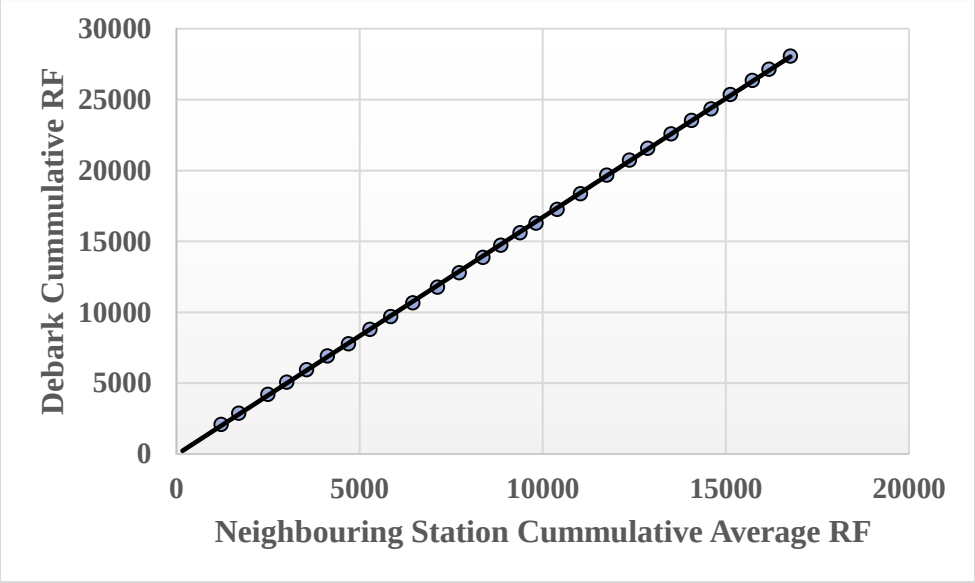

Appendix Figure 1: Double mass curve of Debark station

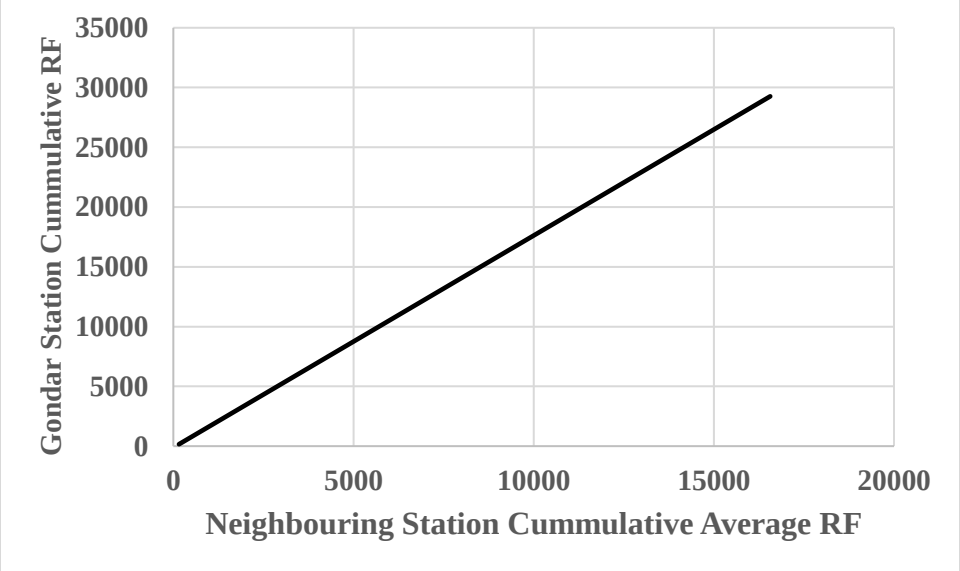

Appendix Figure 2: Double mass curve of Gondar station

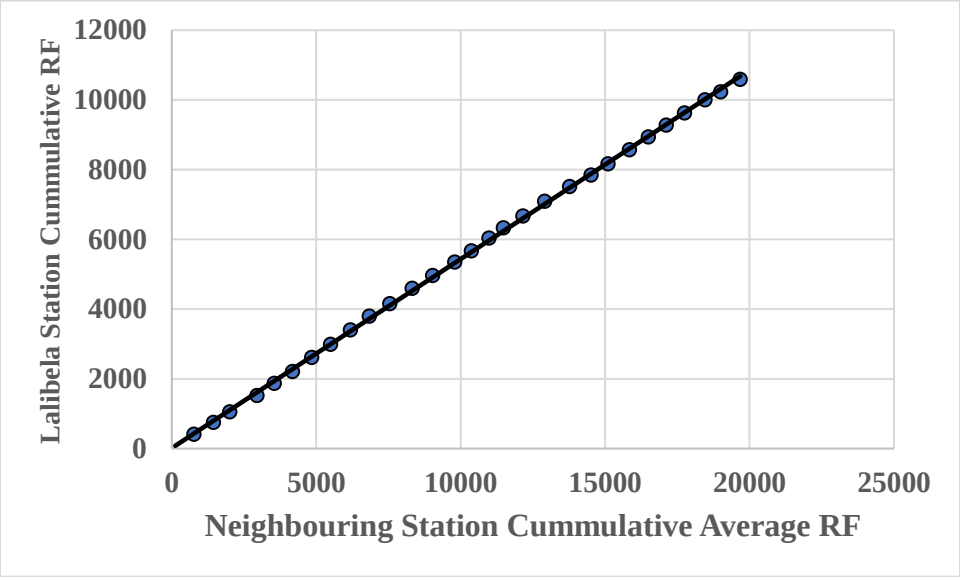

Appendix Figure 3: Double mass curve of Lalibela station

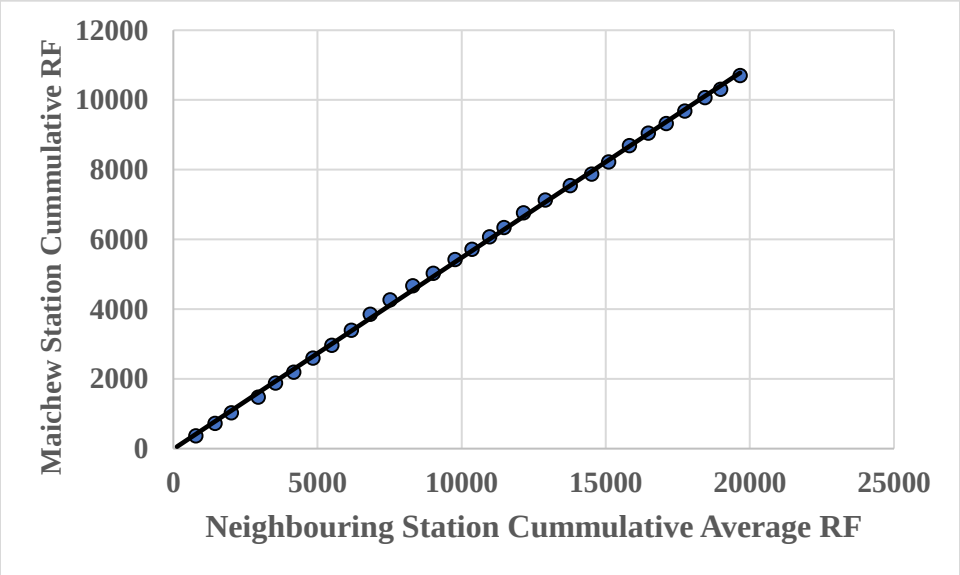

Appendix Figure 4: Double mass curve of Maichew station

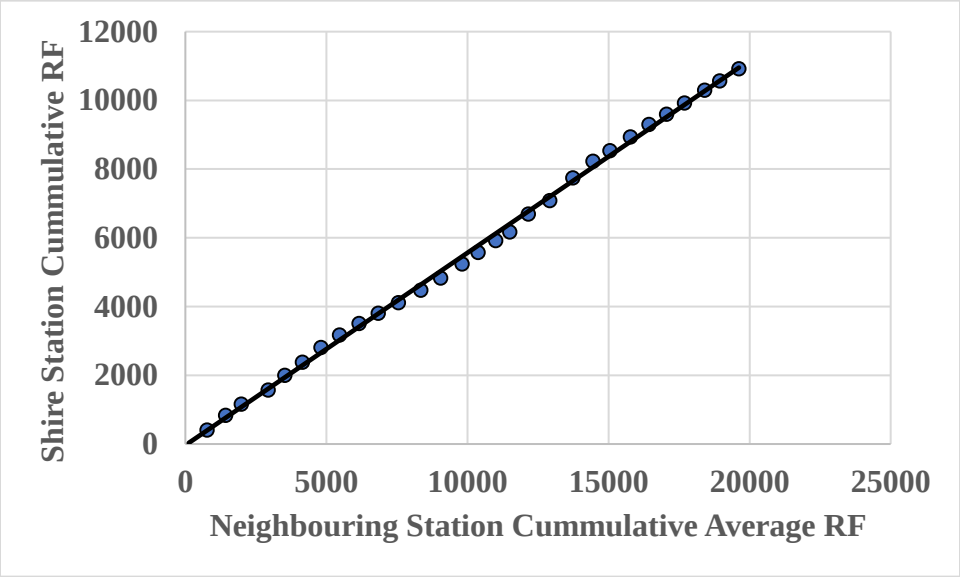

Appendix Figure 5: Double mass curve of Shire station